Performance Analysis and Protocol Design for Wireless Cooperative Networks

by

Yuanqian Luo

A Dissertation Submitted in Partial Fulfillment of the Requirements for the Degree of

DOCTOR OF PHILOSOPHY

in the Department of Electrical and Computer Engineering

Performance Analysis and Protocol Design for Wireless Cooperative Networks

B.Sc., Southeast University, 2005
M.Sc., Southeast University, 2008

Supervisory Committee

Dr. L. Cai, Supervisor
(Department of Electrical and Computer Engineering)

Dr. X. Dong, Departmental Member
(Department of Electrical and Computer Engineering)

Dr. K. Wu, Outside Member
(Department of Computer Science)

Supervisory Committee

Dr. L. Cai, Supervisor
(Department of Electrical and Computer Engineering)

Dr. X. Dong, Departmental Member
(Department of Electrical and Computer Engineering)

Dr. K. Wu, Outside Member
(Department of Computer Science)

ABSTRACT

This thesis presents packet-level channel modeling, spectrum efficiency optimization and channel estimation for wireless cooperative communication systems with diversity combining. Cooperative transmission in a wireless network allows neighboring nodes to share their communication resources to create a virtual antenna array by distributed transmission and signal processing, which is useful to exploit spatial diversity, increase channel capacity, and attain wider service coverage with single-antenna terminals. How to exploit spatial diversity and leverage the multi-hop channel structure is an important research issue for the cooperative network.

In this thesis, two cooperative schemes are considered, amplify and forward (AF) and demodulation and forward (DMF). For AF cooperative systems, finite state Markov chain (FSMC) models are designed in analyzing the system performance considering time-varying channel behaviors and facilitating fast channel simulation. For DMF cooperative systems, first we formulate the optimization problem that jointly chooses the modulation schemes at the source and relay nodes, to maximize the throughput of cooperative systems under the BER constraint. Second, we propose to use the soft values of each bit to devise a simple and effective combining scheme, which can be applied for both AF and DMF cooperative systems. Third, as the soft values from demodulation process can also be used for measuring the channel estimation

accuracy, a soft value-assisted channel estimation has been proposed by iteratively utilizing soft values to refine the accurate channel estimation. In addition, we also implement the soft value module in OFDM-based transceiver system based on a GNU Radio/USRP2 platform, and verify the effectiveness and performance improvement for the proposed SVC systems.

As considering wireless cooperative systems has attracted increasing attentions from both academic and industry to meet the demanding of the high data rate transmission, the packet-level channel modeling, adaptive modulation, spectrum efficiency improvement frameworks based on soft value combining and accurate channel estimation algorithms proposed in this thesis are essential for future proliferation of high data rate, reliable and efficient wireless communication networks.

Contents

List of Figures

List of Tables

ACKNOWLEDGEMENTS

I would like to express my deepest gratitude to my supervisor, Dr.Lin Cai, whose expertise, understanding, and patience, added considerably to my graduate experience. Without her support, motivation, guidance and persistent help, this dissertation would not have been possible.

I would like to thank the other members of my committee, Dr.Xiaodai Dong, and Dr.Kui Wu for the assistance they provided at all levels of the research work and the dissertation. Also, I would like to thank Dr.Hai Jiang from the Department of Electrical and Computer Engineering, University of Alberta, for taking time out from his busy schedule to serve as my external examiner.

A special thanks goes out to Dr.Ruonan Zhang, Northwestern Polytechnical University, whose guidance and suggestions, inspired me with the research direction of channel modeling. I am also pleased to thank colleagues and friends who supported and helped me at University of Victoria, especially Siyuan, Zhe, Min, Xuan, Lei, Kan, Bojiang, Haoling and Ahmad.

I am fortunate to have Qin, Yuchen, Lu, Yun, Zhengya as my friends who encouraged and supported me along the way.

I would also like to thank my parents and my sister for the support they provided me through my entire life. It is hard to put into word how much I appreciate their love. And in particular, I must acknowledge my father and best mentor, without whose love, encouragement and guidance, I would not have chosen this path.

In conclusion, I recognize that this research would not have been possible without the financial assistance of CSC (China Scholarship Council), NSERC, the Department of Electrical and Computer Engineering at University of Victoria (Teaching Assistantships, Graduate Research Scholarships), and express my gratitude to those agencies.

Yuanqian Luo, Victoria, BC, Canada

DEDICATION

This thesis is dedicated to my parents and my sister.
For their endless love, support and encouragement

Chapter 1

Introduction

1.1 Background and Objective

A major driven force for the intensive research efforts in wireless communications and networking is that the limited wireless spectrum may not satisfy the ever-growing demand for inexpensive but effective wireless services, such as wireless Internet access and ubiquitous multimedia distribution. Cooperative communication has emerged to exploit spatial diversity from multiple nodes to improve the wireless spectrum utilization and quality of wireless services. In particular, using cooperative communication, wireless terminals can benefit from relaying messages for each other to propagate the same signal over multiple paths in the network. This path diversity allows the ultimate receivers to combat channel variations resulting from fading, shadowing, and other forms of interference.

Cooperative communication can be applied in many scenarios, including cellular networks, ad-hoc networks, sensor networks, and vehicular networks. Different scenarios call for diverse cooperation methods which can be categorized to two main classes.

1. Amplify and Forward (AF). As the name implies, the relay node amplifies the received signal as well as noise and forwards it to the destination. Although the noise is also amplified with the signal, the destination will achieve the diversity gain by combining two independently faded copies. Because of the light functionality requirement in the relay node, AF is a simple method to implement and analyze. There are two types of AF schemes based on the choice of amplification factor α. If the relay node knows the channel state information between

the source and the relay, h_{SR}, the *fixed gain relays* set α to,

$$\alpha = \sqrt{\frac{E_{RD}}{E_{SR}\mathrm{E}[|h_{SR}|^2] + N_0}}, \tag{1.1}$$

where E_{SR} and E_{RD} denote the average transmission power at the source and the relay, respectively. N_0 is the power of white Gaussian noise. On the other hand, if the relay has the instantaneous channel knowledge of the source to relay h_{SR}, the *variable gain relays* set α to

$$\alpha = \sqrt{\frac{E_{RD}}{E_{SR}|h_{SR}|^2 + N_0}}. \tag{1.2}$$

2. Decode and Forward (DF). Another cooperative scheme is the Decode and Forward. In this scheme, the relay decodes the incoming signal and transmits an re-encoded signal to the destination. Again, independent replicas of the source signal are received at the destination and spatial diversity gain can be achieved. In an uncoded system with the DF protocol, as the relay always forwards the signal to the destination no matter whether the signal is detected correctly or not, an error propagation may occur when the erroneous decoded signal is forwarded by the relay which degrades the system performance. To cope with this problem, DF cooperation incorporated with cyclic-redundancy-check (CRC) codes has been discussed [63], [43]. With CRC codes at the relay, only a correctly decoded signal is allowed to be forwarded by the relay to avoid error propagation. Meanwhile, DF with CRC codes also increases the hardware complexity of the relay and requires additional time to decode and re-encode CRC codes at the relay which results in longer delay.

As cooperative communication systems are more complex than the traditional point-to-point communications with multi-hop multi-path structures, the objective of this thesis is to develop a packet-level channel model of cooperative systems to characterize the statistic properties, and also to investigate new techniques to exploit the spatial diversity of cooperative networks with adaptive modulation and accurate channel estimations, in order to improve the reliability and spectrum efficiency of wireless cooperative systems.

1.2 Contributions

1.2.1 Packets Level Channel Models for Cooperative Systems

Finite-state Markov chain (FSMC) models can capture the essence of time-varying fading channels by preserving their statistic features. How to build FSMC models for multi-hop and multi-path wireless systems remain an open issue. In this thesis, the FSMC channel models are developed for amplify-and-forward (AF) cooperative systems with selection combining (SC) and maximum ratio combining (MRC) techniques, respectively. First, the second-order statistics, such as level-crossing rate (LCR) and average fade duration (AFD) are derived based on the statistical properties of each individual path, for both SC and MRC systems. Then, simple and computational efficient approximations are used to further simplify the proposed model. Numerical and simulation results verify the accuracy and applicability of the proposed FSMC models. Finally, the models are used to optimize the configuration for scalable video streaming in an AF cooperative diversity system. Experimental results show the feasibility and advantage of applying the proposed FSMC model for cross-layer design and optimization.

1.2.2 Soft Value Combining for Cooperative Systems with Adaptive Modulation

User cooperative communication is promising to improve wireless spectrum and energy efficiency. For user cooperative systems, how to maximize the efficiency using adaptive modulation and effectively combine signals with different modulations without sophisticated signal processing is an open issue. A simple soft value combining (SVC) scheme has been proposed. The soft value is a numerical number related to the confidence level in demodulating the bit. With SVC, the receiver sums up the soft values of each information bit from the direct transmission path and the relay path, no matter whether the two transmissions using the same modulation scheme or not. Analytical framework has been developed to quantify the bit error performance of SVC and to optimize the configuration of modulation in demodulate-and-forward (DMF) cooperative systems. Analytical and simulation results have demonstrated that the proposed DMF cooperative system with SVC and adaptive modulation is

simple to implement and can substantially improve the spectrum and energy efficiency of wireless systems, compared to the existing amplify-and-forward cooperative systems and multi-hop relay systems.

1.2.3 Enhanced Channel Estimation for Cooperative Systems with Soft Value-assistance

Inaccuracy of channel estimation is among the main factors that could cause performance degradation in wireless communication. In the cooperative communication, multiple-path and multi-hop scenarios require an even higher accuracy in channel estimation. We propose a channel estimation approach for demodulation-and-forward (DMF) system with the assistance of soft value. The soft values indicating the reliability of demodulated bits are utilized to improve the channel estimation quality. Based on the Expectation-Maximization (EM) algorithm, iterative estimation schemes are proposed which can benefit from the initial estimation results and the soft value information. Numerical results show that the proposed soft value-based channel estimation (S-CE) substantially improve the channel estimation quality in terms of mean square error (MSE), and it thus can improve the spectrum efficiency by reducing the pilot overhead as well as the bit error rate (BER).

1.3 Dissertation Outline

This work focuses on performance enhancement of wireless cooperative network using emerging wireless communication technologies. In order to obtain the statistic information on fading channel of cooperative system, the packet level channel model has been formulated which plays an important role in the network protocol design. Modulation and error recovery for the cooperative system have also been proposed for the throughput enhancement.

The rest of this dissertation is organized as follows.

In Chapter 2, the packet-level channel modeling of wireless cooperative network has been discussed. First, we briefly review the existing work on channel modeling with finite state Markov chain. Then, based on the statistic of the relay and the direct Rayleigh fading channels, two essential second-order parameters level crossing rate (LCR) and average fade duration (AFD), are derived which are important for effective error coding design in the physical and the upper layers.

Adaptive modulation related research issues are discussed in Chapter 3. First, We use an approximate BER expression of M-QAM modulation to formulate an easy-to-solve optimization problem, so the modulation types for the source node and the relay node in the wireless cooperative system can be optimized in real time to maximize the throughput under the BER constraint. To maximize the throughput for the whole network, we further use a worst-link-first (WLF) matching algorithm for selecting appropriate cooperators.

In Chapter 4, an error recovery protocol for user cooperative networks utilizing the soft values of each bit from the physical layer has been proposed. First, we give the definition of soft value in our scheme, and then the closed-form BER expression of AF cooperative systems is derived, both in AWGN and fading channels. We also extend the proposed error recovery scheme in DMF cooperative systems. Significant performance improvement has been noticed from the preliminary results. Spectrum optimization problem with soft value combining is a future research issue.

Chapter 5 focuses on channel estimation algorithm in cooperative systems with the help of soft value. We propose a soft value-assisted channel estimation (S-CE) scheme, by utilizing the reliable information about the initial channel estimation, to improve the accuracy of channel estimation. Several channel refinement schemes are proposed to balance the channel estimation accuracy and the computational complexity.

Chapter 6 concludes the dissertation and suggests the future research directions.

1.4 Bibliographic Notes

Most of the works reported in this dissertation have appeared in research papers. The works in Chapter 2 and Appendix have been published in [44, 49]. The work in Chapter 3 has been published in [45], and those in Chapter 4 have appeared in [46, 48]. The work in Chapter 5 has appeared in [47].

Chapter 2

A Packet-level Channel Model for Wireless Cooperative Diversity Systems

2.1 Motivation and Contributions

As discussed in Chapter 1, the packet-level channel model is used to describe statistical properties of fading channels, and it can track the time-varying channel and capture the dynamics of the packet error rate (PER), on a packet-to-packet basis. A good packet-level channel model is not only important for the simulation of networking algorithms and protocols, but also critical for their performance analysis and optimization.

Wireless cooperative diversity technologies have attracted extensive attention as an essential option to improve the throughput and coverage of wireless communication systems [38]. To overcome the attenuation and distortion caused by the multi-path propagation of wireless channels, neighboring nodes can cooperate to enhance the reliability and stability of wireless transmissions. Depending on the relay functionality, cooperative network can be categorized as amplify-and-forward (AF) by which the relay node amplifies the received signal and retransmits it to the destination, or decode-and-forward (DF) by which the relay node decodes the received signal before forwards it to the destination. In the literature, there are extensive research work on the performance analysis of cooperative diversity systems in terms of capacity and bit error rate (BER) under different cooperative assumptions and diversity combining

techniques [32, 75].

The previous performance analysis for cooperative diversity systems mainly focused on the overall average system performance. For example, BER measures the average error rate in the receiver, determined by the average duration that the received signal envelope falls beneath a certain level. We are also interested in the higher-order statistics of wireless channels, such as how frequently the received envelope crosses a threshold and how long the fading duration is below the threshold each time. These channel statistics have a great impact on the design and performance prediction of wireless systems. For instance, for the queue performance in the link layer, not only the average transmission rate, but also its variation (or the variation of service time) plays an important role.

It is well-known that the Finite State Markov Chain (FSMC) model is a simple and effective tool to capture the first and second-order statistics of fading channels. In 1960s, the classical two-state Gilbert-Elliott (FSMC) model [17] was developed, and then it has been extended to multi-state Markov chain model in [80]. Since then, FSMC models have been extensively studied and widely adopted for protocol design, analysis and simulation purposes [10, 25, 24, 11, 71]. In the literature, FSMCs for a single fading channel (Rayleigh, Rician, or Nakagami-m) [25], for identical channel environments such as multihop relay systems [24, 11], and for diversity systems with multiple identical branches [10] have been studied. However, for cooperative diversity systems with non-identical relay and direct paths, proper channel modeling using FSMC remains an open issue.

In this chapter, we fill the gap by developing the FSMC channel models for AF cooperative diversity system with selection combining (SC) and maximum ratio combining (MRC) diversity techniques, respectively, and applying it to optimize the control strategy for scalable video streaming applications. The main contributions of this chapter are as follows:

1. Considering the statistic properties of the AF two-hop relay path and the direct Rayleigh fading channel, we derive the second-order statistic parameters, i.e., the level crossing rate (LCR) and the average fade duration (AFD), for both SC and MRC cooperative diversity systems. Using the widely adopted SNR partitioning method, the state transition matrix and steady state probabilities, which form the FSMC model, have been derived. To make the exact expression computational attractive for practical applications, we further apply the approximation theorem to simplify the model.

2. Numerical and simulation results have been provided to validate the accuracy of the proposed FSMC models.

3. The proposed FSMC models are applied to optimize the adaptation for scalable video streaming in AF cooperative diversity system, which leads to better user-perceived quality of experience (QoE).

2.2 Related Work

2.2.1 Second-order Statistics

Second-order statistics, such as LCR and AFD determine the frequency and the burst length of the fading channel in certain status, which play an important role in system performance [66, 20, 29, 70]. For AF relay systems with multiple hops, authors in [20] have obtained the analytical expressions for the second-order statistics by modeling the cascaded channel as the product of N fading envelopes. In [29], the statistical properties for diversity techniques in Nakagami-m fading channels have been discussed, where each channel has identical channel distribution. Authors in [70] have studied the statistics of the output from two non-identical Nakagami-m fading channels with MRC. However, none of the above work considers the diversity combining for AF cooperative systems with non-identical relay and direct paths.

2.2.2 SNR Partitioning

Another important issue for FSMC modeling is the state partitioning, which is used to separate the received signals into K nonoverlapping SNR regions. The equiprobable partitioning method (EPM) has been proposed and adopted in [80, 78]. Other partitioning criteria, including equal time duration method and quantization MSE method, have been discussed in [91, 71]. On the other hand, [28] showed that the difference of all partition methods may diminish as the number of the states K increases. In the following, we choose EPM for simplicity.

2.2.3 Video Over Wireless Application

Currently, video applications account for the highest percentage of the network traffic mix. It has been forecasted that two-thirds of the mobile data traffic will be video by

2014 [9]. Given the highly dynamic network conditions, adaptive video transmission gains high attention which can adjust the video source rate according to the available network bandwidth. Authors in [88] proposed adaptive transmission schemes to achieve the inherent gain for a scalable multi-layered video system with quality of service (QoS) guarantee. In [86], the rate adaptation problem was formulated as a Markov Decision Process (MDP), aiming to find an optimal streaming strategy in terms of user-perceived QoE. For the optimization problem, the state transition matrix of the link-layer throughput is a key component. [86] assumed that the transition matrix can be obtained from wireless channel models, but how to obtain the channel models was not considered. Inaccurate channel modeling may under-estimate the available bandwidth which leads to low average video quality, or over-estimate the bandwidth which leads to more playback interruptions. We need to investigate the impact on the video QoE of using different channel models. This case study can reveal the importance of channel modeling on upper layer protocol performance and design.

2.3 Wireless Cooperative Diversity System Models

2.3.1 System Model

We consider the user cooperative system with a relay path and a direct path, as shown in Fig. 2.1. In the first time slot, the source node (S) broadcasts to the relay node (R) and the destination (D). In the second slot, R amplifies the received signal and retransmits it to D. In the system, the maximum Doppler frequency shifts induced by the motion of the mobile stations for the SR, RD and SD, are denoted by f_{m_1}, f_{m_2} and f_{m_3}, respectively. The symbol list is given in Section 2.8 for easy reference.

After the two-hop transmission, the overall received signals at the destination can be written as

$$\begin{bmatrix} r_R \\ r_D \end{bmatrix} = \begin{bmatrix} G_r h_1 h_2 \\ h_3 \end{bmatrix} s + \begin{bmatrix} G_r h_2 n_1 + n_2 \\ n_3 \end{bmatrix}, \tag{2.1}$$

where s is the transmitted signal with the average power normalized to unity, h_1, h_2 and h_3 are the channel gains of SR, RD, and SD, respectively, and n_1, n_2, and

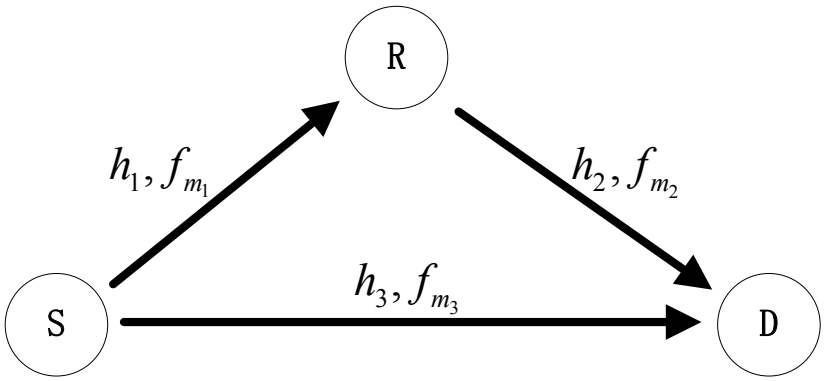

Figure 2.1: System model.

n_3 are the additive complex Gaussian noise with average power N_0. G_r is the fixed amplification gain in R, $h_r = G_r h_1 h_2$ is the overall channel gain of the relay path, and $n_r = G_r h_2 n_1 + n_2$ is the overall noise of the relay path. Note that the direct path and the relay path do not have the identical noise power due to the amplification process at the relay. Thus, the received SNR before the diversity combining is affected by G_r. Following the definition in [59], the fixed gain is given by

$$G_r^2 = \frac{1}{CN_0}, \tag{2.2}$$

where C is a positive constant. The instantaneous end-to-end SNR of the relay path and the direct path can be expressed as $\gamma_R = \gamma_1\gamma_2/(C + \gamma_2)$ and $\gamma_D = \gamma_3$, where $\gamma_i = |h_i|^2/N_0, i = 1, 2, 3$ are the instantaneous SNRs of S-R, R-D and S-D channels, respectively.

In this chapter, we assume that h_1 and h_2 are statistically independent, so the relay amplification factor G_r can be absorbed in the average energy of h_2 for convenience.

To develop the FSMC model for the above cooperative diversity system, there are two essential technical problems. First, as mentioned above, due to the amplifying action in the relay node, the received signal from the relay path contains colored noise, which should be treated carefully. Second, depending on the diversity technique employed by the receiver, combined signals have different properties. Thus, we develop the FSMC models for different combining techniques separately in Sections 2.4 and 2.5, respectively.

2.3.2 Statistical Properties of Direct and Relay Channels

To build the FSMC model for the cooperative diversity system, we need to analyze the statistical properties of the received SNR of both paths, denoted by Γ_D and Γ_R for the direct path and the relay path, respectively.

General Expression of LCR and AFD for Fading Channel

Here, we give the general expression of the second-order statistics for the received signal's envelope. Let y be the value of the fading channel envelope Y. The LCR $N_Y(y)$ is defined as the expected rate at which the random envelope crosses a given threshold y in the downward direction, as described in detail in [71, 91]. It can be

calculated from the joint PDF of the envelope and its time derivative by

$$N_Y(y) = \int_0^\infty \dot{y} f_{Y\dot{Y}}(y, \dot{y}) d\dot{y}, \tag{2.3}$$

where $\dot{}$ denotes the time derivative, and $f_{Y\dot{Y}}(y, \dot{y})$ is the joint PDF of Y and $\dot{Y}$.

Another second-order statistical parameter used to describe the fading channel properties is AFD, $T_Y(y)$, defined as the average time that the channel envelope remains below the threshold y after crossing it in the downward direction. It is given by

$$T_Y(y) = \frac{F_Y(y)}{N_Y(y)}, \tag{2.4}$$

where $F_Y(y)$ is the cumulative distribution function (CDF) of Y.

Statistical Properties for Rayleigh Channel

For the direct path, which is a classical Rayleigh fading channel, the PDF, CDF and LCR of the received SNR can be found as [91]

$$f_{\Gamma_D}(\gamma) = \frac{1}{\bar{\gamma}_3} \exp\left(-\frac{\gamma}{\bar{\gamma}_3}\right), \tag{2.5}$$

$$F_{\Gamma_D}(\gamma) = 1 - \exp\left(-\frac{\gamma}{\bar{\gamma}_3}\right), \tag{2.6}$$

$$N_{\Gamma_D}(\gamma) = f_3 \frac{\sqrt{2\pi\gamma}}{\bar{\gamma}_3} \exp\left(-\frac{\gamma}{\bar{\gamma}_3}\right), \tag{2.7}$$

where $\bar{\gamma}_3 = E\{|h_3|^2\}/N_0$ is the mean SNR of the channel gain, and $E\{.\}$ denotes expectation. f_3 is the maximum Doppler frequency shift between the source and the destination. If one of them is stationary, f_3 equals the Doppler frequency induced by the motion of the mobile station. In our case, $f_3 = f_{m_3}$.

Statistical Properties for AF Relay Channel

From the analysis in Section 2.3.1, the relay path can be modeled as a fixed gain AF fading channel.

The CDF of SNR Γ_R for the relay path is given by

$$\begin{aligned} F_{\Gamma_R}(\gamma) &= Pr(\Gamma_R < \gamma) \\ &= Pr\left(\frac{\gamma_1\gamma_2}{\gamma_2 + C} < \gamma\right), \end{aligned} \tag{2.8}$$

which can be derived as

$$\begin{aligned} F_{\Gamma_R}(\gamma) &= \int_0^\infty Pr\left(\frac{\gamma_1\gamma_2}{\gamma_2 + C} < \gamma | \gamma_2\right) p_{\gamma_2}(\gamma_2) d_{\gamma_2} \\ &= \int_0^\infty \frac{1}{\bar{\gamma}_2}\left[1 - \exp\left(-\frac{\gamma}{\bar{\gamma}_1}\left(1 + \frac{C}{\gamma_2}\right)\right)\right] e^{-\frac{\gamma_2}{\bar{\gamma}_2}} d_{\gamma_2} \\ &= 1 - 2\sqrt{\frac{C\gamma}{\bar{\gamma}_1\bar{\gamma}_2}} e^{-\frac{\gamma}{\bar{\gamma}_1}} K_1\left(2\sqrt{\frac{C\gamma}{\bar{\gamma}_1\bar{\gamma}_2}}\right), \end{aligned} \tag{2.9}$$

where $K_v(.)$ is the v-th order modified Bessel function of the second kind [18].

From (2.9), the PDF of SNR can be obtained by taking the derivative with respect to γ,

$$f_{\Gamma_R}(\gamma) = \frac{2}{\bar{\gamma}_1} e^{-\frac{\gamma}{\bar{\gamma}_1}} \left[\sqrt{\frac{C\gamma}{\bar{\gamma}_1\bar{\gamma}_2}} K_1\left(2\sqrt{\frac{C\gamma}{\bar{\gamma}_1\bar{\gamma}_2}}\right) + \frac{C}{\bar{\gamma}_2} K_0\left(2\sqrt{\frac{C\gamma}{\bar{\gamma}_1\bar{\gamma}_2}}\right)\right]. \tag{2.10}$$

From the definition in (2.3), the LCR for SNR of AF channels can be derived following the method proposed in [66], and obtained as

$$\begin{aligned} N_{\Gamma_R}(\gamma) &= \frac{2\sqrt{2\pi\gamma}}{\bar{\gamma}_1\bar{\gamma}_2} \exp\left(-\frac{\gamma}{\bar{\gamma}_1}\right) \\ &\int_{x=0}^\infty \frac{\sqrt{f_1^2\bar{\gamma}_1 x^4(x^2 + C) + C^2 f_2^2 \bar{\gamma}_2\gamma}}{x^2} \quad \exp\left(-\frac{\bar{\gamma}_1 x^4 + C\bar{\gamma}_2\gamma}{x^2\bar{\gamma}_1\bar{\gamma}_2}\right) dx, \end{aligned} \tag{2.11}$$

where $f_i, i = 1, 2$ are the maximum Doppler frequency shifts for each hop, which depend on the channel mode. For a fixed-to-mobile (F2M) channel, $f_i = f_{m_i}$, where f_{m_i} is the maximum Doppler frequency shift caused by the motion of the mobile station. For a mobile-to-mobile (M2M) channel, the overall maximum Doppler frequency shift can be represented as $f_i = \sqrt{f_{m_{i,s}}^2 + f_{m_{i,r}}^2}$ [65], where $f_{m_{i,s}}$ and $f_{m_{i,r}}$ are the maximum Doppler frequency shifts caused by the motion of the sender and the receiver, respectively. The above properties are crucial in the analysis of the second-order statistical parameters of a cascaded Rayleigh fading channel.

2.3.3 Spatial Diversity

In the destination, two copies of the transmitted signals are received through independent channels, which leads to the diversity gain. With the SC scheme, the receiver selects the signal from the path with the higher received SNR, and ignores the other copy. The output of the SC combiner can be expressed as

$$\gamma = \max\{\gamma_R, \gamma_D\}. \tag{2.12}$$

The MRC scheme takes the advantage of spatial diversity provided by the two independent paths of the cooperative system. With the MRC scheme, signals from each path are weighted with respect to their instantaneous SNR. The resulting overall received SNR can be obtained by

$$\gamma = \gamma_R + \gamma_D. \tag{2.13}$$

Comparing the performance of the SC and the MRC schemes, SC is inferior to MRC from the perspective of the received SNR, due to the lower diversity gain. On the other hand, the SC scheme has lower processing complexity than MRC. SC requires a measurement of the received SNR from each path only, while MRC requires the accurate measurements of both the channel gain and phase. Hence, depending on the tradeoff between complexity and performance, both SC and MRC are widely implemented in the wireless communication systems.

In the following sections of this chapter, we describe our FSMC modeling for two-path cooperative diversity systems. The modeling method can be readily extended to N multi-path cooperative systems, as briefly discussed in Appendix I.

2.4 FSMC Channel Modeling for AF Cooperative System with SC

In this section, we derive the FSMC model for the AF cooperative diversity system with selection combining. Based on the existing work on the statistical properties of AF relay and Rayleigh fading channels, we first derive the second-order statistics (LCR and AFD) for the AF cooperative diversity system with SC. Then, by partitioning the received SNR into K non-overlapping states, the state transition matrix

and steady state probabilities are obtained. The main challenges here are to analyze the statistic properties of the overall combined signals. To overcome the above challenges, we adopt the mapping relationship between the input and output signals of the SC combiner, and derive the expressions in terms of existing individual path statistical parameters, such as LCR, PDF and CDF.

2.4.1 Level Crossing Rate

Let γ be the sampled value of the diversity combined SNR, Γ, of the fading channel. From the definition in (2.3), the LCR, $N_\Gamma(\gamma)$, can be calculated as

$$N_\Gamma(\gamma) = \int_0^\infty \dot{\gamma} f_{\Gamma\dot{\Gamma}}(\gamma, \dot{\gamma}) d\dot{\gamma}, \tag{2.14}$$

where $\dot{}$ denotes the time derivation operator with respect to time, and $f_{\Gamma\dot{\Gamma}}(\gamma, \dot{\gamma})$ is the joint PDF between Γ and $\dot{\Gamma}$. Let $f_\Gamma(\gamma)$ and $F_\Gamma(\gamma)$ be the PDF and CDF of the received SNR of the combined fading channel, respectively. Then the LCR can be rewritten as

$$N_\Gamma(\gamma) = \int_0^\infty \dot{\gamma} f_{\dot{\Gamma}|\Gamma}(\dot{\gamma}|\gamma) f_\Gamma(\gamma) d\dot{\gamma}. \tag{2.15}$$

The value of the received SNR at the output of the combiner, denoted by γ, is given by $\gamma = \max\{\gamma_D, \gamma_R\}$. Then the PDF of the received SNR after SC, $f_\Gamma(\gamma)$, can be represented by

$$\begin{aligned} f_\Gamma(\gamma) &= \sum_{j\in\{D,R\}} P(\Gamma = \gamma_j | \gamma_j = \gamma) f_{\Gamma_j}(\gamma) \\ &= \sum_{\{j,l\}\in\{D,R\}} P(\Gamma_l < \gamma, l \neq j | \gamma_j = \gamma) f_{\Gamma_j}(\gamma) \\ &= \sum_{\{j,l\}\in\{D,R\}, l\neq j} F_{\Gamma_l}(\gamma) f_{\Gamma_j}(\gamma). \end{aligned} \tag{2.16}$$

Given the LCR of the relay and direct paths, $N_{\Gamma_D}(\gamma)$ and $N_{\Gamma_R}(\gamma)$, by taking (2.16)

into (2.15), the average LCR for the SC scheme, $N_\Gamma(\gamma)$, can be obtained as

$$\begin{aligned} N_\Gamma(\gamma) &= \sum_{j\in\{D,R\}} P(\Gamma=\gamma_j|\gamma_j=\gamma) f_{\Gamma_j}(\gamma) \int_0^\infty \dot{\gamma}_j f_{\dot{\Gamma}_j|\Gamma_j}(\dot{\gamma}_j|\gamma_j) d\dot{\gamma}_j \\ &= \sum_{\{j,l\}\in\{D,R\},l\neq j} F_{\Gamma_l}(\gamma) N_{\Gamma_j}(\gamma) \\ &= N_{\Gamma_D}(\gamma) F_{\Gamma_R}(\gamma) + N_{\Gamma_R}(\gamma) F_{\Gamma_D}(\gamma), \end{aligned} \tag{2.17}$$

which implies the number of time that the received signal crosses the threshold γ.

Taking (2.6), (2.7), (2.9) and (2.11) into (2.17), the LCR of the received SNR for SC can be expressed as a function of the SNR threshold γ.

2.4.2 Average Fade Duration

As shown in (2.4), the AFD for cooperative systems with SC is governed by the LCR and the CDF of the combined SNR. The CDF of the SC channel SNR at the receiver can be expressed as

$$\begin{aligned} F_\Gamma(\gamma) &= P(\gamma_D<\gamma, \gamma_R<\gamma) \\ &= F_{\Gamma_D}(\gamma) F_{\Gamma_R}(\gamma). \end{aligned} \tag{2.18}$$

which uses the independence property of each path.

Thus, by taking (2.17) and (2.18) into (2.4), the AFD for the cooperative system with SC, $T_\Gamma(\gamma)$, can be obtained as the average duration that the received signal is below the threshold γ.

2.4.3 SNR Partitioning and Steady State Probabilities

Let $\mathcal{S} = s_1, s_2, ..., s_K$ denote the received SNR state space with K states. Generally, the SNR range of each state should be large enough so the channel most likely remains in the same state during one packet transmission time. On the other hand, the SNR range should be small enough to ensure the corresponding BER performance within the range is similar. Based on the above requirements, [80] proposed EPM for SNR partitioning as a simple and applicable solution, so that the steady-state probabilities

π_k of each state are all equal, i.e.,

$$\pi_k = \int_{\Gamma_k}^{\Gamma_{k+1}} f_\Gamma(\gamma)d\gamma = F_\Gamma(\Gamma_{k+1}) - F_\Gamma(\Gamma_k) = \frac{1}{K}, \tag{2.19}$$

for $k = 0, 1, ..., K$. By numerically solving the above equations, the SNR thresholds $\Gamma_k, k = 1, 2, ..., K-1$ can be obtained.

2.4.4 State Transition Probabilities

Once the number of states and the corresponding SNR partitioning have been determined, we next calculate the state transition probabilities. In a first-order Markov model, we assume a slow fading environment with appropriate SNR partitioning, and that the state transitions are possible only between adjacent states. Let $P_{i,j}$ denote the state transition probability between state s_i and s_j, which can be approximated as [80]

$$P_{k,k+1} \approx \frac{N_\Gamma(\Gamma_{k+1})T_p}{\pi_k}, \quad k = 1, 2, ..., K-1 \tag{2.20}$$

$$P_{k,k-1} \approx \frac{N_\Gamma(\Gamma_k)T_p}{\pi_k}, \quad k = 2, ..., K \tag{2.21}$$

where T_p is the transmission time for one packet.

2.5 FSMC Channel Modeling for AF Cooperative System with MRC

In this section, the FSMC channel model is derived for AF cooperative system with MRC. Different from the approach adopted for SC, we first obtain the second-order statistics by applying the variance properties of the AF relay path and the direct Rayleigh fading path. Then an approximated expression of LCR is given to further simplify the analytical results. Given the SNR partitioning, the state transition probabilities and steady state probabilities are then obtained.

2.5.1 Level Crossing Rate

To derive the LCR defined in (2.3), our approach does not require the explicit expression of joint probability $f_{\Gamma\dot{\Gamma}}(\gamma,\dot{\gamma})$ to obtain the analytical result of LCR. The detail of the derivation is presented below.

As for $f_{\Gamma\dot{\Gamma}}(\gamma,\dot{\gamma})$, it can be expressed as follows:

$$\begin{aligned} f_{\Gamma\dot{\Gamma}}(\gamma,\dot{\gamma}) &= \int_0^\infty f_{\Gamma,\dot{\Gamma}|\Gamma_D}(\gamma,\dot{\gamma}|\gamma_D) f_{\Gamma_D}(\gamma_D) d\gamma_D \\ &= \int_0^\infty f_{\dot{\Gamma}|\Gamma,\Gamma_D}(\dot{\gamma}|\gamma,\gamma_D) f_{\Gamma|\Gamma_D}(\gamma|\gamma_D) f_{\Gamma_D}(\gamma_D) d\gamma_D. \end{aligned} \tag{2.22}$$

By taking (2.22) into (2.3), the LCR expression for MRC can be rewritten as

$$\begin{aligned} N_\Gamma(\gamma) &= \int_0^\infty \dot{\gamma} \int_0^\infty f_{\dot{\Gamma}|\Gamma,\Gamma_D}(\dot{\gamma}|\gamma,\gamma_D) f_{\Gamma|\Gamma_D}(\gamma|\gamma_D) f_{\Gamma_D}(\gamma_D) d\gamma_D d\dot{\gamma} \\ &= \int_0^\infty \left(\int_0^\infty \dot{\gamma} f_{\dot{\Gamma}|\Gamma,\Gamma_D}(\dot{\gamma}|\gamma,\gamma_D) d\dot{\gamma} \right) f_{\Gamma|\Gamma_D}(\gamma|\gamma_D) f_{\Gamma_D}(\gamma_D) d\gamma_D. \end{aligned} \tag{2.23}$$

Since the relay and the direct paths are independent to each other, the derivative of the received SNR of the MRC scheme, γ, can be expressed as

$$\begin{aligned} \dot{\gamma} &= \dot{\gamma}_D + \dot{\gamma}_R \\ &= 2\sqrt{\gamma_D}\dot{\alpha}_D + \dot{\gamma}_R, \end{aligned} \tag{2.24}$$

where $\gamma_D = \alpha_D^2$, and $\alpha_D = |h_D|/\sqrt{N_0}$ is the normalized envelope.

For isotropic scattering, the derivative of the direct path envelope α_D is Gaussian distributed with zero mean and variance $\sigma^2_{\dot{\alpha_D}} = \pi^2 \bar{\gamma}_D f_3^2$ [30]. As we know from Section 2.3.2, LCR of the received SNR from the AF relay path, N_{Γ_R}, can be described as

$$\begin{aligned} N_{\Gamma_R}(\gamma) &= f_{\Gamma_R}(\gamma) \int_0^\infty \dot{\gamma} f_{\dot{\Gamma}_R|\Gamma_R}(\dot{\gamma}|\gamma) d\dot{\gamma} \\ &= f_{\Gamma_R}(\gamma) \frac{\sigma_{\dot{\Gamma}_R}}{\sqrt{2\pi}}. \end{aligned} \tag{2.25}$$

Thus, the standard deviation of the derivative of the AF relay path SNR can be obtained as

$$\sigma_{\dot{\Gamma}_R} = \sqrt{2\pi} \frac{N_{\Gamma_R}(\gamma)}{f_{\Gamma_R}(\gamma)}. \tag{2.26}$$

Based on the statistic properties of the AF relay and direct paths, the variance of the derivative of the receiver SNR for MRC, $\sigma_{\dot{\Gamma}}$, has the following expression:

$$\sigma_{\dot{\Gamma}}^2 = \sigma_{\dot{\Gamma}_D}^2 + \sigma_{\dot{\Gamma}_R}^2, \tag{2.27}$$

where the standard derivations, $\sigma_{\dot{\Gamma}_D}$ and $\sigma_{\dot{\Gamma}_R}$ are, respectively,

$$\sigma_{\dot{\Gamma}_D} = 2\pi\sqrt{\gamma_D\bar{\gamma}_D}f_3 \tag{2.28}$$

$$\sigma_{\dot{\Gamma}_R} = \frac{\sqrt{2\pi}N_{\Gamma_R}(\gamma-\gamma_D)}{f_{\Gamma_R}(\gamma-\gamma_D)}. \tag{2.29}$$

The detailed proof of the above assumption (2.27) is presented in Appendix II.

Based on the above discussion, the bracketed integral in (2.23) is obtained by using (2.27) as

$$\int_0^\infty \dot{\gamma} f_{\dot{\Gamma}|\Gamma,\Gamma_D}(\dot{\gamma}|\gamma,\gamma_D)d\dot{\gamma} = \frac{\sqrt{\sigma_{\dot{\Gamma}_D}^2+\sigma_{\dot{\Gamma}_R}^2}}{\sqrt{2\pi}}, \tag{2.30}$$

which is the function of γ and γ_D.

Also, the PDF of the received SNR Γ conditioned on the direct path SNR Γ_D can be rewritten as the known function f_{Γ_R}

$$f_{\Gamma|\Gamma_D}(\gamma|\gamma_D) = f_{\Gamma_R}(\gamma-\gamma_D). \tag{2.31}$$

In principle, by substituting (2.30) and (2.31) into (2.23), we can obtain the final formula for LCR of the received SNR with the MRC scheme as

$$N_\Gamma(\gamma) = \int_0^\infty \sqrt{2\pi f_3^2 f_{\Gamma_R}^2(\gamma-\gamma_D)\gamma_D\bar{\gamma}_D + N_{\Gamma_R}^2(\gamma-\gamma_D)}\, f_{\Gamma_D}(\gamma_D)d\gamma_D. \tag{2.32}$$

However, since $N_{\Gamma_R}(\gamma)$ in (2.11) has no closed-form but integral expression, (2.32) becomes computationally difficult given the double integration with complex function (i.e., Bessel functions), and it is hard to apply multidimensional numerical integration. By applying the multivarible Laplace approximation theorem [83], a tight closed-form approximation of $N_{\Gamma_R}(\gamma)$ can be obtained as

$$N_{\Gamma_R}(\gamma) = \frac{\sqrt{2}\pi}{\bar{\gamma}_1\bar{\gamma}_2}\exp\left(-\frac{\gamma}{\bar{\gamma}_1}-2\sqrt{\frac{C\gamma}{\bar{\gamma}_1\bar{\gamma}_2}}\right)\sqrt{f_1^2\gamma\bar{\gamma}_2(\sqrt{C\gamma\bar{\gamma}_1\bar{\gamma}_2}+C\bar{\gamma}_1)+Cf_2^2\bar{\gamma}_1\bar{\gamma}_2\gamma}. \tag{2.33}$$

The detailed proof of (2.33) is given in Appendix III. It is noted that with the approximation, the above integral (2.32) can be easily and quickly computed using the well-known mathematical software tools, such as Mathematica or Matlab.

2.5.2 Average Fade Duration

The CDF of the received SNR with the MRC scheme can be expressed as

$$\begin{aligned} F_\Gamma(\gamma) &= P(\Gamma < \gamma) \\ &= P(\Gamma_R < \gamma - \gamma_D | \Gamma_D = \gamma_D) P(\Gamma_D = \gamma_D) \\ &= \int_0^\gamma F_{\Gamma_R}(\gamma - \gamma_D) f_{\Gamma_D}(\gamma_D) d\gamma_D. \end{aligned} \tag{2.34}$$

By definition, (2.34) together with (2.32) provide the AFD as described in (2.4).

2.5.3 Steady State Probability and Transition Probability

Based on the same SNR partitioning method as discussed in Section 2.4.3, the steady state probabilities and the state transition probabilities can be obtained as

$$\pi_k = \int_{\Gamma_k}^{\Gamma_{k+1}} f_\Gamma(\gamma) d\gamma = F_\Gamma(\Gamma_{k+1}) - F_\Gamma(\Gamma_k) = \frac{1}{K} \tag{2.35}$$

$$P_{k,k+1} \approx \frac{N_\Gamma(\Gamma_{k+1}) T_p}{\pi_k}, k = 1, 2, ..., K-1 \tag{2.36}$$

$$P_{k,k-1} \approx \frac{N_\Gamma(\Gamma_k) T_p}{\pi_k}, k = 2, ..., K. \tag{2.37}$$

2.6 Performance Evaluation

In this section, we first evaluate the accuracy of the proposed FSMC models for AF cooperative systems with SC and MRC, by comparing the analytical results with the Monte Carlo simulation results. Then we apply the proposed FSMC models to the adaptive scalable streaming system and compare the user-perceived QoE with those using other channel models.

Based on the system model, the source, relay and destination nodes form two different mathematical scattering models for Rayleigh channels in the simulation. Assume that the source and relay nodes are mobile stations, and the destination node is fixed. Then the channels from S to D and R to D become F2M channels

that are modeled by the standard Jakes model using sum-of-sinusoids (SOS) . And the channel from S to R is M2M channel [65] by using a modified Akki and Habber's channel model. At the relay node, the fixed relay gain G_r is chosen to maintain a constant average power of output [59]. We assume that the average channel gain of SR is known at R, then the fixed relay gain G_r can be calculated as $G_r^2 = 1/E[|r_{S-R}|^2] = 1/(\bar{\gamma}_1 + 1)N_0$. Compared to (2.2), $C = \bar{\gamma}_1 + 1$.

2.6.1 FSMC Modeling for SC and MRC

Figs. 2.2-2.3 compare the LCR and AFD results derived in Sections 2.4 and 2.5 for AF cooperative systems with SC and MRC diversity schemes, among with the AF relay path (without combining with the direct path) as the bench-mark. The maximum Doppler frequency shift caused by the motion of each node are set as $f_{m1} = 1$ Hz, $f_{m2} = f_{m3} = 5$ Hz with the packet transmission time $T_p = 0.001$s. The average SNR for channel SR, RD, and SD are $\bar{\gamma}_1 = \bar{\gamma}_2 = 15$ dB, and $\bar{\gamma}_3 = 10$ dB, respectively. Since we adopt the EPM for SNR state partitioning and the diversity combining schemes, SC and MRC, lead to different distributions, state threshold γ_{th} are different for these two schemes in order to ensure the equal probability of each state.

From Fig. 2.2, it is observed that the LCR for SC is higher than that for MRC when the SNR threshold γ_{th} is small, and lower than that for MRC when the value of γ_{th} is large. While for the AF relay channel, with even a smaller value of threshold, it has a larger value of LCR compared with the other two diversity schemes. Specifically, the received signal crosses the lower-value thresholds more frequently when the AF relay (without combining) is used, while the trend is reversed for higher SNR. This is consistent with the observation made in [29] for identical Nakagami-m diversity system.

Combined the results of AFD in Fig. 2.3, we have more insights. As shown in Fig. 2.3, first, with a small value of the SNR threshold γ_{th}, both SC and MRC almost remain the similar value for AFD, which means that once the combined signal from the AF cooperative diversity system drops beneath the low value threshold, it will remain in the poor channel condition states for the similar amount of time. On the other hand, the LCR results indicate that the signal with MRC crosses the low threshold less often than that with SC, so on average it will stay less time in deep fades. Second, the signal with MRC always has a lower AFD than that with SC and AF relay for all SNR thresholds, so on average a stronger received signal is obtained

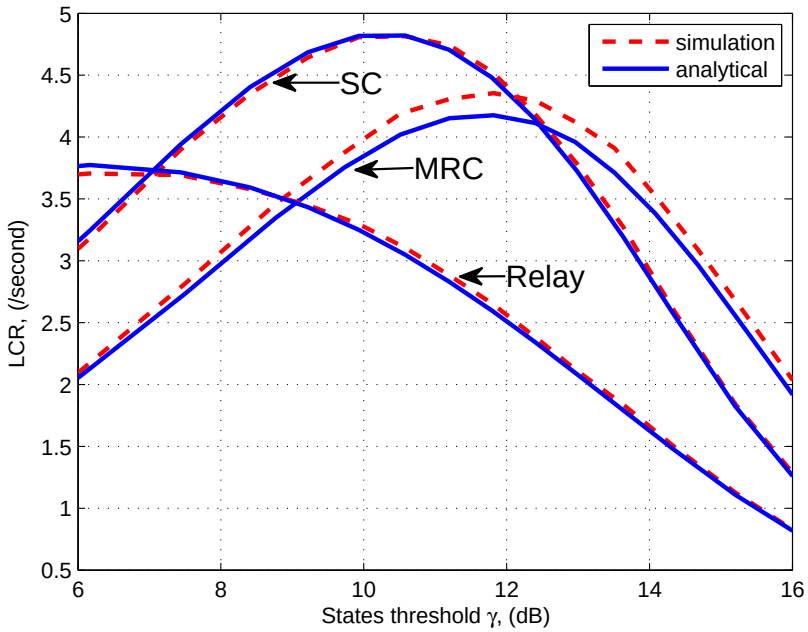

Figure 2.2: LCR for SC and MRC cooperative diversity system compared with AF relay channel.

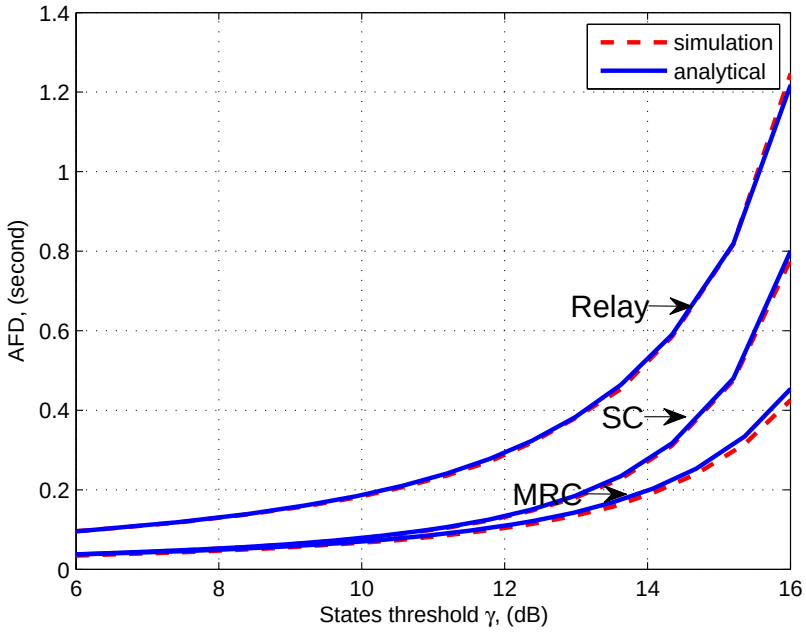

Figure 2.3: AFD for SC and MRC cooperative diversity system compared with AF relay channel.

from the higher order diversity scheme (i.e., MRC). Meanwhile, both cooperative diversity schemes outperform the AF relay case with a lower AFD. In summary, the higher order diversity technique used in the AF cooperative system not only brings the larger average received SNR, but also improves the second-order statistical properties of the received signal.

Similar tendency can be observed from Fig. 2.4, showing the transition probabilities and steady state probabilities, respectively, for SC and MRC. As mentioned above, we adopt equal probability method for SNR partitioning to separate SNR region into K equal probability states with different boundaries for SC and MRC cases, and have verified by steady state probability shown in Fig. 2.4.

Fig. 2.5 demonstrates the LCR for SC and MRC, respectively, for various mobility environments. From the figure, we can observe that with the increase of mobility, in terms of maximum Doppler frequency shifts, LCR for both SC and MRC will be enlarged accordingly, due to the severity of fading channels. Overall, as shown in Figs. 2.2-2.5, the analytical results using the developed channel models match well with the simulation results.

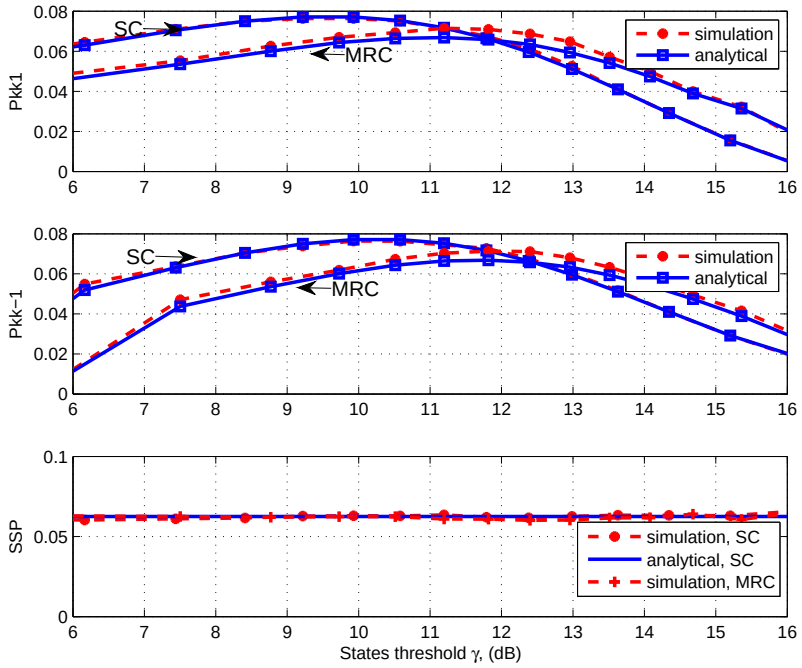

Figure 2.4: Transition probabilities and steady state probabilities for SC and MRC cooperative diversity system.

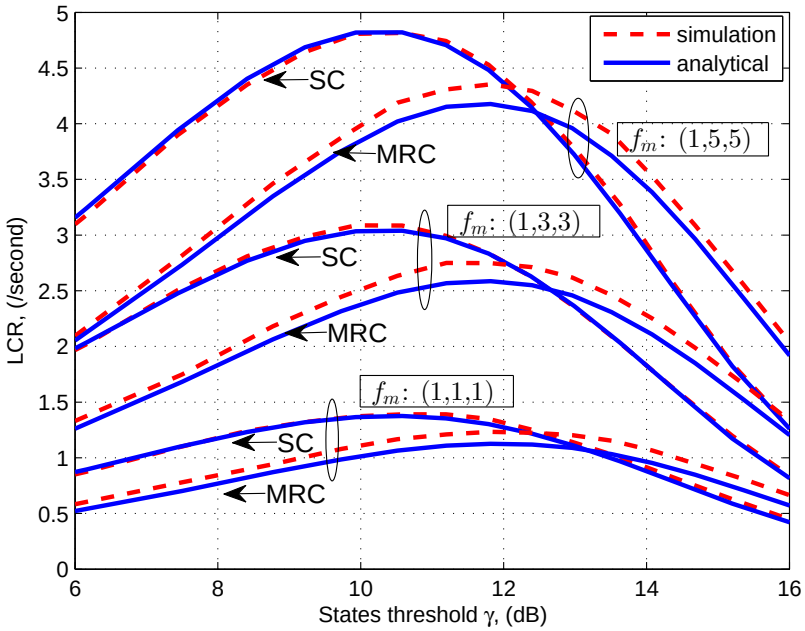

Figure 2.5: LCR for SC and MRC cooperative diversity system with various mobility environments, $f_m : (f_{m1}, f_{m2}, f_{m3})$ (Hz).

Table 2.1: Layer Configuration

Resolution	2	3	Y-PSNR	Layer index
320x180	112.84	39.01	35.47	1
320x180	238.94	88.84	39.44	2
640x360	363.82	140.33	35.90	3

2.6.2 Scalable Video Streaming for AF Cooperative System with FSMC Modeling

We next use the scalable video streaming testbed [85] to evaluate the streaming strategy based on the proposed FSMC models and compare it with other FSMC models. The scalable video streaming testbed uses `Lighttpd` as the streaming server and the sample video ("Big Buck Bunny" [85]) is encoded into three layers by the open-source SVC codec JSVM. The detailed configurations are listed in Table 2.1. Each layer of the scalable video is chopped into small segments of 17 frames, with the total number of segments $N_T = 200$. The frame rate is 24 frame per second.

The wireless link data rate can be adjusted according to the wireless channel quality by using the adaptive modulation and coding techniques. When the channel quality is good, a higher data rate Modulation and Coding Scheme (MCS) is used, and vice versa. Based on the resolution choices listed in Table 2.1, we used a four-state Markov channel model to capture the variation of the available bandwidth in the AF cooperative diversity system. Assuming that the first state of the FSMC channel can support 90 Kbps bandwidth with MCS index 8 in the 3GPP standard [1], we can adjust the MCS configurations for the other states according to the average received SNR as [67]. The average bandwidth, MCS index and received SNR of the cooperative system for each states are listed in Table 2.2. The received SNR for the SR, RD and SD channels are $\bar{\gamma}_1 = \bar{\gamma}_2 = 15$ dB, $\bar{\gamma}_3 = 10$ dB, and $f_{m1} = 1$ Hz, $f_{m2} = f_{m3} = 5$ Hz with packet transmission time $T_p = 0.01$s. We use the Monte Carlo simulation results as the real channel trace to test the received video quality. The video adaptation control algorithm proposed in [86] relies on a Markov model for the available bandwidth. We use our proposed FSMC models to assist the video adaptation decision process. Since there is no existing FSMC model for AF cooperative diversity systems and AF relay path has larger received SNR than the direct path, we choose the FSMC model for AF relay path as a bench-mark for comparison. In other words, to compare the video performance, we use the same wireless channels and the same video adaptation

Table 2.2: Available Bandwidth and SNR

State	1	2	3	4
Bandwidth (Kbps)	90	151.6	280.5	410.96
MCS index [1]	8	12	18	24
Average SNR $\bar{\gamma}$ (dB)	6.65	9.94	14.94	20.83

Table 2.3: QoE Comparison

Case	Model	IR	APQ	PS	Max queue
SC	FSMC	0	1.20	789.12	19.9
	AF	0	1.16	548.19	19.7
MRC	FSMC	0	1.25	629.98	19.8
	AF	0	1.24	406.34	19.9

control algorithm, and use different channel models (the proposed channel models for the cooperative diversity systems vs. the existing channel model for AF relay path only) to assist the video adaptation.

We use the following QoE performance metrics to evaluate the streaming performance [86]: the interruption ratio (IR), equal to the playback interruption duration over the total playback duration; the average playback quality (APQ), a larger value of APQ means a better playback quality; and playback smoothness (PS), a larger value of PS means the longer time of continuous playback of a particular video layer, thus less frequently layer switching. Besides, the max queue denotes the maximum number of buffered segments in the receive buffer, which is used to evaluate how well the streaming strategy can avoid buffer overflow. Since the streaming strategy always try to keep the buffered segment size smaller than the target buffer size.

Figs. 2.6-2.7 show the playback traces for the AF cooperative diversity system with SC and MRC. As shown in the figures, the playback using the proposed FSMC models is smoother than that using the AF relay path model for both SC and MRC cases. Table 2.3 summarizes and compares the QoE performance using different models. From the table, we can see that although using both the proposed FSMC models and the AF relay model can ensure that there is no playback interruption and the maximum queue length is kept less than the target buffer size (20), using the proposed FSMC model can outperform the AF relay model in terms of both APQ and PS. In summary, an accurate channel model can improve the effectiveness of video adaptation control algorithm and enhance the user perceived video quality at no extra energy or spectrum cost.

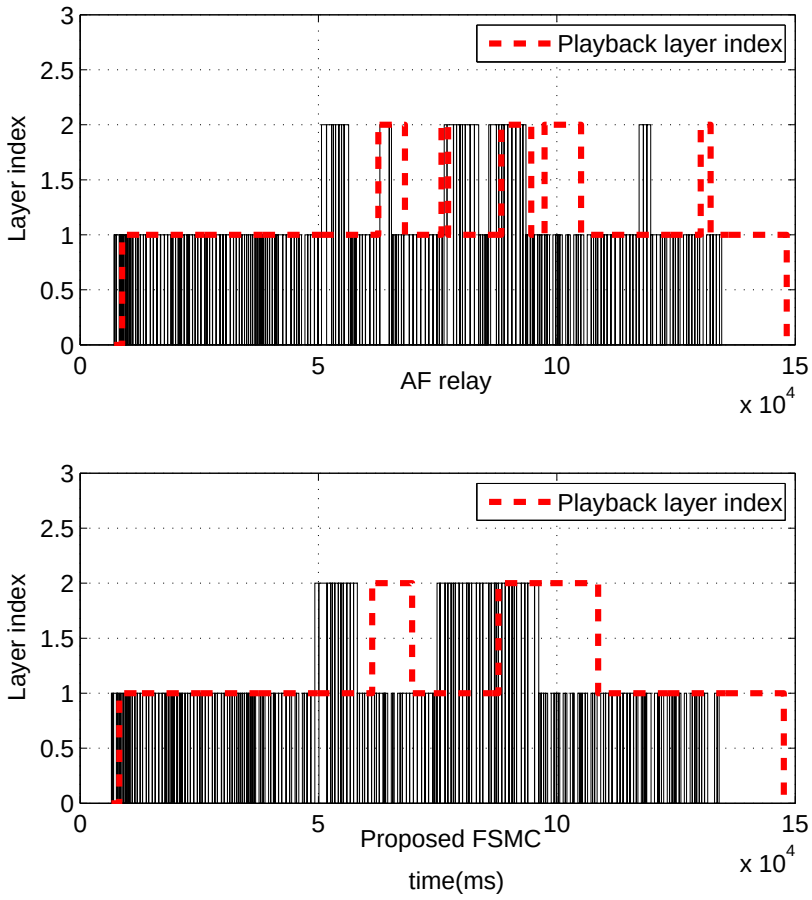

Figure 2.6: Video playback performance comparison between AF relay and proposed model for SC.

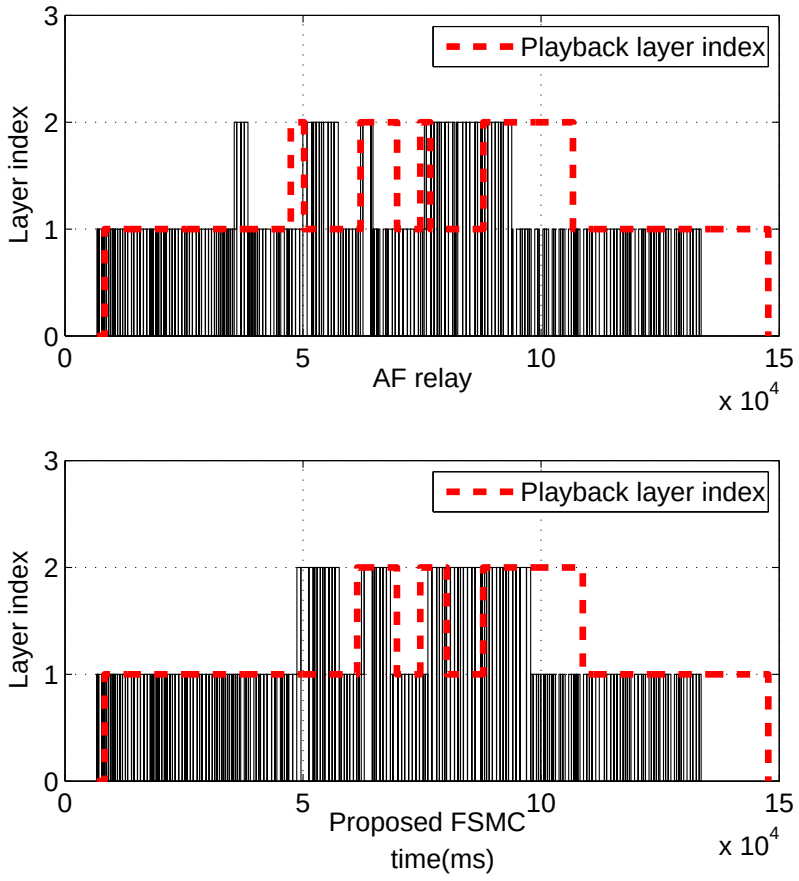

Figure 2.7: Video playback performance comparison between AF relay and proposed model for MRC.

Table 2.4: Notations for Chapter 2

Symbol	Explanation
s	transmitted symbol
h_i	channel gain for i_{th} channel
G_r	fixed amplification gain in R
f_i	maximum Doppler frequency shift for i_{th} channel, i$\in${SR, RD, SD}
f_{m_i}	maximum Doppler frequency shift caused by the motion of the mobile station for i_{th} channel
$N_Y(y)$	LCR of channel envelope y
$T_Y(y)$	AFD of channel envelope y
$(\dot{y})$	time derivation of y
f_Γ, F_Γ	PDF and CDF of received SNR Γ
$\mathcal{S} = s_1, s_2, ..., s_K$	received SNR state space with K states
π_k	steady-state probability for state s_k
$P_{i,j}$	state transition probability between state s_i and s_j
T_p	transmission time for one packet

2.7 Summary

In this chapter, we have developed a channel modeling framework for the AF cooperative diversity systems with SC and MRC. Second-order statistics for the received SNR, such as LCR and AFD, have been derived and simplified by using the Laplace approximation theorem. Then, based on the EPM SNR partitioning scheme, the state transition probabilities and steady state probabilities have been obtained. Accuracy and applicability of proposed FSMC models have been illustrated by comparing the numerical results and simulation results.

A case study of using the proposed channel model to assist the adaptive video streaming over the wireless cooperative systems with SC and MRC has been presented. The testbed results have shown that the proposed channel model can improve the effectiveness of the video adaptation control algorithm to enhance the user perceived video quality, which demonstrates the importance of accurate channel modeling.

2.8 Symbol List

The symbol list is shown in Table 2.4.

Chapter 3

Throughput Maximization for User Cooperative Wireless Systems with Adaptive Modulation

3.1 Motivation and Contributions

In Chapter 2, we have investigated the packet-level channel modeling for wireless cooperative communication systems, which provides statistical properties for system analysis and design. On the other hand, spatial diversity gain from the multi-hop multi-path structure of cooperative systems can also benefit the performance improvement. Since each individual link has distinct channel condition, assigning different modulation schemes, i.e., implementing adaptive modulation becomes a promising solution for spectrum efficiency problem of cooperative systems.

Adaptive modulation has been widely adopted in modern wireless communication systems to improve spectrum efficiency, while user cooperative diversity has also been investigated to improve system coverage and efficiency. How to take the advantage of adaptive modulation for user cooperative transmissions to maximize network throughput under the constraint of the bit error rate (BER) requirement is an open issue.

Different from the previous approaches, in this chapter, to fully utilize adaptive modulation to maximize the throughput of cooperative systems, we propose the demodulation-and-forward (DMF) cooperative protocol. In short, a source node will transmit its information bits in one time slot choosing a modulation type, and both

the destination and a relay node will receive the message, successfully or in-error. The relay then demodulates the received bits and sends it out in the following slot, using another modulation type. The two slots may be of different durations, due to the different modulation types used. One main difference of DMF and DF is that, the relay in the proposed DMF protocol only demodulates the received signal without decoding it. Decoding process is only conducted at the destination. This design can not only reduce the decoding load at the relay, so the latency between the first and second slot can be minimized, but also it allows the destination to use advanced signal processing techniques to process the two copies of the signals to improve BER performance.

The main contributions of this chapter are:

1. We propose the DMF cooperative protocol which can utilize adaptive modulation to enhance spectral efficiency or throughput.

2. We formulate an optimization problem to jointly choose the best modulation types for the source and the relay, so the throughput can be maximized under the BER constraint. Different from [69], where the average symbol error probability (SEP) of a multi-branch cooperative system under general fading channels was analyzed using the method of [82], we derive a closed-form approximation of BER for the DMF cooperative system.

3. We further extend the work to consider how to maximize the whole network throughput by appropriately grouping users in the network, and the worst-link-first (WLF) matching algorithm has been employed.

4. Extensive simulations have been conducted, and the results demonstrate that the proposed DMF protocol with adaptive modulation can effectively improve network throughput.

3.2 Related Work

Multiple-Input-Multiple-Output (MIMO) techniques have been widely accepted as one of the key components for the next generation wireless communication system [16]. However, due to the size and cost limitations of terminals, spatial diversity using multiple antennas may be hard to achieve in practice. Thus, it has been proposed to use

the user cooperative diversity techniques to provide spatial diversity by allowing different individuals to relay the signal, forming virtual antenna arrays without installing multiple antennas in each device. Several cooperative transmission protocols based on half-duplex schemes were proposed [38], which can be classified into two main categories: the amplify-and-forward (AF) protocols by which relays amplify the received signal and retransmit it to the destination, and the decoded-and-forward (DF) protocols by which relays decode the received signal before forward it to the destination. For both AF and DF protocols, since extra channel bandwidth is needed by the relay, how to improve spectral efficiency for cooperative system becomes a key issue [87, 39]. The approach in [87] improves the bandwidth efficiency by using a network coding which allow each user to transmit its own information with the relayed one simultaneously. Superposition coding, originally proposed in [39], has been proved to be able to improve the throughput of cooperative system.

On the other hand, spectral efficiency can be enhanced by employing adaptive transmission techniques, which could fully utilize the time-varying wireless channels by adjusting transmission parameters, such as transmission power, time, symbol rate and constellation size. For instance, in [19], with the partial channel information estimated at the transmitter, the dynamic allocation of system resource, namely time and power, has been discussed. However, only a few studies have considered adaptive modulation in cooperative system [26, 41, 54, 77, 89]. In [26], two-way AF cooperative system with adaptive modulation has been proposed to increase throughput. For DF cooperative protocol, [54] and [77] proposed to combine adaptive modulation and Quality of Service(QoS) constraints from the upper layer to reduce the retransmission time in the link layer. In [89], rotation matrix was employed in order to achieve signal space diversity by changing the signal modulation. To the best of our knowledge, how to take the advantage of adaptive modulation for user cooperative transmissions to maximize network throughput under the constraint of the bit error rate (BER) requirement is an open issue.

3.3 System Model and DMF Protocol

We first consider the cooperative model shown in the Fig. 3.1, where one relay node (R) helps the source node (S) to deliver information to the destination (D). Similar to the DF protocol, two time slots are used for each data transmission. A symbol list in Section 3.8 for easy reference.

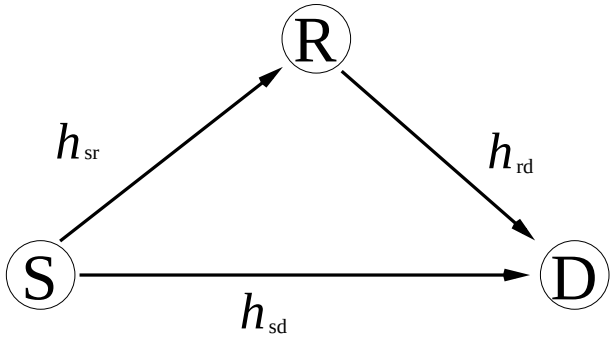

Figure 3.1: Simplified cooperative system model.

In the first time slot, S sends its information to both R and D. The received signals by R and D are denoted as y_{sr} and y_{sd}, respectively, which can be written as

$$y_{sd} = \sqrt{E_s} h_{sd} x + n_{sd}, \tag{3.1}$$

$$y_{sr} = \sqrt{E_s} h_{sr} x + n_{sr}, \tag{3.2}$$

where E_s is the transmission power by S, x is the transmitted signal, and h_{sd} and h_{sr} are the fading coefficients from S to R and S to D, respectively. In this chapter, we use Rayleigh fading as an example. n_{sd} and n_{sr} are additive complex Gaussian noise with average power N_0.

Different from the DF protocol where the relay forwards the information to the destination if it can decode it successfully, in the proposed DMF protocol, the relay only demodulates the received signal and forwards it using another modulation type. Then, the demodulated signal, denoted as $\hat{x}_r$, is re-modulated and subsequently transmitted to D during the second time slot. The received signal at D in the second time slot can be expressed as

$$y_{rd} = \sqrt{E_r} h_{rd} \hat{x}_r + n_{rd}, \tag{3.3}$$

where E_r denotes the transmission power by R and $\hat{x}_r$ is the demodulated signal. h_{rd} and n_{rd} represent the channel coefficient and Gaussian noise from R to D, respectively.

Since the proposed DMF protocol does not request the relay to decode the source information, relay may transmit bits even there are transmission errors during the first slot. The advantages of this design are two-fold: first, the process of the relay can be simplified and the latency can be reduced; second, the distorted relay signal may still be valuable for the destination when an advanced signal processing scheme is used, which is an interesting further research issue. In this chapter, we assume that all nodes use the same transmission power E for transmission and relay, and the source node and the relay choose appropriate modulation types jointly to maximize the throughput under the constraint of BER, which will be discussed in Section 3.4.

In Section 3.5, we further consider the network scenario of a cellular system using the proposed DMF protocol. Users cooperate with each other in the uplink transmissions. The instantaneous SNR between any user i and j is denoted as $\gamma_{i,j} = \bar{\gamma}_i |h_{i,j}|^2$, in which $|h_{i,j}|^2$ is the amplitude of Rayleigh fading channel with the exponential dis-

tribution. $\bar{\gamma}_{i,j} = \sigma_{i,j}^2 E_i/N_0$ is the average received SNR and the pathloss parameter $\sigma_{i,j}^2$ is determined by the distance between user i and j, i.e., $\sigma_{i,j}^2 = d_{i,j}^{-\alpha}$.

3.4 BER Performance Analysis and Protocol Optimization

To maximize the spectrum efficiency without violating the BER requirement, we first investigate the BER performance of the proposed DMF protocol. Then, we formulate an optimization problem to optimize the modulation types chosen by the source and the relay, respectively.

3.4.1 Error Performance Analysis

The channel decoding process happens at the destination only, and the raw error performance without coding is our focus. We consider the average symbol error probability (SEP) of the M-QAM modulation system. Set $\beta = |h|^2$. Using Rayleigh fading channel as an example, β has an exponential distribution, defined as $p(\beta) = e^{-\beta}$. Then, the average SEP of the link between user i and user j can be expressed as

$$P_E = \int_0^\infty P_E(\beta) p(\beta) d\beta, \tag{3.4}$$

where $P_E(\beta)$ is the instantaneous SEP which is the integration of Gaussian functions. The expression of the average SEP is very complicated. To simplify it, we use the method introduced in [82], which evaluates the SEP for high average SNR cases by concentrating the error probability performance of the instantaneous SNR close to zero which triggers the majority of symbol errors. Considering the Gray coding in the system, the simple approximate expression of BER for M-QAM system is obtained as

$$\begin{aligned} P_{BER} \approx & \frac{1}{M}\left[\frac{4b}{\pi}\frac{\sqrt{M}-1}{\sqrt{M}}\left(\frac{2(M-1)}{3}\right)^d \right. \\ & \left.\left(\int_0^{\frac{\pi}{2}} \sin^{2d}\theta \mathrm{d}\theta - \frac{\sqrt{M}-1}{\sqrt{M}}\int_0^{\frac{\pi}{4}} \sin^{2d}\theta \mathrm{d}\theta\right)\right](\bar{\gamma})^{-1} \end{aligned} \tag{3.5}$$

where the fading channel parameters b and d are both equal to one for Rayleigh fading channel [82].

To further simplify the above BER expression so the optimization decision of mod-

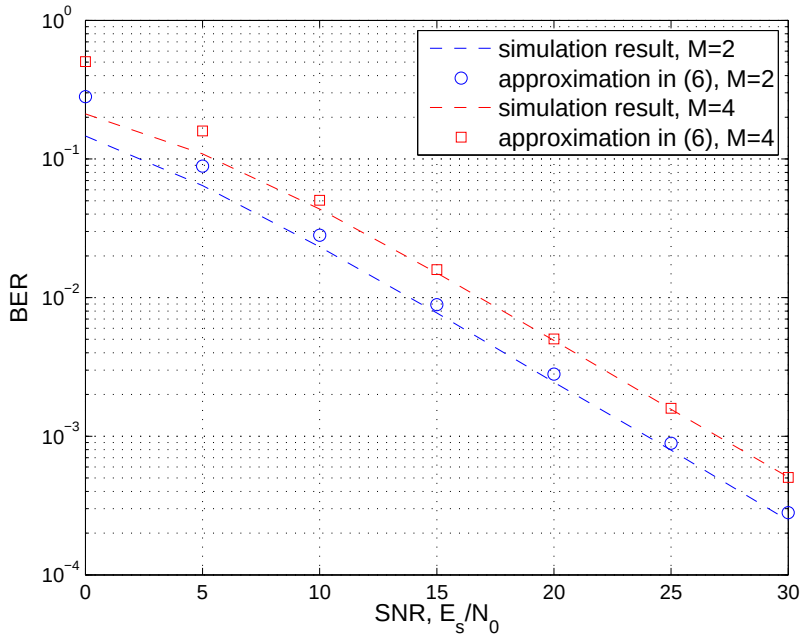

Figure 3.2: Exact vs approximate expression of BER for Rayleigh fading channel.

ulation schemes can be done in real time, we use MATLAB to obtain the polynomial approximation function for P_{BER}:

$$P_{BER} \approx a(1) \exp\left(a(2) \cdot k\right) (\bar{\gamma})^{-1} \tag{3.6}$$

where $a = [0.157,\ 0.583]$ is the approximation vector measured from numerical curve fitting method, and $k = \log_2(M)$ is the number of bits represented by a symbol with the M-QAM modulation scheme. As shown in Fig. 3.2, the simulation results and the approximated fitting curve in (3.6) match well with each other.

3.4.2 Throughput Optimization

The throughput with the adaptive modulation scheme is determined by the modulation type used. The optimization problem to maximize the spectrum efficiency or total throughput for the DMF cooperative system with adaptive modulation under the constraint of the received BER requirement $P_{e,max}$ is formulated as

$$\begin{aligned} \max_{k_s,k_r} \quad & R_{total}(k_s, k_r) \\ s.t.: \quad & P_{BER} \leq P_{e,max} \end{aligned}$$

where R_{total} is the total throughput which is determined by the modulation types chosen by the source and the relay, k_s and k_r, respectively.

Since the source and the relay may transmit signal in different constellation size, the transmission time $T_i(k_i)$ of each hop can be written as $L/(k_i W)$, where L (bit) is the frame size and W (symbol/sec) is the symbol rate. Without loss of generality, we assume that symbol rate W and frame size L are constant. Therefore, the total throughput is $R = \frac{1}{T_s+T_r}$ bps. As for the cooperative system shown in Fig. 3.1, the information has two independent copies at D which could improve the BER performance. However, since the modulation types through direct and relay links are different, traditional maximal ratio combining (MRC) receiver no longer works here. We choose selection combining (SC) where the error bit will only occur when the two copies were wrong at the destination. The performance of the DMF scheme can be further improved if more advanced signal processing technique is used to better utilize the two copies than the SC, which can be a future research issue.

Given the SC scheme used, the upper bound BER at the destination that the error bit will only happen when both paths are in error, can be written as

$$\begin{aligned} P_{BER}^{upper} &= P_e^{direct} \cdot P_e^{relay} \\ &= P_e^{sd}\left[1-(1-P_e^{sr})(1-P_e^{rd})\right] \\ &= P_e^{sd}P_e^{sr} + P_e^{sd}P_e^{rd} - P_e^{sd}P_e^{sr}P_e^{rd}, \end{aligned} \tag{3.7}$$

where P_e^{sd}, P_e^{sr}, and P_e^{rd} are the bit error probabilities for the channels from S to D, S to R, and R to D, respectively.

Thus, the optimization problem can be formulated as follows

Problem 1. *(P1)*

$$\begin{aligned} \max_{k_s,k_r} \quad & \left(\frac{1}{T_s(k_s)+T_r(k_r)}\right) \\ s.t. \quad & P_e^{sd}P_e^{sr} + P_e^{sd}P_e^{rd} - P_e^{sd}P_e^{sr}P_e^{rd} \le P_{\max} \end{aligned}$$

The objective is to maximize the throughput of the cooperative system which is determined by jointly selected modulation types at the source and the relay, i.e. k_s and k_r. For the nonlinear optimization problem above, there is no simple close-form expression for the optimal modulation selection k_r and k_s. Although (P1) is a nonlinear and complicated problem, the number of candidates for the M-QAM modulation is limited. In a practical system, the integer value k as the number of

bits per symbol normally is within a small range, e.g., [1, 8] so the group size of all potential combinations is $8^2 = 64$ only. Therefore, a simple searching algorithm can solve the above optimization problem and find the optimal modulation scheme [k_s, k_r] in real time.

If in the situation that both the source and the relay nodes should use the same modulation type for transmission, we can add one more constraint $k_s = k_r$ into the optimization problem (P1), and obtain the optimal modulation type.

3.5 Network Matching

In a cellular system, we intend to group users appropriately to maximize the whole network throughput. In this section, we will discuss the matching algorithm for this purpose.

Assume that there are n mobile users (nodes) in a cell, and they randomly locate in the cell which is covered by a base station (BS) in the center of the cell, as shown in Fig. 3.3. We assume that two groups of nodes exist in the network: source nodes with data to transmit to the BS in the upper link, and idle ones. A number of nodes are willing to cooperate or act as a relay to enhance the whole system performance. We assume that there exists incentive schemes for the ones contributing to the improved system performance by using their own energy, which is out of the scope of this chapter. If a source node can find a relay to improve the throughput, the two nodes will use the DMF protocol for cooperation; otherwise, the source node will just transmit directly to the BS using the highest modulation scheme under the BER constraint. The problem is that two or more source nodes may prefer the same node to serve as the relay. Since a node may have the capacity to serve as the relay for a single source node only, an appropriate matching algorithm is needed to optimize the whole system performance when such confliction occurs.

The design of the matching algorithm directly affects the whole network performance, and the algorithm should be simple enough to match users in real time. Our observation is that assigning a good relay to the source node with the worst channel condition can benefit the whole network throughput most. Therefore, we use a worst link first (WLF) matching algorithm which assigns a higher priority to the source node with a worse channel condition to choose its relay. The WLF matching algorithm was first proposed in [53], which has one order lower computational complexity than the optimal maximum weighted matching algorithm, yet with very close perfor-

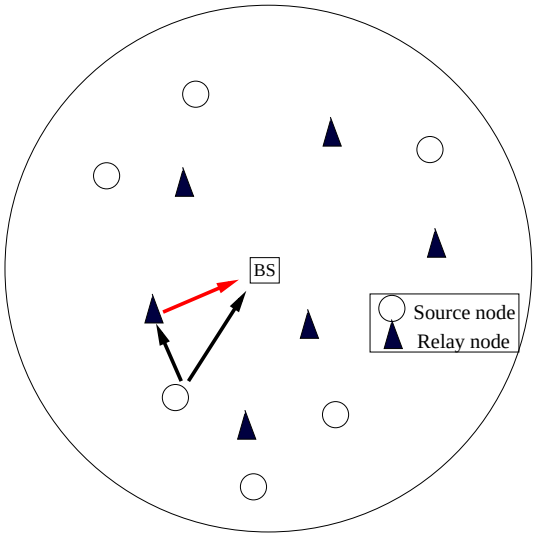

Figure 3.3: Network cooperative system with users are randomly around the BS.

mance to the optimal one. We revise the WLF algorithm according to our context, which is described in Algorithm 1.

In short, based on the location information of all nodes $\vec{r}$, the source node with the worst uplink channel u_i will be the first one to choose the relay. Then, we group the source node u_i and the chosen relay u_{j^*} (if such one exists) and remove them from the source node set U_{source} and relay candidate set U_{relay}, respectively. This procedure repeats till all source nodes have been considered. If a source node cannot find any relay who can help to improve the throughput, the source node just transmits directly to the destination using the adaptive modulation scheme.

3.6 Performance Evaluation

In this section, results from Monte Carlo simulations are presented to evaluate the performance of various cooperative and non-cooperative protocols. Using the proposed DMF cooperative scheme, the relay node only demodulates the received signal without decoding. We assume $\bar{\gamma}_{ref}$ is the reference SNR for nodes at the boundary of the cell, so they have the lowest SNR among all nodes. The average SNR $\bar{\gamma}_i$ of node i will be obtained according to the relative distance, i.e., $\bar{\gamma}_i = \left(\frac{d_i}{d_{ref}}\right)^{-\alpha} \bar{\gamma}_{ref}$, while d_i and d_{ref} is the distance from node i and the boundary of the cell to the BS, respectively. The raw BER requirement at the destination is set as $P_{max} = 10^{-3}$. The pathloss exponent α typically has the range between 2 to 6. Here, we set α to 2, and we can achieve even higher cooperation gain if a higher value of α is used.

Algorithm 1 Worst Link First Algorithm

Require: location $\vec{r}$
Ensure: optimal U_{pair}

for U_{source} is not empty **do**
  find the user $u_i \in U_{source}$ with the worst channel condition;
  calculate the throughput for direct transmission $R_{direct,i}$
  $R\_MAX = 0$
  for each $u_j \in U_{relay}$ **do**
    calculate the cooperative throughput $R_{i,j}$;
    if $(R_{i,j} < R\_MAX)$ **then**
      $j^* = j$;
    end if
  end for
  if $(R\_MAX > R_{direct,i})$ **then**
    remove u_{j^*} from U_{relay};
    add the pair $[u_i, u_{j^*}]$ into U_pair;
  end if
  remove u_i from U_{source};
end for

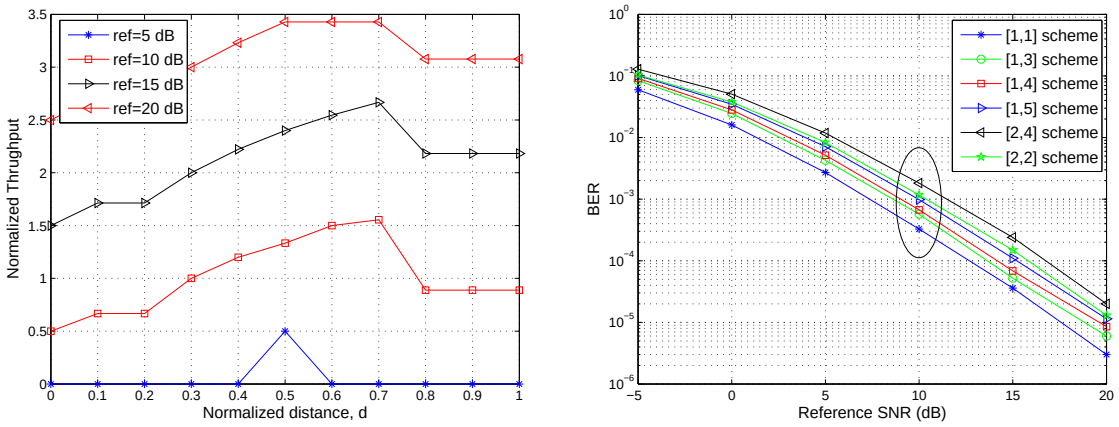

(a) Throughput for different location.

(b) BER performance, $d_{sr} = 0.7$

Figure 3.4: Performance results for one dimension structure

3.6.1 Cooperation Gain and BER Performance for Single Source

In this subsection, we consider a simple system with one source node, one relay node and the destination located on a line. The source node is located at the origin, and we adjust the position of the relay along the line between the source and the destination. Given the location of the relay, the optimal modulation schemes for both the source and the relay can be obtained, using the solution to the optimization problem (P1).

In Fig. 3.4(a), the x-axis represents the relative location of the relay, where the distance of the source and destination is normalized to one. Different curves correspond to different received SNR from the source to the destination. The y-axis represents the normalized throughput (normalized by assuming symbol rate is 1 symbol/sec). The normalized throughput is proportional to the number of bits that can be delivered to the destination per second. Zero throughput means that the cooperative system cannot ensure the minimum BER requirement, no matter which modulation types are used. As shown in the figure, the best relay location for a given source/destination pair is around 0.5 to 0.7, i.e., the d_{sr} is about 0.5 to 0.7 of d_{sd}. The results in the figure can be an important guideline for fast searching good relays, e.g., used by the WLF matching algorithm. Taking $\bar{\gamma} = 10dB$ as an example, $d_{sr} = 0.7$ is the best location with the modulation schemes of $[k_s, k_r] = [1, 4]$, i.e., the source uses BPSK and the relay uses 16-QAM.

Next, we further obtain the BER results from simulations for various modulation schemes to verify whether the suggested modulations obtained from the optimization

algorithm can ensure the BER performance or not. Rayleigh fading channels are simulated and the bits cannot be correctly decoded by the destination are counted. The reference SNR is 10 dB and $d_{sr} = 0.7$. The optimization algorithm solution is to use $[k_s, k_r] = [1, 4]$ for modulation. From Fig. 3.4(b), not only scheme $[1, 4]$ can satisfy the BER constraint, but also $[1, 5]$ can achive to the BER slightly below 10^{-3}, so we can maximize the throughput by using $[1, 5]$ instead. The reason that the solution from the optimization problem (P1) is slightly more conservative is due to the BER approximation in (3.5), which is an upper-bound for BER. Nevertheless, the approximation is reasonably close to the real value, especially with higher SNR.

3.6.2 Network Throughput Evaluation

Next, we evaluate the performance of a network with N_s source nodes and N_r relay candidates which are randomly located in a cell. We assume $N_s = N_r$ equal to half of the total number of nodes in the cell. The WLF matching algorithm is used to group the source nodes and the relay nodes. If a source node cannot find any relay node that can further improve the throughput, the source node just transmits directly to the BS.

We compare four cases: the proposed DMF protocol with joint optimized modulation schemes at the source and the relay, the DMF protocol with optimized modulation while $k_s = k_r$ (both the source and the relay using the same modulation), the pure relay strategy (the destination only relies on the received signal from the relay for decoding), and the direct transmission (the source node directly sends information to the destination without any relay.) In the direct transmission case, since there is only one user participating for transmission, the transmission power at the source is doubled to be fair to compare. Both the pure relay and direct transmission schemes use the AMC, i.e., the sender always chooses the highest modulation scheme under the BER constraint.

In Fig. 3.5(a), we change the total number of users in the network from 10 to 30, which covers both the low density and high density cases. As shown in the figure, the proposed DMF with joint optimization always outperforms the DMF scheme with the constraint of $k_s = k_r$, and both of them can achieve significant throughput gain compare to the pure relay and direct transmission schemes. In addition, the cooperation gain increases w.r.t. the number of users. This is because the source nodes have better chance to find ideal relays in a higher dense network.

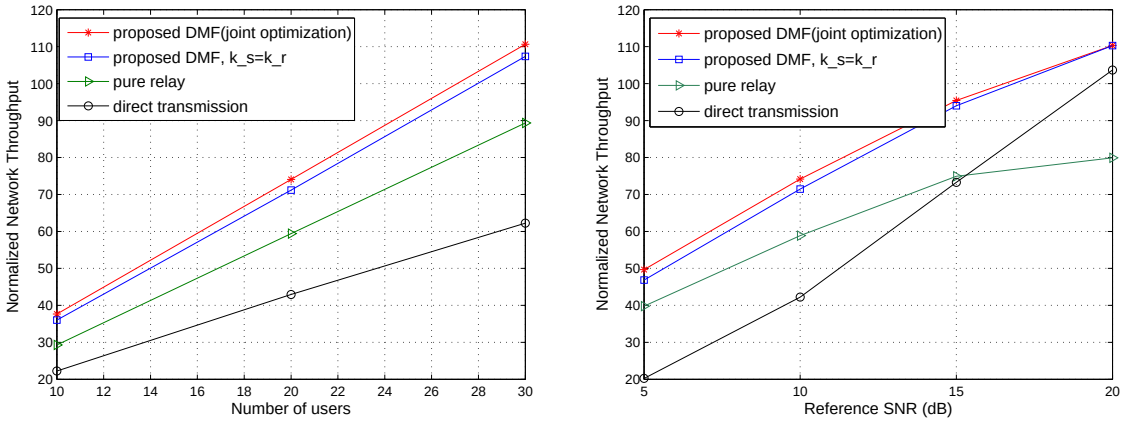

(a) Network throughput, $\bar{\gamma}_{ref} = 10dB$

(b) Network throughput, 20nodes.

Figure 3.5: Network performance results

In Fig. 3.5(b), we fix the number of nodes and change the cell size so the reference SNR varies from 5 dB to 20 dB. Again, the proposed cooperative scheme can achieve 5% to 150% throughput gain, compared with the direct transmission scheme. The gain becomes less significant when the reference SNR reaches 20 dB, as the majority of source nodes can directly transmit to the destination with the highest modulation considered, 64-QAM. Overall, the proposed cooperative schemes can always achieve cooperation gain and outperform the pure relay (which even becomes less favorable than direct transmission when the reference SNR is above 15 dB).

3.7 Summary

In this chapter, we have proposed the Demodulation-and-Forward user cooperation protocol, which can flexibly choose the modulation types for the source node and the relay node to maximize throughput with the BER constraint. Closed-form BER expression with the proposed DMF protocol has been derived and validated using Monte Carlo simulations. We have further proposed to use a WLF matching algorithm to group users for cooperation in a network, aiming to maximize the whole network throughput. Simulation results have been given, which demonstrate that the proposed protocol can effectively improve network throughput by taking the advantage of both adaptive modulation and cooperation.

3.8 Symbol List

The symbol list is shown in Table 3.1.

Table 3.1: Notations for Chapter 3

Symbol	Explanation
x, $\hat{x}_r$	transmitted signal, demodulated signal
h_i	channel gain for i_{th} channel
$\gamma_{i,j}$	instantaneous SNR between any user i and j
$\bar{\gamma} = \sigma^2 E_i / N_0$	average received SNR
σ^2	pathloss parameter
P_E	average symbol error probability (SEP)
$P_{e,max}$	constraint of the received BER requirement
R_{total}	total throughput for optimization
L (bit)	transmission frame size
W (symbol/sec)	transmission symbol rate
$\vec{r}$	location information of all nodes
u_i	source node with the worst uplink channel
U_{source}	source node set
U_{relay}	relay candidate set

Chapter 4

Soft Value Combining for User Cooperative Systems with Adaptive Modulation

4.1 Motivation and Contributions

Wireless cooperative communication can exploit the spatial diversity to improve the efficiency and coverage of wireless communication systems [38, 51, 52]. Two well-known cooperative systems, AF and DF, are discussed in Chapter 1. Another key technology to further improve the spectrum efficiency is adaptive modulation and coding (AMC), which can adjust the modulation to optimize the data rate according to the channel conditions [74, 42]. To utilize AMC in cooperative systems, demodulate-and-forward (DMF), where the relay node demodulates the signal and forwards it using an independent modulation scheme configured according to the channel quality, has been investigated in Chapter 3. As the complexity of DF is high for relay node, in this chapter, we focus on AF and DMF systems only.

One of the important open issues for AF and DMF cooperative systems is the combining scheme at the receiver. For AF systems, the optimal signal combining scheme is the maximal ratio combining (MRC), and the modulation can be configured considering the SNRs of all the links involved, referred as AF-MRC [36]. However, the strict synchronization requirement causes a complex hardware structure for AF-MRC. For DMF system, as it is difficult if not impossible to directly combine signals with different modulation schemes due to the distinct waveform structures, MRC is

not applicable [23].

In this chapter, we propose to use the soft values of each bit to devise a simple and effective combining scheme, which can be applied for both AF and DMF cooperative systems. Different from the existing work, the soft value defined, related to the confidence of the PHY layer in demodulating the bit, can be applied for arbitrary modulation and constellation mapping. The main contributions of this chapter are :

1. We develop an analytical framework to quantify the theoretical performance of soft value combining based on both the AWGN and fading channel environments, for general modulation schemes.

2. We propose the soft-value combining (SVC) scheme for AF and DMF cooperative systems considering the error propagation effect. In the AF system, the SVC scheme can achieve close-to-optimal performance. In the DMF system, the probability of error recovery by SVC has been analyzed.

3. We propose to maximize the spectrum and energy efficiency of DMF systems, using SVC and optimal modulation configuration. Analytical and simulation results show that the proposed solution can substantially outperform the existing AF cooperative systems and multi-hop relay systems.

4. We design a OFDM-based transceiver system with soft values from the demodulation module in GNU Radio/USRP2 platform. The experimental result has verified the effectiveness of soft value module with easy implementation, and the performance improvement with SVC.

4.2 Related Work

Many existing approaches took the advantage of spatial diversity of wireless communications to improve system performance [34]. By combining symbols from different copies, MRC, Selection Combining (SC), and Equal Gain Combining (EGC) can improve system throughput with a higher effective received SNR. Rate adaptive transmission in AF cooperative systems was also discussed [60]. By adjusting the modulation scheme used by both the source and relay nodes, the performance is limited by the worst link in the cooperative system. More importantly, the tight synchronization requirement makes practical implementation of the previous combining techniques difficult. In [56], the spatial diversity of multiple access points (which

are wired connected) was considered. Each packet is chopped into multiple blocks. When a packet error occurs, the receiver can resolve the corrupted packet by trying all block combinations with the assumption that each block has at least one correctly received copy by one of the APs. Its computational complexity becomes higher as the number of blocks increases.

On the other hand, confident information has been used to identify collisions or optimize the performance for error recovery protocols and bit-error detection [31, 84, 5, 37]. PPR [31] uses SoftPHY hints to detect corrupted bits without extra error detection codes, and only retransmits those bits most likely in error. Driven by SoftPHY hints from the PHY layer, SOFT [84] combines soft values associated with individual bits from multiple copies of access points (APs) in 802.11 WLANs. The soft packet forming from the corresponding soft values will be decoded in the link layer to obtain the transmitted packet. [5] proposed an automatic repeat request (ARQ) scheme with soft error detectors: instead of discarding the blocks with errors, such blocks are stored temporarily for error recovery purpose. In DMF relay systems, [37] designed a symbol selection threshold to minimize the transmission BER. The relay node will only forward the most likely correct bits to the destination, as determined by the comparison of the LLR with the designed threshold. [6] proposed soft-bit MRC (SB-MRC) to combine signals with different modulation schemes. Defining the soft value as an approximated expression of Log Likelihood Ratio (LLR), specified for M-QAM Gray labelling modulations, SB-MRC can convert signals with various M-QAM modulations into soft bits for combining. However, SB-MRC is not suitable for non-Gray labelled or non-square-QAM modulations which are also important for various applications. For example, the trellis modulation, such as bit interleaved coded modulation with iterative decoding (BECM-ID), can achieve significant BER performance improvement compared to the Gray labelling modulation and it has been widely adopted in practical communication systems [79, 58, 8]. Furthermore, [6] assumed error-free source to relay communication which also limits the application of SB-MRC in cooperative systems.

As the user cooperative system has both the single-hop direct transmission path and the multi-hop relay path which use independent modulation schemes with various constellation mappings, none of the above approaches is directly applicable, which motivates this work to fit the gap.

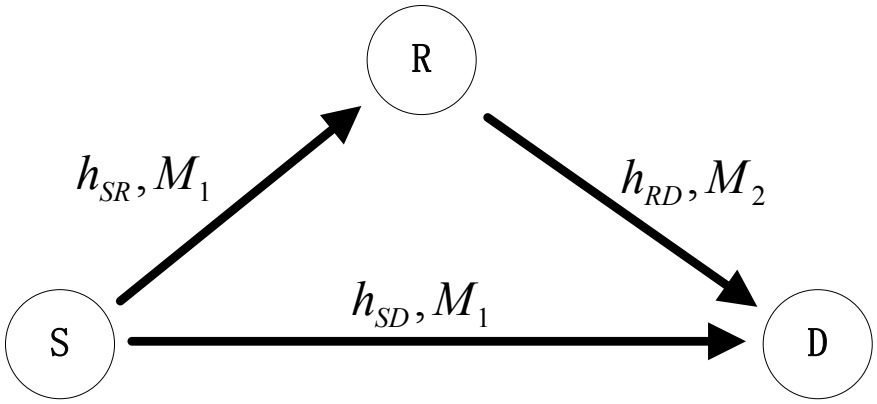

Figure 4.1: System model.

4.3 System Model and Soft Value Combining

4.3.1 System Model

We consider the user cooperative system shown in Fig. 4.1. The source node (S) communicates with the destination node (D) with the help of the relay node (R). S transmits the symbols to D in the direct communication path, and the transmissions are also received by R. R forwards the processed symbols to D. D combines both copies from the direct and relay paths to recover the information. A notation list is given in the Symbol List in Section 4.9 for easy reference.

To avoid collisions at R, we assume that a frame transmission takes two time slots. In each slot, the message will be transmitted in a frame whose header contains the information of the type of the modulation used. In the first time slot, S broadcasts the modulated symbol x to R and D using M_i Quadrature Amplitude Modulation (M_i-QAM). Each M_i-QAM symbol $x_{i,j}$ contains $\log_2(M_i) = m_i$ bits (named $b_1, b_2, ..., b_{m_i}$). Without loss of generality, we assume that the noise terms of link SR and SD, n_{SR} and n_{SD}, have equal variances σ_0^2, and are Gaussian distributed $\mathcal{CN}(0, \sigma_0^2)$. All the links, namely h_{SR}, h_{SD} and h_{RD}, are assumed to subject to i.i.d. Rayleigh fading. The received symbol by R and D are y_{SR} and y_{SD}, respectively, given by $y_{SR} = h_{SR}x + n_{SR}$ and $y_{SD} = h_{SD}x + n_{SD}$.

During the second time slot, the processed symbol, denoted as x_{RD}, is subsequently transmitted to D with the same average power. The duration of the second time slot may be different from that of the first slot if different modulations are used by S and R. The received symbol at D is $y_{RD} = h_{RD}x_{RD} + n_{RD}$, where $n_{RD} \sim \mathcal{CN}(0, \sigma_0^2)$ is the noise at D.

For the AF cooperative system, the received symbols are amplified and forwarded by R to D with a fixed gain G_r. Denote $\bar{\gamma}_i, (i = SR, RD, SD)$ as the average received SNR of link i. Following the definition in [59], to maintain a constant average power of output, the fixed gain can be given as $G_r = (E[|y_{SR}|^2])-1 = ((\bar{\gamma}_{SR} + 1)\sigma_0^2)^{-1}$. In this case, the instantaneous end-to-end SNR of the relay path and the direct path can be expressed, respectively, as

$$\gamma_R = \frac{\gamma_{SR}\gamma_{RD}}{\bar{\gamma}_{SR} + \gamma_{RD} + 1}, \tag{4.1}$$

$$\gamma_D = \gamma_{SD}. \tag{4.2}$$

For the DMF cooperative system, instead of transmitting with the same modulation type as the direct transmission, R first demodulates the received signal with a modulation type M_1 and transmits it in a separate modulation type M_2. The processed symbols x_{RD} will have the same average power with probably a different modulation type based on the SNR of RD only, so DMF can typically achieve a higher throughput than AF.

For both systems, two copies of the transmitted signals are received by D through independent channels, which can lead to a diversity gain. To exploit such diversity gain, soft value information for each bit can be employed during the combining at D, as discussed in the following subsections.

4.3.2 Soft Value

Soft value indicates how confident the receiver is on the demodulated signal, which is assigned to each bit with the smaller absolute value representing less confidence. Let $x_{i,j}^{M_i}$ denote the transmitted symbol from node i to node j with M_i-QAM modulation, which contains the bit sequence $b_k, (k = 1, .., m_i)$, where $m_i = \log_2(M_i)$. y denotes the corresponding received signal. Similar to the soft outputs in a Viterbi decoder [21], a maximum likelihood (ML) decision making scheme is implemented at the receiver. When the information bits have equal probability, the ML decoder is equal to the

maximum a posteriori probability (MAP) decoder. Then, the soft value for each bit is defined as the LLR [68]:

$$s_k = \log \frac{Pr(b_k = 1|y, h)}{Pr(b_k = 0|y, h)}. \tag{4.3}$$

Given the channel fading is independent of the transmitted symbols and $f_{y|h,x}\{y|h, x = \alpha\} = \frac{1}{\sqrt{2\pi}\sigma} \exp(-\frac{||y-h x||^2}{2\sigma^2})$, (4.3) can be expressed as

$$s_k = \log \frac{\sum\limits_{\alpha\in\Theta_k} f_{y|h,x}\{y|h, x = \alpha\}}{\sum\limits_{\beta\in\Psi_k} f_{y|h,x}\{y|h, x = \beta\}} = \log \frac{\sum\limits_{\alpha\in\Theta_k} \frac{1}{\sqrt{2\pi}\sigma} \exp(-\frac{||y-h\alpha||^2}{2\sigma^2})}{\sum\limits_{\beta\in\Psi_k} \frac{1}{\sqrt{2\pi}\sigma} \exp(-\frac{||y-h\beta||^2}{2\sigma^2})}, \tag{4.4}$$

where Θ_k (Ψ_k) is the set of constellation points whose k-th bit (b_k) is one (zero). As the log and exp operations are complicated to implement, the MAX-LOG-MAP is used to simplify (4.4) as

$$s_k \approx \frac{1}{2\sigma^2} \left\{ \min_{\beta\in\Psi_k} ||y - h\beta||^2 - \min_{\alpha\in\Theta_k} ||y - h\alpha||^2 \right\}. \tag{4.5}$$

Define $z \triangleq y/h = x + n/h = s + \hat{n}$, where $\hat{n}$ is a complex Gaussian R.V. $\sim \mathcal{CN}(0, \sigma^2/||h||^2)$. Normalizing the LLR s_k by $2/\sigma^2$ and applying the above z, we have

$$\begin{aligned} s_k &= \frac{||h||^2}{4} \left\{ \min_{\beta\in\Psi_k} ||z - \beta||^2 - \min_{\alpha\in\Theta_k} ||z - \alpha||^2 \right\} \\ &= \frac{||h||^2}{4} \left\{ \min_{\beta\in\Psi_k} \left[||\beta||^2 - 2z_I\beta_I - 2z_Q\beta_Q\right] - \min_{\alpha\in\Theta_k} \left[||\alpha||^2 - 2z_I\alpha_I - 2z_Q\alpha_Q\right] \right\} \end{aligned} \tag{4.6}$$

where $z = z_I + jz_Q, \alpha = \alpha_I + j\alpha_Q$ and $\beta = \beta_I + j\beta_Q$.

Gray Mapping

Given the structure of M_i-QAM with Gray mapping shown in Fig. 4.2, we note that the closest constellation points to the received symbol in different sets, Ψ_k or Θ_k, always on the same row or column, due to the symmetry of Gray coding. Thus, taking 16-QAM as example, the LLRs for $b_k(k = 1, 2, 3, 4)$ with Gray mapping can be simplified by interval matrix $\mathbf{S}_k$ and boundary matrix $\mathbf{U}_k$

$$s_k^{(16)} = \mathbf{S}_k \mathbf{U}_k, \tag{4.7}$$

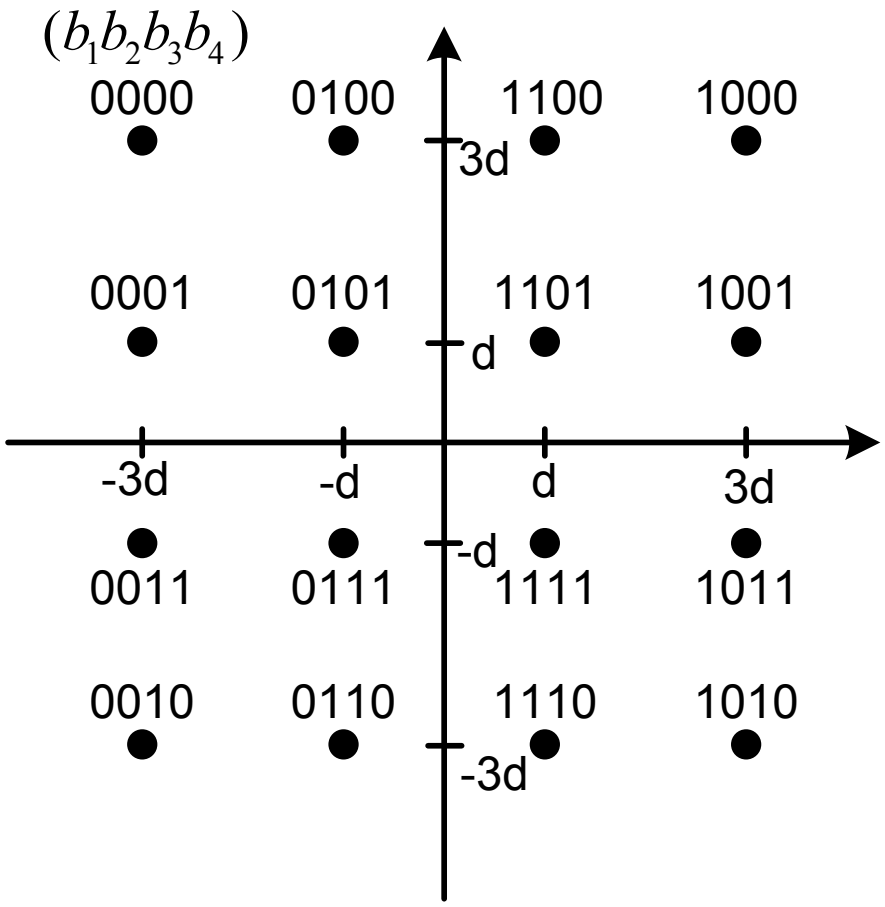

Figure 4.2: 16-QAM constellation Gray mapping.

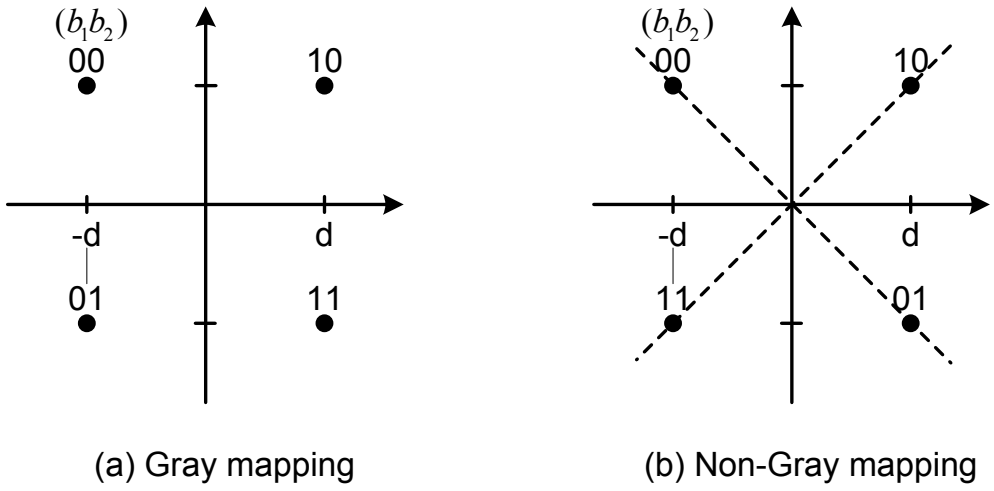

Figure 4.3: QPSK constellation mapping: Gray, non-Gray.

$$\text{where } \mathbf{S}_k = \begin{cases} \left[||h||^2 z_I d, -2||h||^2 d(d-z_I), 2||h||^2 d(d+z_I)\right], & k=1, \\ \left[||h||^2 d\left\{2d-z_I\right\}, ||h||^2 d\left\{2d+z_I\right\}\right], & k=2, \\ \left[-||h||^2 z_Q d, 2||h||^2 d(d-z_Q), -2||h||^2 d(d+z_Q)\right], & k=3, \\ \left[||h||^2 d\left\{2d-z_Q\right\}, ||h||^2 d\left\{2d+z_Q\right\}\right], & k=4, \end{cases} \tag{4.8}$$

$$\mathbf{U}_k = \begin{cases} \left[U(2d-|z_I|), U(z_I-2d), U(-2d-z_I)\right]^T, & k=1, \\ \left[U(z_I), U(-z_I)\right]^T, & k=2, \\ \left[U(2d-|z_Q|), U(z_Q-2d), U(-2d-z_Q)\right]^T, & k=3, \\ \left[U(z_Q), U(-z_Q)\right]^T, & k=4, \end{cases} \tag{4.9}$$

$2d$ is the minimum distance between any two constellation points, and $U(.)$ is the unit step function.

Soft Value for General Modulation and Mapping

Compared with the previous work [6], the soft values we derived based on the above approach are applicable not only for Gray labelled M-QAM, but also for other non-Gray or other modulation types. A QPSK symbol labelled by either Gray-labeling or the non-Gray-labeling are shown in Figs. 4.3(a) and (b), respectively. The LLRs in (4.6) for QPSK in Fig.4.3(a) can be represented with $\beta = -d, \alpha = d$ for the first bit

and $\beta = jd, \alpha = -jd$ for the second bit, i.e., $s_1^{(4)} = ||h||^2 z_I d$ and $s_2^{(4)} = -||h||^2 z_Q d$.

For the non-Gray labeling QPSK in Fig. 4.3(b), we can observe that the received symbols in the same region between the dash lines will share the same α and β for the first bit. The soft value for the first bit $s_1^{(4)}$ can be represented as

$$s_1^{(4)} = \begin{cases} ||h||^2 z_I d, & z_Q > 0, z_Q > |z_I| \\ -||h||^2 z_Q d, & z_I < 0, -z_I < |z_Q| \\ -||h||^2 z_I d, & z_Q < 0, -z_Q > |z_I| \\ ||h||^2 z_Q d, & z_I > 0, z_I < |z_Q| \end{cases} \tag{4.10}$$

For the second bit, the two constellation symbols in Θ_2 and Ψ_2 having the closet distance to the received symbol satisfy the condition $\alpha_I = \beta_I$. Hence the soft value for the second bit is $s_2^{(4)} = -||h||^2 z_Q d$. A similar procedure can be applied to obtain the soft value for other modulation and constellation mappings.

Practical Implementation Discussion

To limit the memory usage and computation cost, we quantize the soft value to a few bits. As shown in the simulation results in Section 2.6, five bits are sufficient to represent the soft value with negligible performance loss due to the quantization error. This is in contrast to other diversity combining technique, such as MRC, which requires a large memory space to store and process the received waveform. For instance, for two-branch MRC, at least eight multipliers with complex arithmetic operations and strict synchronization module are needed to generate co-phased combining signals [35], while our scheme only requires several adders with much smaller size for the soft value calculation. Consequently, the proposed soft value combining is simple and practical to implement.

4.4 BER Analysis of Soft Value Combining

In this section, we study how to combine the soft values from multiple received copies to maximize the chance to recover the original information successfully. Then the BER derivation for SVC of two signals with different modulation schemes are given.

4.4.1 Soft Value Combining

From the definition of soft value in Section 4.3.2, the combined soft value of two received copies is $\bar{s}_k = w_1 s_{1,k}^{(M_1)} + w_2 s_{2,k}^{(M_2)}$, where $w_i, i = 1, 2$ is the combining weight aiming to maximize the received SNR. $s_{i,k}^{(M_i)}$ is the soft value for the k-th bit mapping from the i-th path signal with modulation type M_i. By applying Schwartz inequality [73] and the soft value definition in (4.6), the maximal received SNR after combining can be obtained as

$$(\bar{s}_k)_{max} = \sum_{i=1}^{2} s_{i,k}^{(M_i)}, \text{ with } w_i = 1. \tag{4.11}$$

As discussed in Section 4.3.2, soft value $s_{i,k}$ is defined on the likelihood function, which has the decision threshold of 0. Given the above combined weight w_i, the optimal decision rule for the decoder of $\bar{s}_k$ is to decide the output bits based on the threshold of 0, given by

$$\hat{b}_k = \begin{cases} 1 & \text{if } \bar{s}_k > 0, \\ 0 & \text{if } \bar{s}_k < 0, \end{cases} \tag{4.12}$$

where $\hat{b}_k$ is the output from the decoder at the receiver. In the following, we will omit the subscript k from $s_{i,k}^{(M_i)}$ in the SVC for the simplicity of notation.

4.4.2 BER Derivation of 2-Branch Soft Value Combining

Assume that the same source bit stream has been modulated by M_1-QAM and M_2-QAM modulation schemes, where bits $(b_{1,1}, b_{1,2}, ..., b_{1,m_1})$ and $(b_{2,1}, b_{2,2}, ..., b_{2,m_1})$ are mapped to the complex symbol $x_1 = x_{1I} + jx_{1Q}$ and $x_2 = x_{2I} + jx_{2Q}$, respectively. Thus, the received signals can be written as $y_i = h_i x_i + n_i$, where $h_i, i = 1, 2$ are the complex fading channel gains with unity energy. $y_i (i = 1, 2)$ are the received signals, and the corresponding additive white Gaussian noises are $n_i \sim \mathcal{CN}(0, \sigma_0^2)$.

The error probability of the combined signal for bit b_k, $\Pr\{e, b_k\}$, can be given as

$$\Pr\{e, b_k\} = (\Pr\{e|b_k = 1\} + \Pr\{e|b_k = 0\})/2. \tag{4.13}$$

We have

$$\Pr\{e|b_k = c\} = \sum_{j=1}^{L} \Pr\{e, b_k = c|A_{k,c,j}\}\Pr\{A_{k,c,j}\}, \quad \text{for } k = 1, 2, ..., \max(m_1, m_2) \tag{4.14}$$

and $A_{k,c} = \{A_{k,c,j}, j = 1, 2, ...L\}$ is the set of events that contains all of the possible transmitted symbols for signal y_i with the length of L, when the k-th bit equals c. When $c = 1$, the element of $A_{k,1}$ is $A_{k,1,j} = \{x_1 = D_{1,j} \in \Theta_{1,k}, x_2 = D_{2,j} \in \Theta_{2,k}\}$, where $\Theta_{i,k}$ is the set of states for signal y_i whose k-th bits is 1. $A_{k,0,j} = \{x_1 = D_{1,j} \in \Psi_{1,k}, x_2 = D_{2,j} \in \Psi_{2,k}\}$, where $\Psi_{i,k}$ is the set of states of signal y_i whose k-th bits is 0.

When $c = 1$ and under the condition of event $A_{k,1,j}$, the error probability of $b_k = 1$ is

$$\begin{aligned} \Pr\{e, b_k = 1|A_{k,1,j}\} &= \Pr\{s_1(n_1) + s_2(n_2) < 0|A_{k,1,j}\} \\ &= \Pr\{n_1 \in \mathbf{U}_k, n_2 > \mathbf{V}_k|A_{k,1,j}\} \end{aligned} \tag{4.15}$$

where $\mathbf{V}_k = \{n_2 = f(n_1)|n_1 \in \mathbf{U}_k\}$, $f(n_1)$ is the remapping function by solving $s_1(n_1) + s_2(n_2) = 0$, and $\mathbf{U}_k$ is the boundary matrix as described in (4.9). Since $n_i, i = 1, 2$ are complex Gaussian noises, (4.15) can be written as

$$\Pr\{e, b_k = 1|A_{k,1,j}\} = \sum_{i=1}^{N_{b_k}} \int_{n_1 \in \mathbf{U}_{k,i}} \frac{e^{-n_1}}{\sqrt{\pi}} Q(\mathbf{V}_{k,i}) dn_1, \tag{4.16}$$

where N_{b_k} is the number of definition intervals for s_k, which equals the length of vector $\mathbf{U}_k$.

Since each bit has the same transmission probability, the average BER of SVC of M_1-QAM and M_2-QAM can be obtained as

$$\Pr\{e, SVC_{M_1}^{M_2}\} = \frac{1}{K} \sum_{k}^{K} \Pr\{e, b_k\}, \quad \text{where } K = \max\{m_1, m_2\}. \tag{4.17}$$

To further illustrate the above results, we use the following SVC of 16-QAM and BPSK signals as an example, with $M_1 = 16$ and $M_2 = 2$. We first consider the error probability of the combined bit b_1, $\Pr\{e, b_1\}$. Due to the symmetry structure of

the constellation maps and equal probability of all the transmitted symbols, we have $\Pr\{e, b_1 = 1\} = \Pr\{e, b_1 = 0\}$. Then, with $k = 1$, (4.13) can be rewritten as

$$\Pr\{e, b_1\} = \sum_{j=1}^{L} \Pr\{e, b_1 = 1 | A_{1,1,j}\}. \tag{4.18}$$

From Fig. 4.2, the decision boundary for set partitions Θ_k and Ψ_k are horizontal or vertical. Consequently, $b_1 = 1$ implies that the real part of the transmitted symbol x_1 can be either d_1 or $3d_1$, and x_2 is $-d_2$. The the length of set $A_{1,1}$ is $L = 2$, and

$$A_{1,1} = \cup_{j=1,2} A_{1,1,j} = \{(x_{1I} = d_1, x_{2I} = -d_2), (x_{1I} = 3d_1, x_{2I} = -d_2)\}. \tag{4.19}$$

Since the expression of LLR for b_1 in 16-QAM is defined on three definition intervals, i.e., $N_{b_1} = 3$, $\Pr\{e, b_1 = 1 | A_{1,1,j}\}$ in (4.18) has to be calculated piecewise. When $j = 1$, with $A_{1,1,1} = \{(x_{1I} = d_1, x_{2I} = -d_2)\}$, (4.16) can be rewritten as

$$\Pr\{e, b_1 = 1 | A_{1,1,1}\} = \sum_{i=1}^{3} \int_{n_{1I} \in \mathbf{U}_{1,i}} \frac{e^{-n_{1I}}}{\sqrt{\pi}} Q(\sqrt{2}\mathbf{V}_{1,i}) dn_{1I}, \tag{4.20}$$

where $\mathbf{U}_1 = [(-3d_1, d_1), (d_1, \infty), (-\infty, -3d_1)]$, and $\mathbf{V}_1 = \{{s_2}^{-1}\{-s_1(n_1)\} | n_1 \in \mathbf{U}_1\}$. We have

$$\begin{aligned} \mathbf{V}_1 \quad = \tfrac{1}{||h_2||^2 d_2} \quad & \left[||h_1||^2 d_1^2 + ||h_2||^2 d_2^2 + ||h_1||^2 d_1 n_{1I}, \quad ||h_2||^2 d_2^2 + 2||h_1||^2 d_1 n_{1I}, \right. \\ & \left. 4||h_1||^2 d_1^2 + ||h_2||^2 d_2^2 + 2||h_1||^2 d_1 n_{1I}\right]. \end{aligned} \tag{4.21}$$

When $j = 2$, $A_{1,1,2} = \{(s_{1I} = 3d_1, s_{2I} = -d_2)\}$, $\Pr\{e, b_1 = 1 | A_{1,1,2}\}$ can be obtained as

$$P\{e, b_1 = 1 | A_{1,1,2}\} = \sum_{i=1}^{3} \int_{n_{1I} \in \mathbf{U}_{1,i}} \frac{e^{-n_{1I}}}{\sqrt{\pi}} Q(\sqrt{2}\mathbf{V}_{1,i}) dn_{1I} \tag{4.22}$$

where $\mathbf{U}_1 = [(-5d_1, -d_1), (-d_1, \infty), (-\infty, -5d_1)]$ and

$$\begin{aligned} \mathbf{V}_1 \quad = \tfrac{1}{||h_2||^2 d_2} \quad & \left[3||h_1||^2 d_1^2 + ||h_2||^2 d_2^2 + ||h_1||^2 d_1 n_{1I}, \quad 4||h_1||^2 d_1^2 + ||h_2||^2 d_2^2 + ||h_1||^2 d_1 n_{1I}, \right. \\ & \left. 8||h_1||^2 d_1^2 + ||h_2||^2 d_2^2 + ||h_1||^2 d_1 n_{1I}\right]. \end{aligned} \tag{4.23}$$

Then taking (4.20) and (4.22) into (4.18), and using the fact that $\sigma_I^2 = \sigma_0^2/2$ and

$\frac{d_1}{\sigma_I} = \sqrt{\frac{\gamma_1}{10}}, \frac{d_2}{\sigma_I} = \sqrt{\gamma_2}$, we can obtain the overall error probability of the combined bit b_1.

For error probability of combined bit b_2, $\Pr\{e, b_2\}$, $b_2 = 1$ implies that the real part of transmitted symbol s_1 can be either d_1 or $-d_1$, and s_2 is $-d_2$. $b_1 = 0$ implies that the transmitted symbol s_1 can be either $3d_1$ or $-3d_1$, s_2 is d_2, i.e., $A_{2,1} = \{(s_{1I} = d_1, s_{2I} = -d_2), (s_{1I} = -d_1, s_{2I} = -d_2)\}$ and $A_{2,0} = \{(s_{1I} = 3d_1, s_{2I} = d_2), (s_{1I} = -3d_1, s_{2I} = d_2)\}$. $\Pr\{e, b_2\}$ can be obtained following the same procedure as that for $\Pr\{e, b_1\}$.

It can be shown that $\Pr\{e, b_1\} = \Pr\{e, b_3\}$ and $\Pr\{e, b_2\} = \Pr\{e, b_4\}$, by switching from the real to imaginary part of modulated symbols. Eventually, the bit error probability of SVC of 16-QAM and BPSK transmissions can be obtained by $\Pr\{e, SVC_{16}^2\} = \frac{1}{2}(\Pr\{e, b_1\} + \Pr\{e, b_2\})$.

4.4.3 Fading channel

We use λ_i to denote the square of the magnitude of the Rayleigh fading channel coefficient $||h_i||^2$, and it follows an exponential distribution as $f_{\lambda_i}(\lambda) = \frac{1}{\bar{\lambda}_i} e^{\frac{-\lambda}{\bar{\lambda}_i}}$, where $\bar{\lambda}_i = \mathrm{E}[||h_i||^2]$.

Plugging the distribution of the R.V.s λ_1 and λ_2 into the BER expression in (4.17), the average BER of SVC for Rayleigh channel can be obtained by

$$\overline{\Pr\{e, SVC_{M_1}^{M_2}\}} = \int_0^\infty \int_0^\infty \Pr\{e, SVC_{M_1}^{M_2}\}(\lambda_1, \lambda_2) \prod_{i=1}^{2} f_{\lambda_i}.(\lambda_i) d\lambda_1 d\lambda_2 \qquad (4.24)$$

As there are many existing approaches to approximate the Q function or to use fast algorithm to evaluate it, numerical evaluation results of (4.24) can be obtained accurately with low computational cost.

4.5 SVC for Cooperative Systems

In this section, we will apply the above soft value combining in the AF and DMF cooperative systems, and study how to optimize the modulation configuration.

4.5.1 AF System with Soft Value Combining

For the AF cooperative system with a fixed amplification gain, the instantaneous received SNRs of the relay path and the direct path based on the system model in Section 4.3 are denoted as γ_R and γ_D, respectively, which are expressed in (4.1) and (4.2). We can obtain the BER expression by replacing the variance of noise σ_1^2 and σ_2^2 in (4.17) by $1/\gamma_R$ and $1/\gamma_D$, respectively. Since the relay and direct link share the same modulation scheme, $M_1 = M_2$.

Due to the AF process, the relay path no longer follows the Rayleigh distribution. From [44], the PDF of the relay path and that of the direct path for the fixed gain AF cooperative system, f_{γ_R} and f_{γ_D}, are expressed respectively as

$$\begin{aligned} f_{\gamma_R}(\gamma) &= \frac{2}{\bar{\gamma}_{SR}} e^{\frac{\gamma}{\bar{\gamma}_{SR}}} \left[\sqrt{\frac{(\bar{\gamma}_{SR}+1)\gamma}{\bar{\gamma}_{SR}\bar{\gamma}_{RD}}} K_1\left(\sqrt{\frac{(\bar{\gamma}_{SR}+1)\gamma}{\bar{\gamma}_{SR}\bar{\gamma}_{RD}}}\right) \right. \\ &\quad \left. + \frac{\bar{\gamma}_{SR}+1}{\bar{\gamma}_{RD}} K_0\left(\sqrt{\frac{(\bar{\gamma}_{SR}+1)\gamma}{\bar{\gamma}_{SR}\bar{\gamma}_{RD}}}\right) \right], \qquad (4.25) \\ f_{\gamma_D}(\gamma) &= \frac{1}{\bar{\gamma}_D} e^{\frac{\gamma}{\bar{\gamma}_D}}, \qquad (4.26) \end{aligned}$$

where $K_v(.)$ is the v-th order modified Bessel function of the second kind [18].

Thus, the average error probability of the Rayleigh fading channel in the AF cooperative system can be derived using (4.24), with $f_{\gamma_1}(\gamma) = f_{\gamma_R}(\gamma)$ and $f_{\gamma_2}(\gamma) = f_{\gamma_D}(\gamma)$.

4.5.2 DMF System with Soft Value Combining

Consider the DMF cooperative system with three nodes, S, R and D, as shown in Fig. 4.1. R will first demodulate the received M_1 modulated signals. If the signal is demodulated incorrectly at R due to the poor channel quality of S-R, the error may be propagated to the destination. Such propagated error can result in severe performance degradation of the DMF system, especially when the S-R link is not reliable. Since the received symbol has been demodulated first, the transmitted symbol will be modulated using the corrupted bits as there is no error correction coding used by R. With SVC, the error in the relay path still has a chance to be recovered at D by the direct transmission from S to D. For instance, in Fig. 4.4, b_1 and b_2 are corrupted during the transmission from S to R. In the direct transmission path, assume that b_2

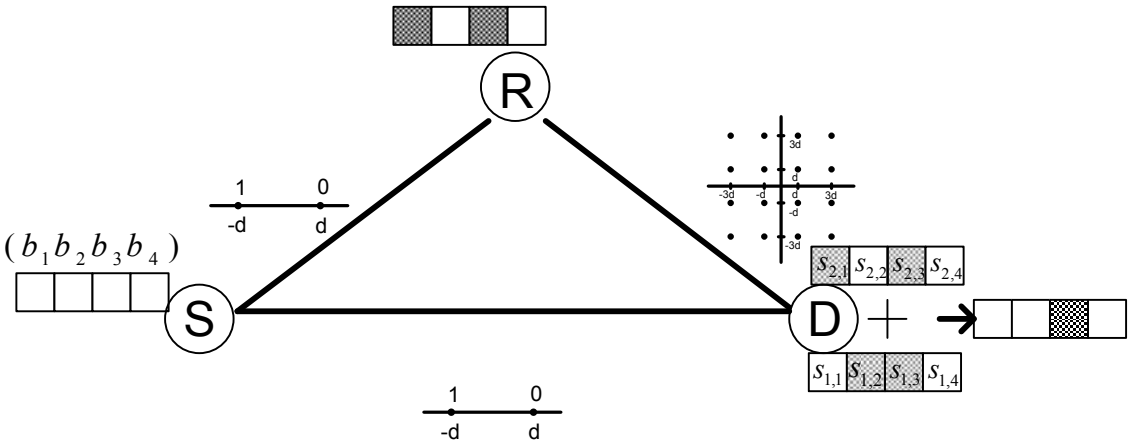

Figure 4.4: Cooperative system with error recovery.

and b_3 are corrupted, and b_2 and b_4 are correct. After SVC, it is possible that the corrupted bit b_1 has being recovered by the signal from the direct path. We will give the detailed analysis below.

Here we still use BPSK ($M_1 = 2$) and 16-QAM ($M_2 = 16$) as an example, and it can be easily extended for other modulations. First, we assume that b_1 is corrupted during the transmission from S to R. Thus, at R, source bit $b_1 = 1$ becomes the corrupted bit $b_1^{'} = 0$, and the real part of the re-modulated symbol x_1 can be either $-d_1$ or $-3d_1$, instead of d_1 or $3d_1$, and $x_{2I} = -d_2$. Hence, the set of events for bits $b_1^{'}$ being corrupted, denoted as $A_{1,c}^{\prime}$, can be expressed as $\bigcup_j \{A_{1,1,j}^{\prime}, A_{1,0,j}^{\prime}\}$, where

$$\{A_{1,1,j}, j = 1, 2\} = \{(x_{1I} = -d_1, x_{2I} = -d_2), (x_{1I} = -3d_1, x_{2I} = -d_2)\}, \quad (4.27)$$

$$\{A_{1,0,j}, j = 1, 2\} = \{(x_{1I} = d_1, x_{2I} = d_2), (x_{1I} = 3d_1, x_{2I} = d_2)\}. \quad (4.28)$$

Taking (4.27), (4.28) and (4.15) into (4.13), the error probability of $b_1^{'}$ can be obtained.

Following the same procedure, we can obtain $\Pr\{e, b_2^{'}\}$ for $b_2^{'}$. Using the property that $\Pr\{e, b_1^{'}\} = \Pr\{e, b_3^{'}\}$ and $\Pr\{e, b_2^{'}\} = \Pr\{e, b_4^{'}\}$, the BER performance of bits that are corrupted during the S-R transmission can be obtained as

$$\Pr\{e, SR^{'}\} = \frac{1}{2}(\Pr\{e, b_1^{'}\} + \Pr\{e, b_2^{'}\}). \quad (4.29)$$

Overall, the BER for the DMF cooperative system using SVC is expressed as

$$\Pr\{e, DMF_{M_1}^{M_2}\} = (1 - \Pr\{e, SR\})\Pr\{e, SVC_{M_1}^{M_2}\} + \Pr\{e, SR\}\Pr\{e, SR^{'}\}, \quad (4.30)$$

where $\Pr\{e, SR\}$ is the BER performance for the S-R transmission, which equals to $Q(\sqrt{\frac{E_s}{2N_0}})$ for BPSK, and $\Pr\{e, SVC\}$ is the BER performance for two-path SVC which is given in Section 4.4.2.

4.5.3 Optimal Modulation Configuration

Given the analytical results for AF and DMF cooperative systems with SVC, the next question is how to choose the best modulation scheme for each transmission under the constraint of BER, p_e. Denote by m_1 and m_2 the bit-per-symbol rates corresponding to the highest modulation schemes that can be supported by the first- and second-hop of the cooperative system, respectively. $P_e(m_1, m_2, P_t) \in \{\Pr\{e, AF\}, \Pr\{e, DMF\}\}$ is the overall received BER, either in AF or DMF systems. Assuming that all nodes transmit using the same power P_t and fixed bandwidth, both the spectrum efficiency measured by the number of bits transmitted per symbol duration and the energy efficiency measured by bit-enery can be maximized by solving the following optimal modulation configuration problem.

Problem 2. *(P1)*

$$\max \quad \frac{m_1 m_2}{m_1 + m_2} \quad (4.31)$$

$$\text{s.t.} \quad m_1, m_2 \in [1, 2, 4, 6] \quad (4.32)$$

$$P_e(m_1, m_2, P_t) \leq p_e \quad (4.33)$$

Since the number of candidate modulation schemes is limited (e.g., typically four M-QAM modulation schemes are used in cellular systems) and the BER results for AF and DMF system can be easily solved numerically, it is feasible to solve the optimization problem by a simple searching algorithm given in Algorithm 2 [1].

[1] In Problem P1, we only use BPSK, QPSK, 16-QAM and 64-QAM as the modulation set. If needed, other modulations, such as 8/32/128-QAM in Digital Television (DTV) system, or even 1024-QAM in microwave system, can be considered. It is anticipated that the performance of the system can be further improved with more choices of modulations.

Algorithm 2 Optimal Modulation Configuration

INPUT P_e as the required BER and P_t as the transmission power for S and R.
$R_{max} = 0$;
for all modulation schemes **do**
    calculate $p_e(m_1, m_2, P_t)$;
    if $P_e(m_1, m_2, P_t) \leq p_e$, and $\frac{m_1 m_2}{m_1+m_2} > R$ **then**
        $R = \frac{m_1 m_2}{m_1+m_2}$;
        set n equal to the index of the modulation scheme
    end if
end for
Return: R, n

4.6 Performance Evaluation

Monte Carlo simulations are conducted to verify the analytical results and investigate the performance of the proposed SVC for both AF and DMF systems. We also compare the efficiency of SVC with the existing user cooperative schemes and non-cooperative relay transmissions.

4.6.1 AF Cooperative Systems with SVC

We first compare the BER performance of the AF cooperative systems with MRC and SVC, all using BPSK. From Fig. 4.5, the BER performance of the proposed SVC (using ≥ 5 bit for each soft value) is close to MRC, the optimal combining scheme. As we mentioned in Section 4.3.2, MRC has a much higher hardware cost, the proposed SVC is more practical to implement.

Fig. 4.5 also compares the BER performance of SVC with different quantization levels. We observe that the BER performance of 5-bit quantization (1 bit for the sign and 4-bits for the magnitude of the soft value) is close enough to that of using the real soft value. From the figure, SVC with 5-bit quantization level is close to MRC and can out-perform SC by more than 2 dB when the BER threshold is $\leq 10^{-3}$.

4.6.2 DMF Systems with SVC

We next study the SVC performance when combining two copies of signals from two single-hop paths. The received SNR for the second path is set as $\gamma_2 = 4$ dB with BPSK modulation, and signals from the first path is modulated by 16-QAM. Fig. 4.6 compares the BER performance of the proposed SVC scheme and that of each individual path, where the x-axis represents the average received SNR in dB for the first path. From the figure, first, we observe that the simulation results match well with the analytical ones. Second, SVC can result in the BER much lower than that of either path, and close to the lower bound (the dashed curve). The lower bound is obtained by the multiplication of the BERs of the two paths. The performance gain of SVC is from the spatial diversity of two independent paths.

Fig. 4.7 compares the average BER performance of the three-node cooperative system shown in Fig. 4.1 w.r.t. the received SNR of the 2nd-hop (R-D). BPSK ($M_1 = 1$) is used by the source node, with $\gamma_{SR} = 7$ dB and $\gamma_{SD} = 5$ dB. After demodulated the received signals, R transmits to D using 16-QAM ($M_2 = 4$). We also

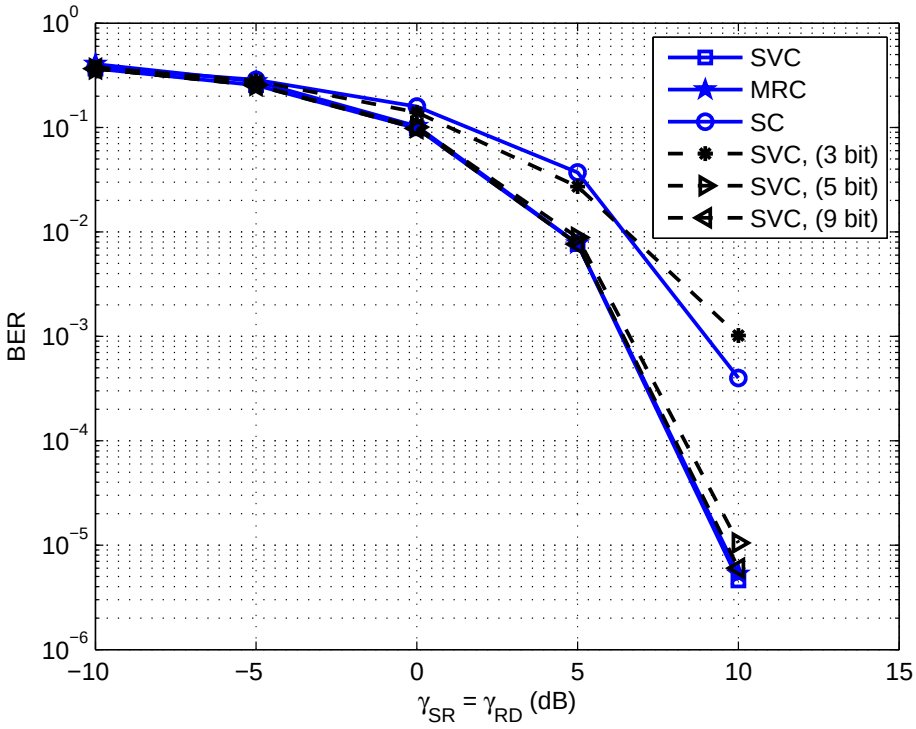

Figure 4.5: Impact of quantization on BER performance.

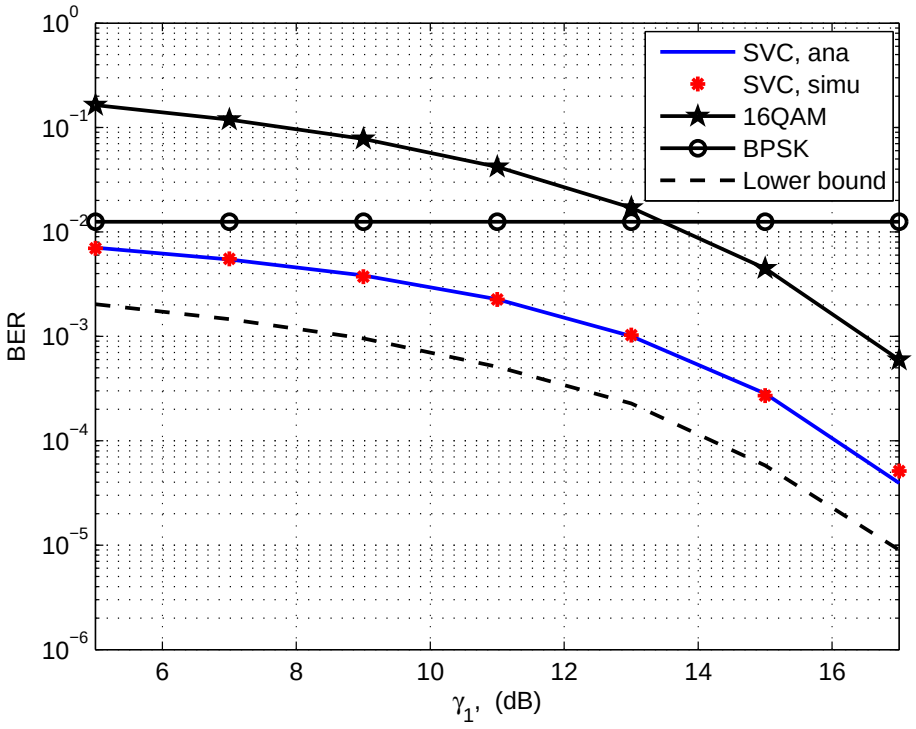

Figure 4.6: BER of SVC of two single-hop paths, AWGN channel, $\gamma_2 = 4$ dB.

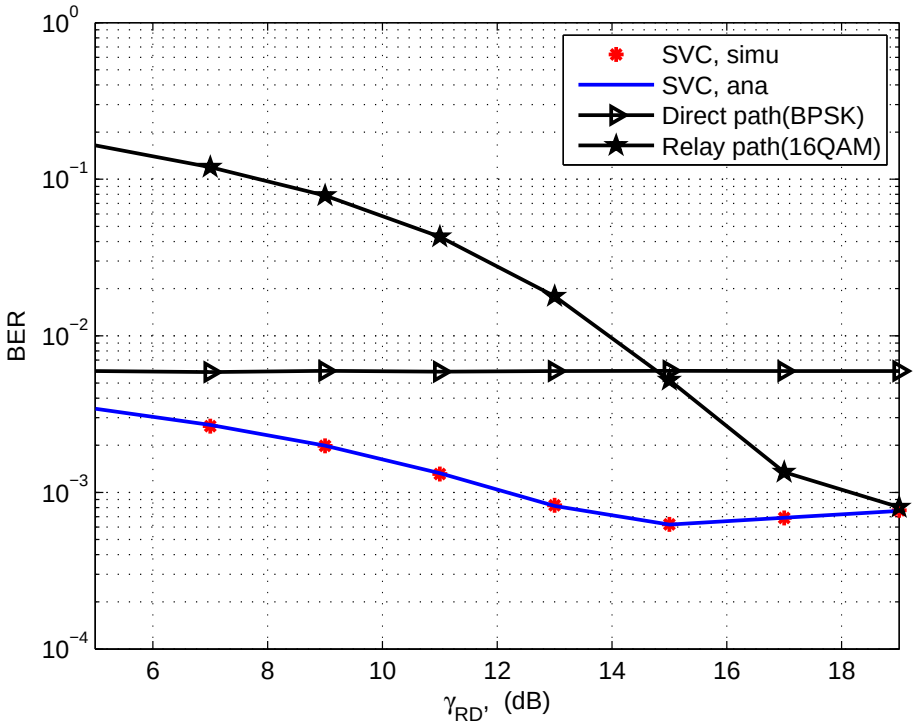

Figure 4.7: BER of cooperative system with SVC, AWGN channels, γ_{SD}=5 dB, γ_{SR}=7 dB, BPSK for the first hop, 16-QAM for the second hop.

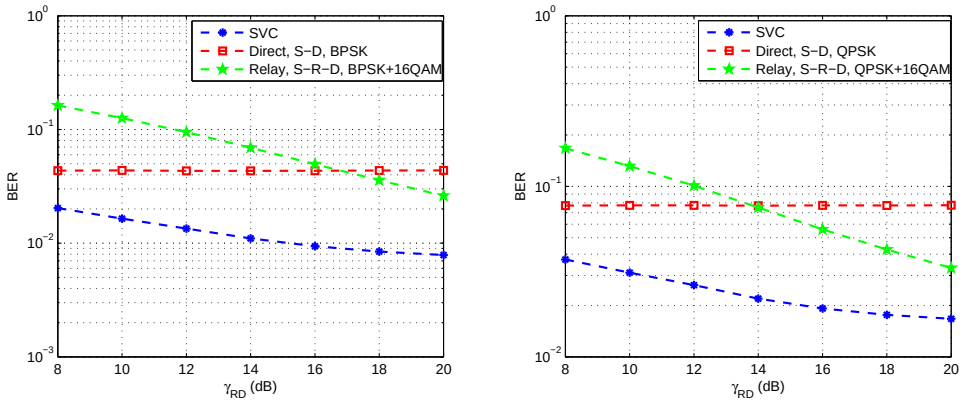

Figure 4.8: BER of cooperative system with SVC in Rayleigh fading channels, γ_{SD}=7 dB, γ_{SR}=15 dB

give BER results of the direct path (S-D) and the relay path (S-R-D) for comparison. From the figure, we can observe that, first, the SVC scheme reduces the BER at D, thanks to the diversity combining. To ensure BER of 10^{-3}, the SNR required for RD using SVC is almost 6 dB lower than that needed using the two-hop relay (without combining). Second, as γ_{RD} increases, the gap of the BER performance of SVC and that of the two-hop relay (without combining) becomes small. This is because the BER of S-D is so high that the direct transmissions contribute little to the combined signal, then the channel quality of S-R become the bottleneck of the system performance. Also, we note that when the SNR of R-D exceeds 15 dB, further increasing it will result in a higher BER. This is because, in this region, the corrupted bits during the S-R transmission have a larger soft value and they have even less chance to be recovered by the direct transmission. The results show that, given fixed modulations, cooperative communication is preferable than the traditional relay until the SNR of the second hop is larger than a threshold (in the example in Fig. 4.7, the threshold is about 19 dB). Later we will show that, considering optimal modulation configuration, the proposed DMF with SVC can always outperform the relay scheme.

A similar tendency can be observed in Fig. 4.8 for Rayleigh fading channels. Significant BER performance improvement can be achieved using SVC for DMF, compared to using the relay path only.

4.6.3 Spectrum and Energy Efficiency

We next evaluate the spectrum and energy efficiency of the cooperative system with SVC using the line topology, i.e., S, R and D are located on a line. For comparison, we implement the traditional relay scheme (the receiver decodes bits from the relay path only) and the AF-MRC scheme, both using adaptive modulation. Assuming that all the transmissions use a fixed bandwidth (with a constant symbol rate), spectrum efficiency can be represented by $\frac{m_1 m_2}{m_1+m_2}$ bit/symbol, where $m_i (i = 1, 2)$ are the number of bits per symbol that the first and second hop modulation schemes can support, respectively. Also the transmission power for the source and relay nodes are fixed at the same level. Thus, the optimal spectrum efficiency solution (highest number of bits transmitted per symbol duration) also leads to the optimal energy efficiency (least bit-energy used). In the following, we mainly present the spectrum efficiency results from which the bit-energy results can be obtained easily.

Without channel coding

We compare the spectrum efficiency performance without channel coding in AWGN channels first. The uncoded BER requirement is $p_e = 10^{-3}$. The distance between S and D is fixed as $d_0 = 1$ unit with the corresponding reference SNR $\gamma_{SD} = 6$ dB. A simple path-loss model is applied, and the corresponding SNR at distance d $(0 \leq d \leq 1)$ can be obtained as $\gamma_{SD}(d/d_0)^{-2}$.

In Fig. 4.9, x-axis represents the relay location (where the source node is located at 0, and the destination node is located at 1), and y-axis represents the spectrum efficiency in terms of bit/symbol. The densest modulation schemes are chosen following Algorithm 2. From the figure, the DMF system with SVC can aways outperform the relay and AF-MRC schemes. In the region $d \in (0.25, 0.8)$, it can achieve 33∼50% spectrum efficiency gain compared with the AF-MRC scheme, and, in the region $d \in (0.4, 0.6)$, 102% gain over the traditional relay scheme. In the above regions, on top of the throughput gain, the proposed solution also achieves about 24∼33% and 50% bit-energy saving compared with the AF-MRC and traditional relay, respectively.

For communication systems, imperfect channel estimation is another critical issue. Over- or under-estimation of the channel conditions can degrade system performance by dropping packets with high BER or choosing lower modulation schemes. To investigate the impact of imperfect channel estimation, the channel estimation error is assumed a Gaussian R.V. with zero mean and 0.2 unit variance. Monte Carlo sim-

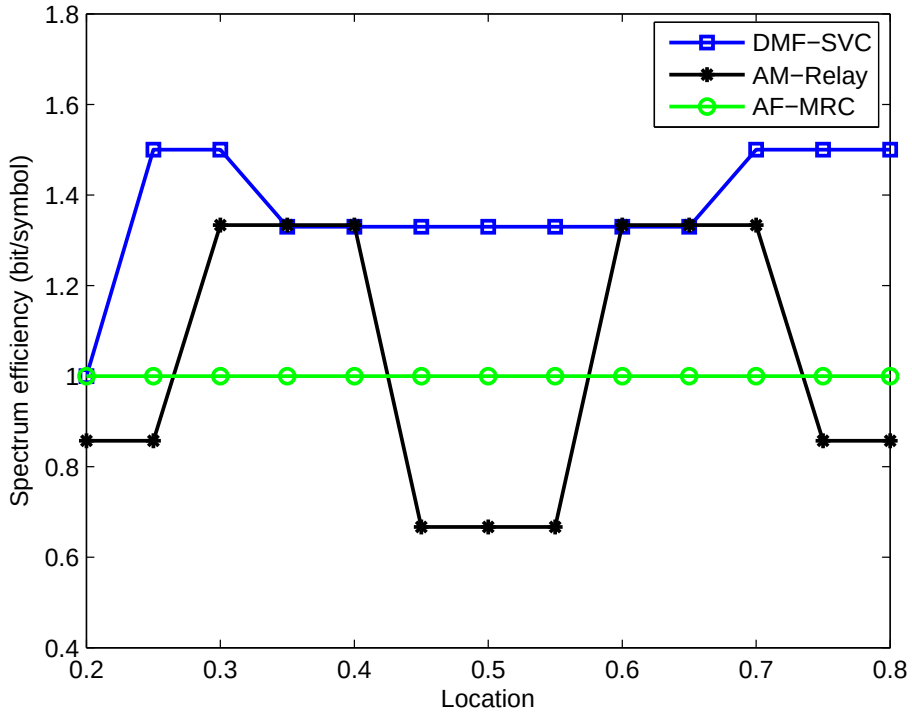

Figure 4.9: Spectrum efficiency, without channel coding, $\gamma_{SD} = 6$ dB

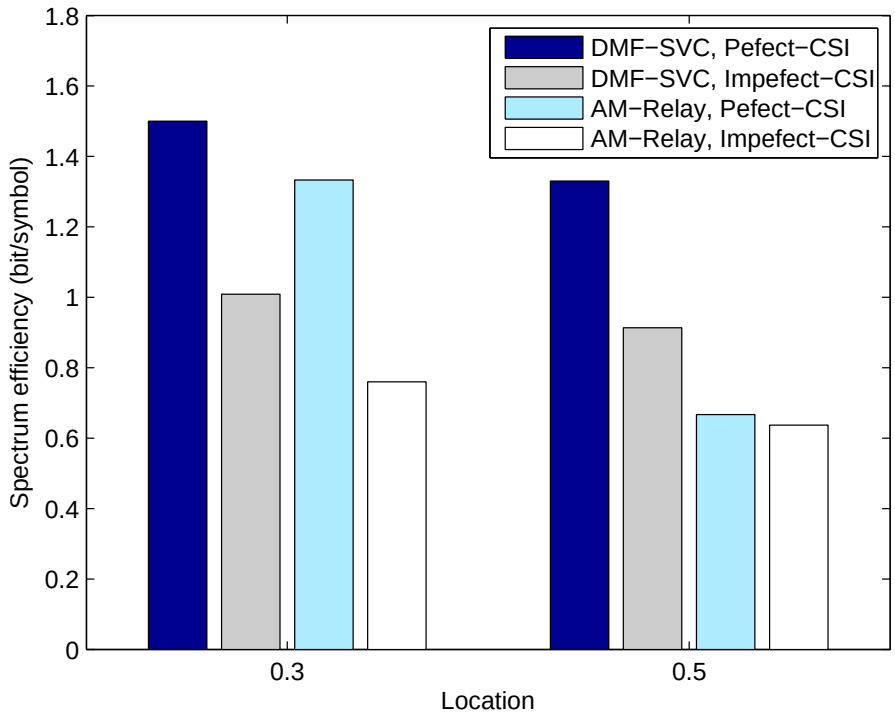

Figure 4.10: Spectrum efficiency for perfect/imperfect CSI, $\gamma_{SD} = 6$ dB

ulations were conducted, where the locations of the relay node are at 0.3 and 0.5, respectively. From Fig. 4.10, although imperfect CSI degrades the performance of both the proposed DMF scheme and the traditional relay scheme, the proposed DMF with SVC can still achieve around 41% and 37% gains (by averaging the results at the two locations) over the traditional relay scheme with perfect and imperfect CSI, respectively.

Considering channel coding

A realistic communication system uses channel coding to reduce the BER. To investigate a realistic system, Fig. 4.11 presents the simulation results with Rayleigh fading channels and the Reed-Solomon (RS) error code [255, 225]. For each setting, we select the best modulation combinations for all the schemes to maximize the spectrum efficiency under the constraint that the coded BER is below 10^{-6}.

The proposed SVC scheme can still bring additional gain to the system performance. When d, the location of the relay, is in the region of $(0.2, 0.6)$, the SVC scheme can obtain 15∼28% spectrum efficiency gain compared to the AF cooperative

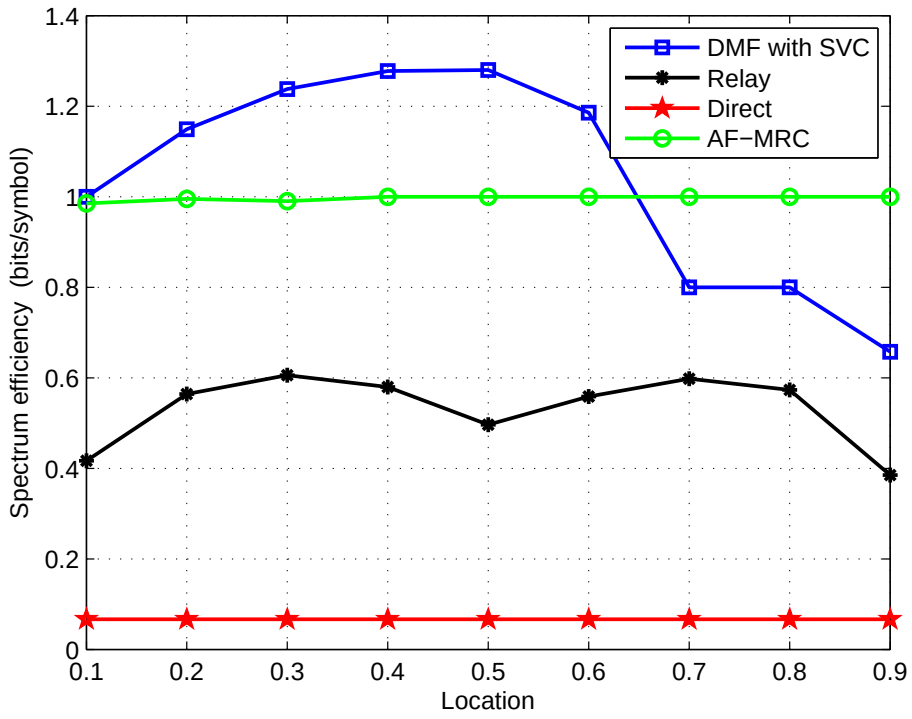

Figure 4.11: Spectrum efficiency, RS[255,225], $\gamma_{SD} = 7$ dB

system with MRC, and it can outperform the relay scheme by 104∼160%. Correspondingly, the bit energy saving compared to the AF-MRC and relay schemes are 13∼22% and 51∼61%, respectively. These results demonstrate that the simple SVC scheme can effectively exploit spatial diversity gain and facilitate adaptive modulation in cooperative systems, and thus achieves higher spectrum and energy efficiency.

4.7 Testbed with GNU Radio and USRP2

In this section, we first briefly introduce the GNU Radio/USRP2 platform which is increasingly popular and flexible for rapid prototyping and verification. Then the OFDM transceiver system with soft values from demodulation is designed and implemented in the GNU Radio/USRP2 platform. Results from the real transmission system demonstrate the effectiveness and performance gain of SVC.

4.7.1 GNU Radio and USRP2

With an exponential growth of modern wireless communications, modifying radio devices easily and cost-effectively has become both a challenge and an advantage. Software defined radio (SDR) brings together the flexibility and cost efficiency to perform the digital signal processing inside a general piece of hardware, making developing radio functionalities easier and faster. GNU Radio [3] is a free software development toolkit for SDR systems. Started in 1998, GNU Radio is now an official GNU project, which provides the signal processing runtime and processing blocks to implement software radios using readily-available, low-cost external RF hardware and commodity processors. By getting code as close to the antenna as possible, GNU Radio turns radio hardware problems into software problems.

Universal Software Radio Peripheral (USRP) [2] is a high-speed USB-based, generalized hardware for GNU Radio. The second version USRP2 [2], made available in September 2008, offers higher performance and increased flexibility. It uses a Gigabit Ethernet interface in place of a USB 2.0 connection. USRP2 has an open design, drivers and free software to integrate with GNU Radio.

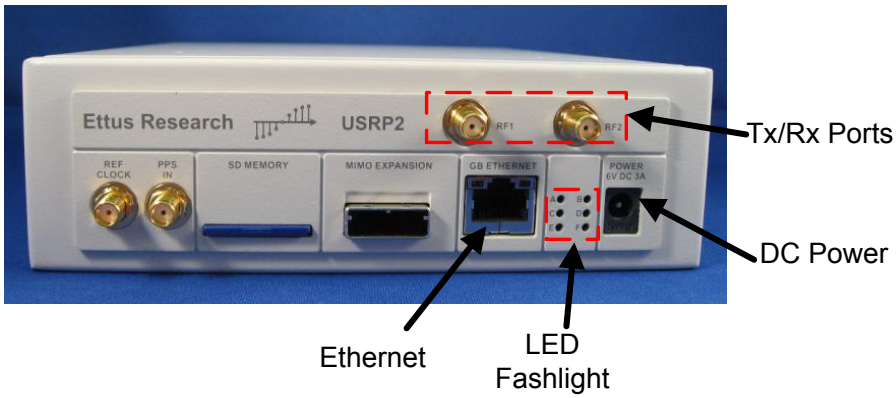

Figure 4.12: Universal Software Radio Peripheral2 (USRP2)[4].

Fig. 4.12 shows how a USRP2 generally looks like. Its product family consists of the motherboards, which contain an FPGA for high-speed signal processing, and interchangeable daughterboards that cover different frequency ranges. Further, there are two 100 mega sample-per-second (MS/s) 14-bit analog-to-digital converters, two 400 MS/s 16-bit digital-to-analog converters, and supports circuitry including a Gigabit Ethernet interface. Together, they bridge between bits in a host computer and one or more antennas. Among the various daughterboards, the USRP2 family has

an overall range of DC to 5 GHz, covering everything from AM radio through Wi-Fi and beyond. Some of the hardware specifications are listed in Table 4.1.

Table 4.1: USRP2 Preliminary Hardware Specifications.

Component	Quantity	Description
ADC	2	capable of 100 MS/s at a resolution of 14 bit, 88dB SFDR(LTC2284)
DAC	4	capable of 400 MS/s at a resolution of 16 bit, 80+dB SFDR (AD9777)
FPGA	1	Xilinx Spartan 3 - XC3S2000 FPGA
Ethernet	1	Gigabit, an open source MAC in the FPGA, a National Semicondutor PHY chip(DP83865)
MIMO Expansion	1	two USRP2 connected by a MIMO cable
Daughterboard capacity	2	1 TX, 1 RX
RF Bandwidth to/from host	1	25 MHz @ 16bits

The corresponding block diagram of USRP2 is shown in Fig. 4.13. After received analogy signals at the front end, the ADC is used to transfer it to digital signals. Then, the digital signals are fed into FPGA for the data rate conversion, and finally to the software code inside the PC.

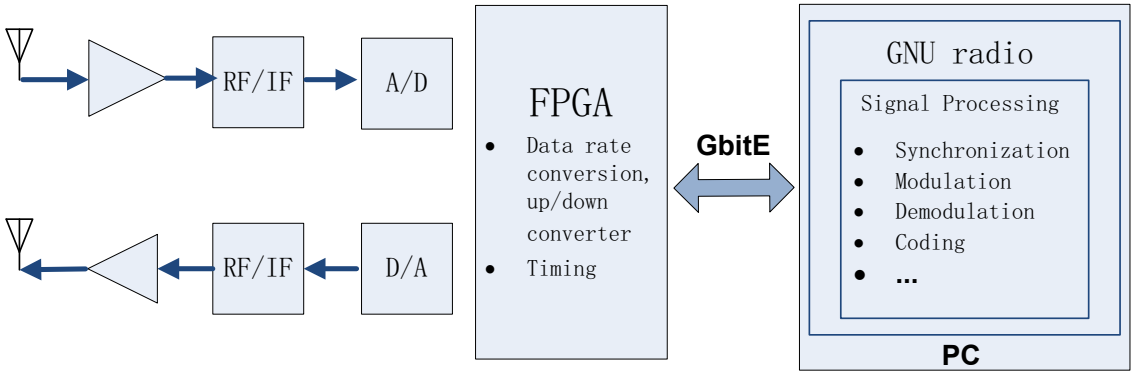

Figure 4.13: Block Diagram of USRP2.

In the PC, all the sources, sinks and processing blocks are implemented as classes in C++, and all the high-level organizing, connecting and gluing are done using Python. Thus, by modifying/adding the processing blocks, proposed scheme or algorithm can be implemented in the real testbed systems with low-cost.

4.7.2 Soft Values from Demodulation

As we have demonstrated before, the soft value is a useful information which can be used to further improve the system performance from different angles. With the significant advantages in terms of rapid prototyping and the availability offered by GNU Radio/USRP2 platform, the implementation of soft values from demodulation process is described as follows.

Our soft value system uses OFDM [61] to transmit data over multiple orthogonal subcarriers. The OFDM transmitter is shown in Fig. 4.14. First, the transmitted data is packeted by adding the MAC header, CRC and whiten payload (to avoid color noise, payload is sent through a whitening filter [12]). Then packeted messages are transmitted from **Msg_queue** to the **OFDM_mapper** where constellation mapping for each subcarrier is applied. After inserting the preamble symbols, frequency domain packets are transfered to time domain by **IFFT** module. To avoid the ISI, CP sequence is implemented before sending the packets to the USRP2 sink. The reverse process is described in Fig. 4.15. As the purpose of this experiment is to obtain the soft values of modulated symbols, we have modified the constellation mapping modules (**OFDM_mapper, ofdm_receiver**) from transmitter and receiver sides respectively, for calculating the soft vales. The input bit streams before the modulation module are recorded in *File_tx*.txt. At the receiver side, **ofdm_receiver** module performs the OFDM receiver function, including frame synchronization, frequency/timing synchronization and FFT. **OFDM_frame_sink** is a signal processing module programmed by C++, which is used for demodulating symbol streams to bits. During the demodulation process, by calculating the soft value as we demonstrated in Section 4.3.2, the soft values for transmitted symbols are obtained and recorded to the log files.

Due to the hardware limitation of USRP2, we choose lower data rate and short packet length to improve the transmission reliability. The system parameters are set as follows. The carrier frequency is 2.49 GHz and the data rate is set as 10 Kbps, with 20 dB transmission gain. One OFDM frame consists 64 subcarriers and 16 CP. QPSK modulation has been adopted for each subcarrier. To obtain the soft values that experience different channel conditions, the same data file has been transmitted twice to obtain the independently received copies for soft value combining. After collecting the transmitted data in *File_tx*.txt and the two copies of soft values in *File_sv*.txt, we use Matlab to analyze the experimental data and the results are shown in Fig. 4.16(a) and (b).

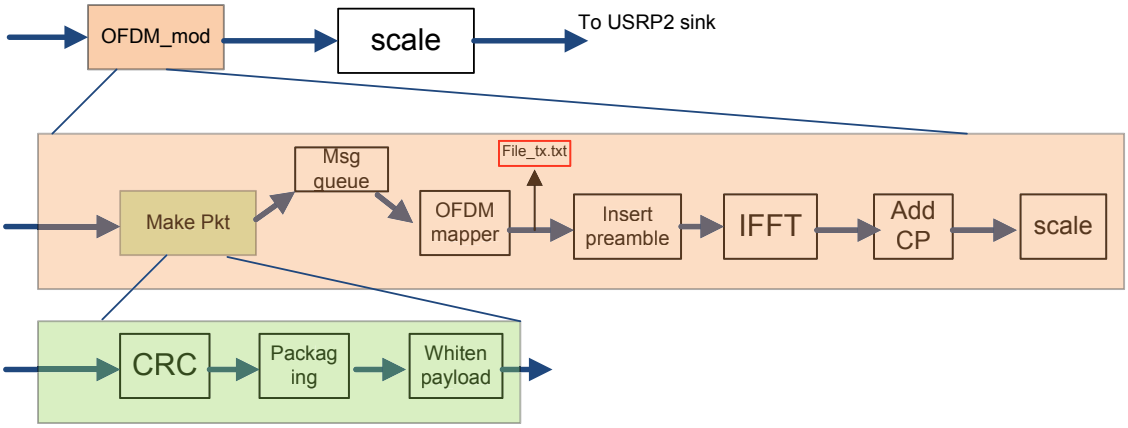

Figure 4.14: Block diagram of OFDM transmitter.

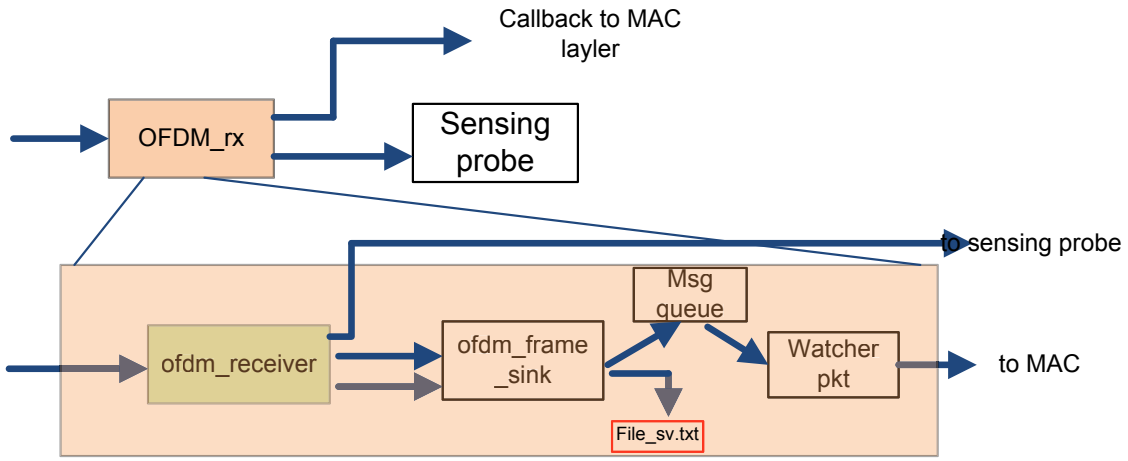

Figure 4.15: Block diagram of OFDM receiver.

In Fig. 4.16(a), the soft values of the transmitted bits b_i=1 are presented. As the demodulation decision boundary is 0, combined soft values have less samples fallen below the threshold, compared with single-copy SV1 or SV2. In other words, with SVC, the BER is reduced. As shown in Fig. 4.16(b), the BER has been reduced from 1.24×10^{-1} (SV_1) and 1.16×10^{-1} (SV_2) to 3.71×10^{-2} with SVC, thanks to the spatial diversity gain exploited from the combining of two independent copies which mitigates the effect of fading.

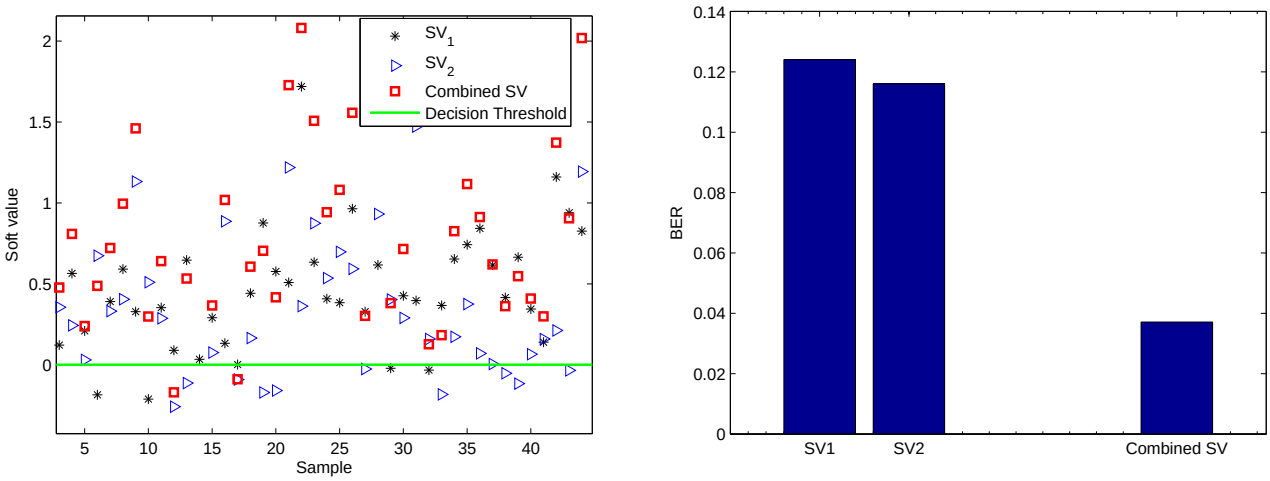

(a) Sample results of soft values for SV1, SV2 and combined SV.

(b) BER performance.

Figure 4.16: Performance results for soft value combining.

4.8 Summary

In this chapter, we have proposed the soft value combining scheme for wireless cooperative systems to effectively improve the spectrum and energy efficiency. The closed-form BER expression for cooperative systems with the proposed soft value combining has been derived and validated by simulation. The proposed soft value combining scheme is simple and practical to implement than the existing optimal combining, and it can achieve close-to-optimal performance. We have further extended our work to the DMF cooperative systems which can flexibly choose the modulation types of the two transmissions by the source and the relay node to improve spectrum efficiency. Simulation and analytical results show that, the DMF cooperative system with SVC can substantially outperform the traditional cooperative systems and the relay-transmission system in terms of both spectrum and energy efficiency. Additionally, a OFDM transceiver system with soft values from demodulation module are designed and implemented in the GNU Radio/USRP2 platform. The experiment results verify the performance improvement from SVC and also demonstrate the flexibility of SDR systems for the rapid prototyping and verification.

4.9 Symbol List

The symbol list is shown in Table 4.2.

Table 4.2: Notations for Chapter 4

Symbol	Explanation
y_i	received signal
x	transmitted symbol, $x = x_I + jx_Q$
$s_{i,k}^{(M_i)}$	soft value for bit b_k from y_i with M_i modulation type
$\Theta_{i,k}$	set of constellation signal y_i whose b_k bit is 1
$\Psi_{i,k}$	set of constellation signal y_i whose b_k bit is 0
z	normalized received symbol, $z = y/h = x + n/h$
$\bar{s}_k$	combined soft value for bit b_k
$\mathbf{S}_k$,$\mathbf{U}_k$	interval matrix $\mathbf{S}_k$ and boundary matrix $\mathbf{U}_k$
$\mathbf{V}_{k,j}$	j-th element of available region $\mathbf{V}_k$, $\mathbf{V}_k = \{n_2 = f(n_1) \vert n_1 \in \mathbf{U}_k\}$
$A_{k,c}$	set of events that contain all the possible transmitted symbols when the k-th bit is c
$A_{k,c,j}$	j-th element of set $A_{k,c}$ $A_{k,1,j} = (x_1 = D_{1,j} \in \Theta_k^1, x_2 = D_{2,j} \in \Theta_k^2)$ $A_{k,0,j} = (x_1 = D_{1,j} \in \Psi_k^1, x_2 = D_{2,j} \in \Psi_k^2)$
$A_{k,c}^{'}$	set of events for corrupted bit b_k, which is $\hat{c}$ from the relay path and is c from the direct path
$Pr\{e, SVC\}$	BER of SVC
$Pr\{e, SR\}$	BER of link S-R
$Pr\{e, SR^{'}\}$	BER of corrupted bits after SVC recovery
$Pr\{e, DMF\}$	BER of DMF cooperative system with SVC

Chapter 5

Soft Value-assisted Channel Estimation for Demodulation and Forward Cooperative Systems

5.1 Motivation and Contributions

In the Chapter 3 and 4, we have discussed the DMF scheme that forwards the demodulated information to the destination with a proper modulation type [45, 90]. With the reliable information for each bit, soft value, receivers can combine the signals from different paths with different modulations. Thus DMF scheme not only simplifies the complexity at the relay by avoiding the coding/decoding process, but also exploit the spatial diversity and adaptive modulation gains by employing different modulation types for two-hop transmissions.

To obtain the potential performance gain of DMF cooperative communication, accurate channel state information (CSI) is essential to determine the optimal modulation configuration. In the majority of existing work, perfect channel knowledge is assumed because of the common belief that the channel estimation approach for DMF can be the same as the traditional direct transmission system. For the DMF scheme, useful information, such as soft values reflecting the reliability of received signals from the demodulation process, has often been overlooked. Soft values from demodulation can be used to indicate the reliability of the transmitted bits, showing how confident the demodulated bits are. Since the reliability of demodulated bits can be caused both by noise and inaccurate estimation of the channel, such soft value

information can also represent the quality of channel estimation, which in turn can be used to improve the existing channel estimation algorithm.

In this chapter, we propose a soft value-assisted channel estimation (S-CE) scheme, by utilizing the reliable information about the initial channel estimation, to improve the accuracy of channel estimation. A channel estimation refinement scheme is derived from the EM algorithm to iteratively approach the ML estimate of the channel. To make a tradeoff between the complexity and performance, a hybrid scheme is proposed to simplify the estimation with near-optimal performance. Simulation results have demonstrated that the proposed S-CE scheme can significantly improve the system performance by providing more accurate CSI.

5.2 Related Work

Effect of channel estimation errors for cooperative communication systems has attracted great attention recently. In [22, 15], the effect of channel-estimation errors on BER performance for AF cooperative system has been investigated. Channel estimation design and analysis for OFDM AF cooperative channels were discussed in [33]. In [13, 64], the optimal training sequence design for channel estimation of the AF system was discussed, as the training sequence being modeled for the optimal MMSE estimator design. For the DF system, channel estimation normally employs the same strategy as that in traditional point-to-point systems. In [14], the optimal training design for the DF system under the total power constraint were studied. Optimization tools were applied to find the optimal training sequence to achieve the best spectrum efficiency. For the DMF system, to the best of our knowledge, no previous work discusses the effect and design for channel estimation. Typically, such as [81, 90, 46], channel state information are assumed to be known, and obtained the same way as that in the DF system, which overlooks the special features of the DMF scheme that each hop of the transmission can be implemented with different modulation types.

On the other hand, using reliable information of received symbols for the channel estimation is not totally new in the traditional point-to-point wireless communication systems. In [76], joint channel estimation and decoding process for turbo coding system was proposed. Soft information from turbo decoder are used to iteratively improve the channel estimation quality. In [40, 72, 62], soft reconstruction schemes of the estimated channel for OFDM system with error correcting code (ECC) were inves-

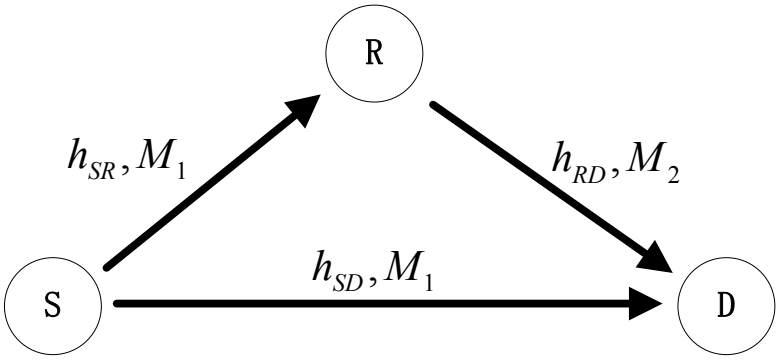

Figure 5.1: System model.

tigated. Reliable information from decoding were used to reconstruct the CSI, which can be iteratively applied for the decoding process. However, the above mentioned soft value information are all from the decoding process which raises the energy and complexity concern in the cooperative communication system, and are not applicable for the DMF system.

To fill the gap, we exploit the reliable information, i.e., soft value, to improve the channel estimation quality which in turn will enhance the performance of the DMF system.

5.3 System Model and Pilot Structure

5.3.1 System Model

Consider the cooperative communication system that the source node (S) transmits information to the destination (D) via a relay node (R) in a frequency flat fading channel as shown in Fig. 5.1. The notation table of this chapter can be found in Section 5.7 for easy reference.

We assume transmissions by S and R are in two non-overlapping time slots to avoid collisions. In the first time slot, S broadcasts the modulated symbol x to R and D using M_i-QAM. Each M_i-QAM symbol $x_{i,j}$ contains $\log_2(M_i) = m_i$ bits (named $b_1, b_2, ..., b_{m_i}$). Without loss of generality, we assume that the noise terms of link

SR and SD, n_{SR} and n_{SD}, are Gaussian distributed with equal variances, $\mathcal{CN}(0, \sigma_0^2)$. All the links, namely h_{SR}, h_{SD} and h_{RD}, are assumed to subject to i.i.d. Rayleigh fading, modeled as a circular complex Gaussian random process with autocorrelation function

$$R_h(k) = J_0(2\pi f_m T_s k), \tag{5.1}$$

where f_m is the maximum Doppler frequency shift, T_s is the symbol duration, and $J_0(.)$ is the Bessel function of zero order.

In the first time slot, the received symbol by R and D are y_{SR} and y_{SD}, respectively, given by

$$y_{SR} = h_{SR}x + n_{SR}, \tag{5.2}$$

$$y_{SD} = h_{SD}x + n_{SD}. \tag{5.3}$$

During the second time slot, instead of transmitting with the same modulation type as the direct transmission, R first estimates the CSI of link SR, and applies it to demodulate the received signal. Then R transmits it in a separate modulation type M_2. Since the processed symbols x_{RD} will have the same average power with probably a different modulation type based on the quality of RD only, DMF can typically achieve a higher throughput than AF. The received symbol at D is

$$y_{RD} = h_{RD}x_{RD} + n_{RD}. \tag{5.4}$$

Two copies of the transmitted signals going through independent channels are received by D, which can lead to a diversity gain. To exploit this diversity gain by combining two copies with different modulations, D will calculate the soft value information for each bit as described in Section 4.3.2, and then apply the soft value combining (SVC) scheme we also have discussed in Chapter 4, to demodulate the two copies with the benefit of the spatial diversity gain. With SVC, soft values from relay and direct paths can be weighted summed at D based on channel qualities.

5.3.2 Pilot Structure for Channel Estimation

For a pilot-based channel estimation, known symbols are inserted into the transmitted sequence periodically. At the receiver, several estimation algorithms, such as Least

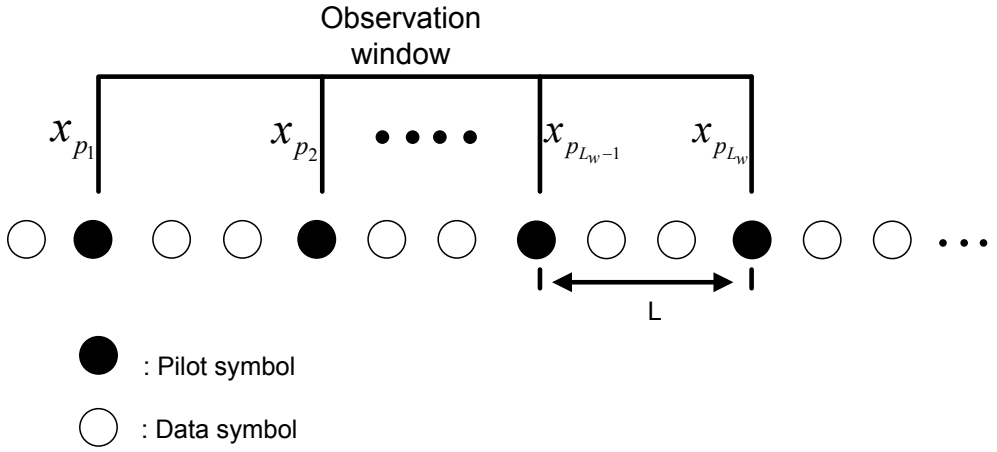

Figure 5.2: Pilot structure.

Squares (LS), Minimum Mean Square Error (MMSE) can be employed to estimate the transmission channel based on the pilot symbols and the pattern insertion [55].

The pilot-based channel estimation structure is shown in Fig. 5.2. Assume that N_p pilots are uniformly inserted into sequence $X(k)$, where L is the pilot interval. For the simple transmission model $Y = HX + N$, the channel response at pilot symbols $H_p(k), k = 1, ..., N_p$, is given by LS estimation, as $H_{p,ls} = \frac{Y_p}{X_p}$.

Since the LS estimation is vulnerable to the noise and the accuracy of channel response at pilot symbols is essential for the following data symbol communication, the MMSE estimator is employed to depress the noise effect [55]. The MMSE estimation of the pilot channel response can be obtained as

$$\hat{H}_{p,MMSE} = R_{H_pH_p}(R_{H_pH_p} + \frac{\beta}{SNR}I)^{-1}H_{p,ls} \tag{5.5}$$

where β is a constant factor related to the modulation scheme (equal to 1, 1.8889 for QPSK and 16-QAM respectively), and $R_{H_pH_p}$ is the auto-correlation matrix for pilot channel response as described in (5.1).

After filtering the pilot channel responses, the MMSE estimator can be used to interpolate the channel response of data symbols between pilots. To reduce the computational complexity, we apply the pilots information within the observation window Γ of limited size L_w,

$$\hat{H}_k = \sum_{k' \in \Gamma_k} w'_k H_{p,ls}(k') \tag{5.6}$$

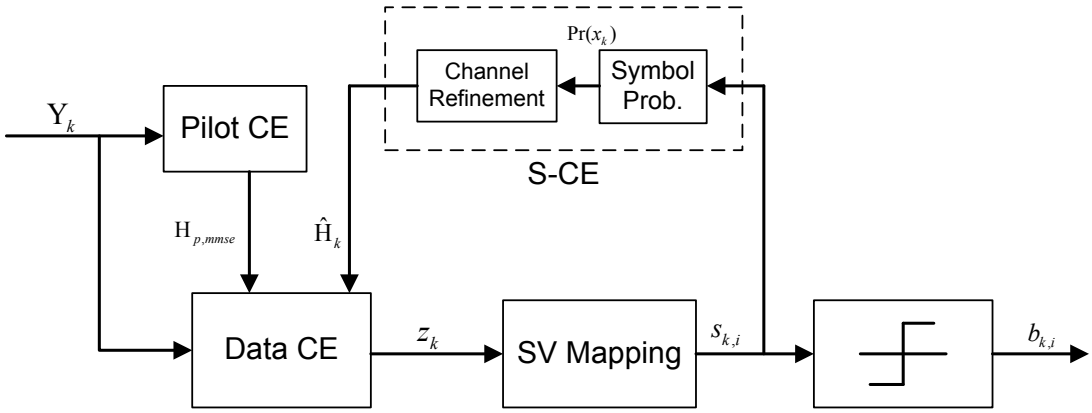

Figure 5.3: Block diagram of receiver with S-CE.

where w_k is the estimation coefficients. w_k can be solved by Wienner-Hopf equation, as

$$\mathbf{w}'_k = (R_h + \frac{\beta}{SNR} I)^{-1} r_h \tag{5.7}$$

where R_h is the autocorrelation matrix with the size of L_x, and $r_h = [R_h(k - p_1), R_h(k - p_2), ..., R_h(k - p_{L_w})]$.

5.4 Soft Channel Estimation

In this section, we study how to utilize the soft values from demodulation to improve the quality of channel estimation, as shown in Fig. 5.3. Based on the EM algorithm, a numerical approach has been proposed to iteratively approach the ML estimation. Then a hybrid scheme has been proposed to simplify the channel refinement scheme for DMF cooperative system with several channel estimation processes.

5.4.1 Soft Value Mapping

Since the channel response is based on each transmitted symbol, we first need to restore the transmitted symbol with the help of SVs. Using SV s_i defined in (**??**) for transmitted bit $b_{k,i}$ from symbol C_k, and the fact that $P\{b_{k,i} = 0\} + P\{b_{k,i} = 1\} = 1$, the probability of the i-th bit of the transmitted symbol x_k given the observation Y

and the initial channel estimation $\hat{H}$, can be expressed as the function of SVs,

$$P\{b_{k,i} = 1|Y, \hat{H}\} = \frac{1 + \tanh(\frac{s_i}{2})}{2}, \tag{5.8}$$

$$P\{b_{k,i} = 0|Y, \hat{H}\} = \frac{1 - \tanh(\frac{s_i}{2})}{2}. \tag{5.9}$$

where $i = 1, 2, ..., \log_2(M)$ for M-QAM modulation.

Thus, the reliability of the transmitted symbol x_{ij}, in terms of the probability of x_k given received symbol Y and $\hat{H}$, can be obtained as

$$P\{x_k|Y, \hat{H}\} = \prod_{i=1,2,...,\log_2(M)} P\{b_{k,i}|Y, \hat{H}\}. \tag{5.10}$$

5.4.2 Channel Estimation Refinement, EM Algorithm

For channel estimation, the ML estimate of H given the observation Y is presented as

$$H^{ML} = \arg\max_{H} \log f(Y|H), \tag{5.11}$$

where $f(Y|H)$ is the conditional pdf of the observed signal Y given H, $f(Y|H)$ can be expressed as

$$f(Y|H) = \sum_{x_i \in \mathbf{X}} f(Y|x_i, H) \Pr(x_i|H), \tag{5.12}$$

where $\mathbf{X}$ is the set of constellation symbols with size L_X.

The channel response H and the input symbols x_i are independent, and the probability of transmitted symbols x_i is equal, $\Pr(x_i|H) = \Pr(x_i) = \frac{1}{L_X}$. The ML estimation is not practical to obtain results directly due to its high complexity. In the presence of unobserved data, the EM algorithm [57, 50] is a well-known alternative method which can iteratively approach to the results using the ML estimation. Basically, the algorithm can be broken down into two steps: the *E-step* for finding the expected log-likelihood function and *M-step* for maximizing the results with respect to the estimate parameters. In our case, the log-likelihood function of the incomplete data is $\log f(Y|H, x)$. Due to the Gaussian noise assumption, we can rewrite the pdf

of the received signal Y given the transmitted symbol x and H as

$$f(Y|H,x) = \frac{1}{2\pi\sigma^2}\exp\{-\frac{1}{2\sigma^2}|Y-Hx|^2\}, \tag{5.13}$$

and from (5.12), the pdf of Y given H can be obtained as

$$f(Y|H) = \sum_{i=1}^{L_X}\frac{1}{2L_X\pi\sigma^2}\exp\{-\frac{1}{2\sigma^2}|Y-Hx_i|^2\}. \tag{5.14}$$

By applying the above results for the ML estimation of (5.11), the EM algorithm for estimating H from Y can be summarized as follows

E-step

$Q(H|H^{(p)}) = E\{\log f(Y|X,H)|Y,H^{(p)}\}$,

M-step

$\tilde{H}^{(p+1)} = \arg\max_H Q(H|H^{(p)})$.

Following the same procedure of the EM algorithm with (5.13) and (5.14), the value of H that maximizing $Q(H|H^{(p)})$ can be found [50] as

$$\tilde{H}^{(p+1)} = \frac{\sum_{i=1}^{L_X}\frac{Y}{x_i}f(Y|x_i,H^{(p)})}{\sum_{i=1}^{L_X}f(Y|x_i,H^{(p)})}. \tag{5.15}$$

By applying Bayes' theorem to (5.13) and the fact that the transmitted symbol x_i is independent of H, (5.13) can be rewritten as

$$\begin{aligned} f(Y|x_i,H) &= \frac{f(x_i|Y,H)\Pr(Y|H)}{\Pr(x_i|H)} \\ &= \frac{f(x_i|Y,H)}{\Pr(x_i)}. \end{aligned} \tag{5.16}$$

Taking (5.16) into (5.15) and replacing the pdf with the conditional probability $\Pr(x_i|Y,H^{(p)})$, the Mean-CSI (M-CSI) scheme is proposed as the channel refinement is shown as

$$\tilde{H}_k = \sum_{i=1,2,\ldots,L_X}\Pr\{x_i|Y,\hat{H}_k\}\frac{Y_k}{x_i}\ . \tag{5.17}$$

5.4.3 Channel Estimation Refinement, Hybrid Algorithm

To assist the channel refinement performance in the low SNR scenario, a hybrid scheme is proposed to combine the EM update information and the initial MMSE estimation $\hat{H}_k$ as

$$\begin{aligned} j &= \underset{i=1,2,\ldots,\log_2(M)}{\arg\max} P\{x_i|Y,\hat{H}_k\}, \\ \tilde{H}_k &= P\{x_j|Y,\hat{H}_k\}\frac{Y_k}{x_j} + (1 - P\{x_j|Y,\hat{H}_k\})\hat{H}_k \end{aligned} \tag{5.18}$$

The motivation behind the *hybrid* scheme is that, for a single-time or a small number of iterations, the initial estimation is important for the accuracy of estimation. When the transmission SNR is low, which makes the SVs of the received symbols less reliable, the initial estimate has an important impact on the channel refinement. In this case, the *hybrid* scheme may achieve a better performance than the M-CSI scheme, especially in the lower SNR range, which will be demonstrated in the simulation section.

5.4.4 MMSE Update

After refining the estimate of channel based on the soft value information, the above $\tilde{H}_k$ needs to be updated based on an MMSE filter to smooth out the results. Similar to the MMSE estimation of the pilot channel responses in Section 5.3.2, the Winner-Hopf function is solved to obtain the weight factor as

$$\hat{H}_{d,SV} = R_h(R_h + \tfrac{\beta}{SNR}I)^{-1}\tilde{H}_d \tag{5.19}$$

where R_h is the auto-correlation function of the Rayleigh fading channel.

5.4.5 Iterative Performance Analysis

As the EM algorithm is a numerical approach for ML estimation, and it requires an iterative process to achieve the optimal results, a nature question is how important the iterative process for our proposed S-CE is. We take BPSK modulation transmission as an example, and compare the performance of several iteration processes.

From Fig. 5.4, the accuracy of channel estimation has not changed substantially when the number of iteration changes from 1 to 5. This is because, unlike the decod-

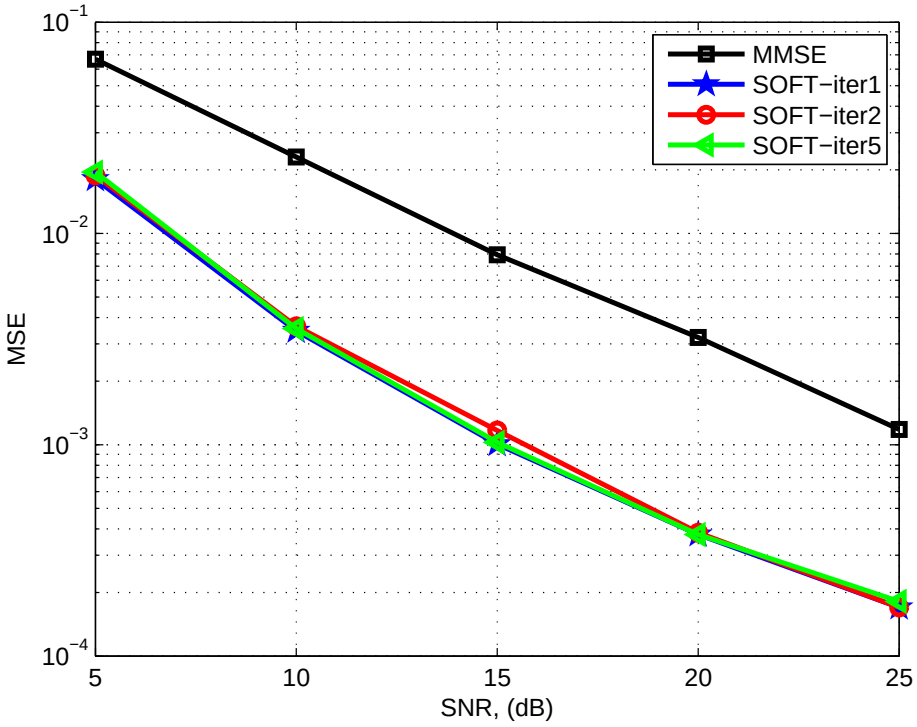

Figure 5.4: MSE performance of BPSK with S-CE.

ing process which has a strong error-correction ability, demodulation has less ability to improve the erroneous symbol. Especially when the MSE is low, the improved reliability of the received symbols (i.e., SVs) from a more accurate channel estimation will be marginal, which limits the performance improvement of the channel refinement. On the other hand, multiple iterations will greatly increase the complexity, especially for the MMSE update. In the following sections, we only apply one time channel refine process in the S-CE scheme given the tradeoff between performance and computational complexity.

5.4.6 DMF Soft Channel Estimation

For the DMF system shown in Fig. 5.1, three channels need to be estimated, i.e., S-R, R-D and S-D channels, which are all applicable with the proposed S-CE. For the relay path, with a more accurate channel response information, error propagation can be depressed, and thus it can achieve better performance, both in BER and MSE measurements. Moreover, an accurate channel estimation can also improve the spectrum efficiency by reducing the pilot overhead of the cooperative system with S-CE. With less pilot symbols, more useful data can be transmitted with a similar transmission quality. An accurate channel estimation can be helpful for the relay process, such as the forward threshold selection in [37], modulation scheme selection in [27] etc.

The procedure of the DMF system with S-CE is described below:

Step 1: The source broadcasts information to the destination and the relay in the first time slot. Then the destination and relay estimate the channel response information of the S-D and S-R links, respectively, and apply the estimated CSI to demodulate the received symbols. Soft values of each bit are calculated as described in Section 4.3.2;

Step 2: The relay forwards the received information to the destination with the best modulation type selected according to the channel estimation;

Step 3: During the second time slot, a joint channel estimation and demodulation process at the destination for the retransmitted symbols (probably with another modulation type) from R to D is performed, and the soft value for each bit is constructed using the same procedure as that in Step 1;

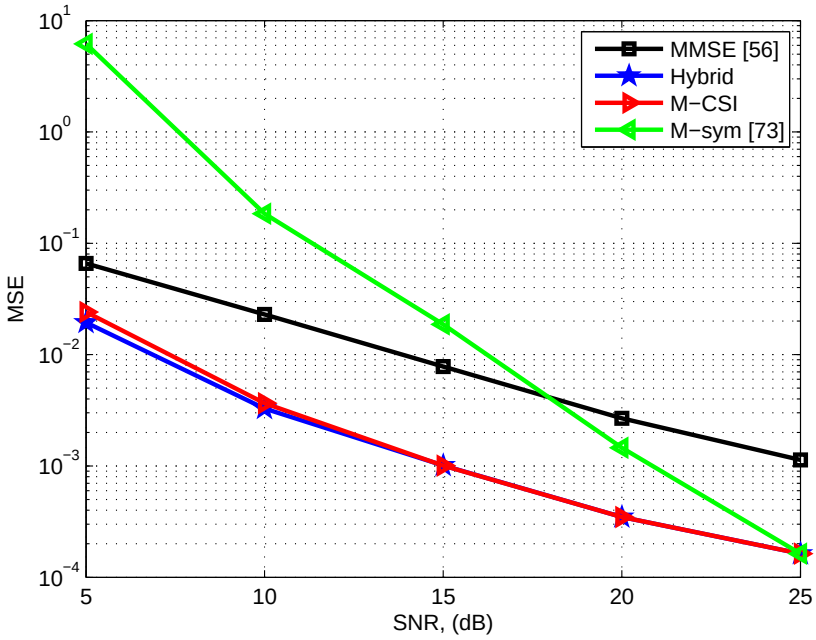

Figure 5.5: MSE performance for MMSE, *hybrid*, M-CSI and *M-sym* channel estimation with BPSK modulation.

Step 4: For each bit, the destination combines the corresponding soft values of the two copies, and obtains the final decoded bit based on whether or not the combined soft information is larger than the demodulation threshold.

5.5 Performance Evaluation

In this section, Monte Carlo simulations are conducted to investigate the performance of the proposed soft channel estimation.

5.5.1 Point-to-point System with S-CE

We first discuss the performance of S-CE in a traditional point-to-point link with Rayleigh fading. The pilot ratio is 10%, and the MMSE estimator is adopted at the receiver as discribed in Section 5.3.2. Assume that the Rayleigh fading channel has f_m=10 Hz and $T_d = 10^{-4}$.

In Fig. 5.5, we first compare the estimation quality in terms of MSE for various soft channel refinement schemes discussed in Section 5.4.1. It is also used to compare

with the mean-symbol scheme (*M-sym*) proposed in [72] that the estimated channel is constructed by dividing the received symbol Y with the mean value of the data symbol, i.e., $\tilde{H}_k = Y_k / \sum_{i=1,2,\ldots,\log_2(M)} P\{x_i\} x_i$. From the figure the proposed *hybrid* scheme outperforms MMSE [55] by 5-10 dB, and outperforms the *M-sym* [72] by up to 10 dB gain. *M*-CSI scheme can achieve a similar performance as the hybrid scheme in the higher SNR range, while slightly worse in the lower SNR range. This is because, when SNR is low which represent a poor channel condition, the soft value of each bit becomes less reliable while the existing MMSE estimation results can be more helpful. In the lower SNR range, the *M-sym* scheme [72] has the worst estimation performance because of the noise effect that dominates the performance. Overall, the *hybrid* scheme can both benefit from the soft value information and the existing MMSE estimation results, and outperform other schemes in all the SNR range. In the following simulation, we use the *hybrid* scheme for S-CE.

In Figs. 5.6-5.7, MSE and BER performance for BPSK and 16-QAM modulations with S-CE are compared. For BPSK and 16-QAM, S-CE outperforms traditional MMSE by 7 dB and 6 dB gain respectively, given the 10^{-2} MSE threshold. With accurate channel estimation, BER performance improvement for both modulation schemes are noticed in Fig. 5.7, especially for higher modulation schemes (16-QAM). The dash curve represents the BER performance for each modulation scheme with the perfect channel response information.

5.5.2 DMF System with S-CE

We next evaluate the performance of S-CE in DMF system with two different modulations for source and relay transmissions. The averaged received SNR for S-R, R-D and S-D are $\gamma_{SR} = 20$ dB, $\gamma_{RD} = 30$ dB and $\gamma_{SD} = 20$ dB, which can support BPSK and 16QAM for the first and second hop transmissions, respectively. The BER and MSE performance of S-CE with various pilot overheads are compared in Figs. 5.8-5.9. It is noticed that with more pilot overheads, both BER and MSE performance can be improved for traditional MMSE and our proposed S-CE scheme. But more pilot overhead means less useful data transmission which would reduce the spectrum efficiency. From the figures, S-CE can improve the system performance for all the pilot overhead scenarios, which means under the same BER requirement, less pilot overheads are needed for the S-CE scheme to achieve the same channel estimation quality (i.e., MSE) and thus the spectrum efficiency can be increased.

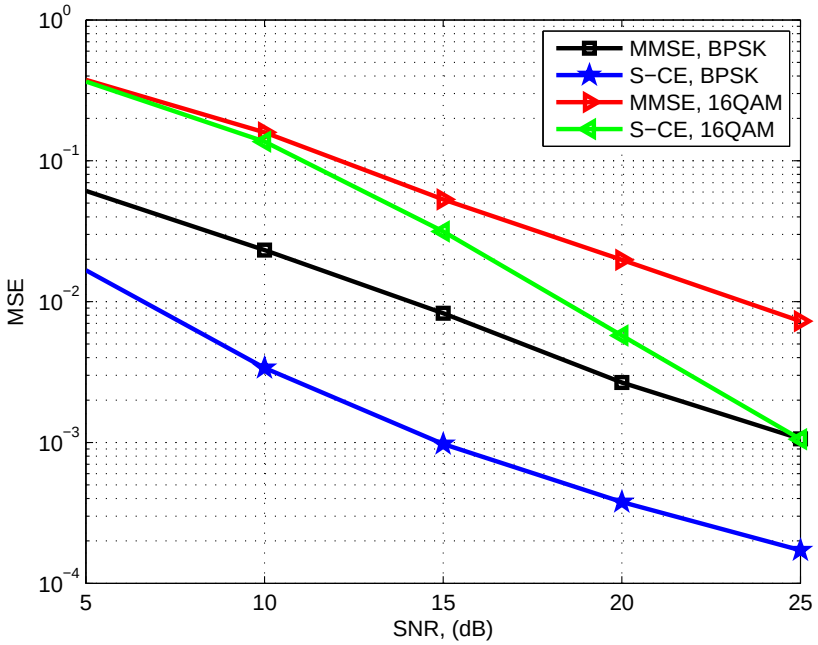

Figure 5.6: MSE performance of channel estimations for BPSK and 16QAM modulations.

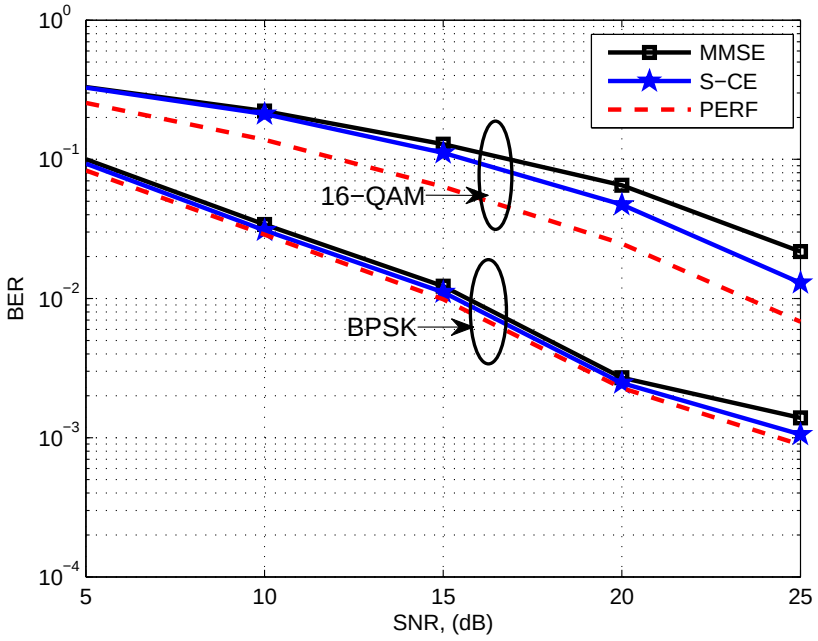

Figure 5.7: BER performance of channel estimations for BPSK and 16QAM modulations.

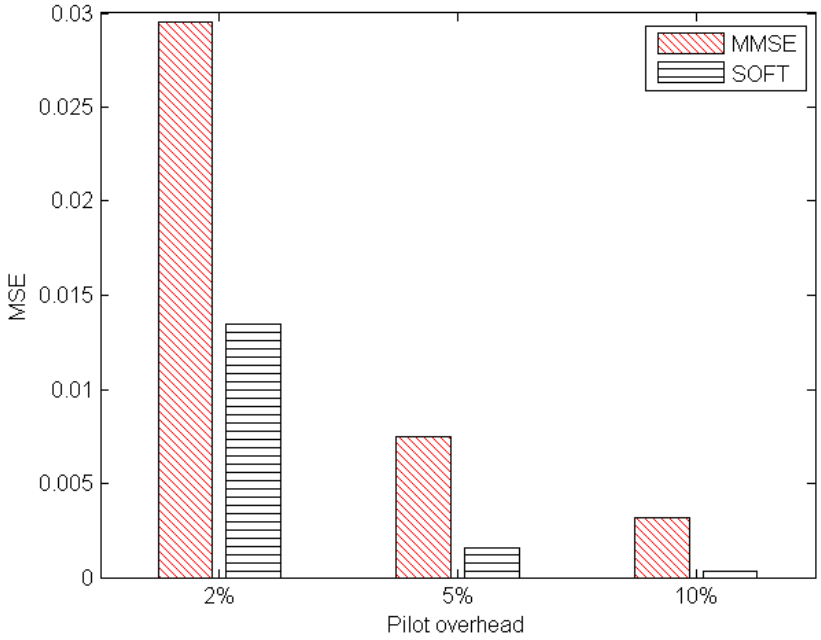

Figure 5.8: MSE performance of channel estimations with various pilot overhead for DMF system.

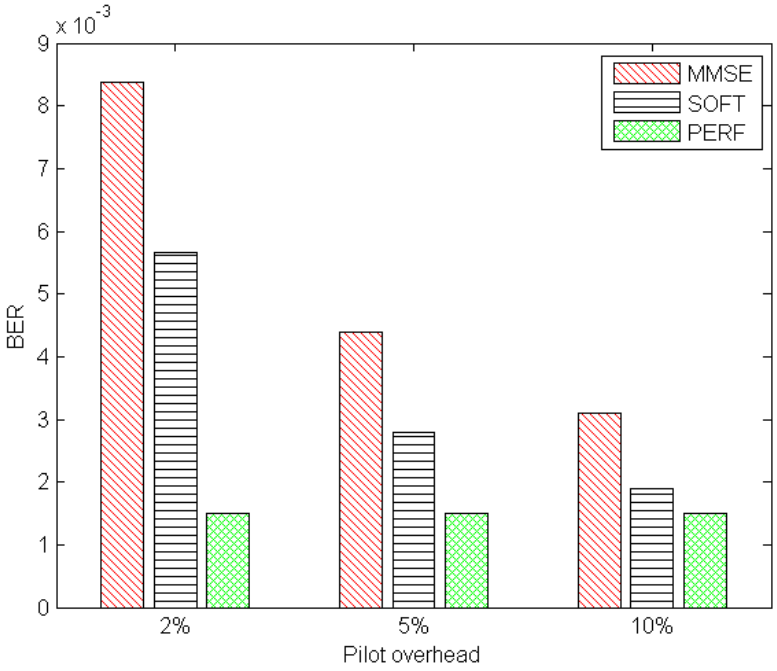

Figure 5.9: BER performance of channel estimations with various pilot overhead for DMF system.

Table 5.1: Notations for Chapter 5

Symbol	Explanation
y_i	received signal
x	transmitted symbol, $x = x_I + jx_Q$
$s_{i,k}^{(M_i)}$	soft value for bit b_k from y_i with M_i modulation type
f_m	maximum Doppler frequency shift
T_s	symbol duration
$\Theta_{i,k}$	set of constellation signal y_i whose b_k bit is 1
$\Psi_{i,k}$	set of constellation signal y_i whose b_k bit is 0
N_p	number of pilot symbols
L	pilot interval
$H_{p,ls}$	LS estimation of the pilot channel response
$\hat{H}_{p,mmse}$	MMSE estimation of the pilot channel response
β	constant factor related to the modulation scheme
$R_{H_pH_p}$	auto-correlation matrix for pilot channel response
w_k	estimation coefficients which can be solved by Wienner-Hopf equation
$\tilde{H}_k$	channel estimation results from EM-algorithm

5.6 Summary

In this chapter, we have proposed the S-CE scheme for DMF cooperative systems to effectively improve the quality of channel estimation. By utilizing the soft value information indicating the reliability of the received symbols, two channel refinement schemes (*hybrid* and M-CSI) based on the EM algorithm are proposed to improve the accuracy of the channel estimation. Numerical results have shown that the proposed S-CE scheme can significantly improve the MMSE channel estimation performance, and leads to obvious performance gains for the DMF system. With accurate channel estimation results, the pilot overhead can be reduced which in turn improves the spectrum efficiency for the DMF cooperative system.

5.7 Symbol List

The symbol list is shown in Table 5.1.

Chapter 6

Contributions and Future Work

6.1 Conclusions

In this thesis, we have tackled three fundamental and critical problems in wireless cooperative systems: (1) channel modeling for wireless cooperative networks that bridges the channel characters and the upper-level QoS design and anlysis. (2) spectrum efficiency and energy optimization problem for cooperative systems with the multi-path multi-hop structure, and (3) accurate channel estimation problem in cooperative systems with the efficient channel refinement scheme. The following outlines the contributions achieved:

1. We have investigated the wireless cooperative systems with spatial diversity over Rayleigh fading channels. The second-order statistic properties, such as LCR and AFD are derived for wireless cooperative systems with SC and MRC diversity combining. Then based on SNR partitioning, a packet-level FSMC channel models for wireless cooperative diversity systems have been developed. Additionally, simulation results on video scheduling problem by using proposed FSMC models are demonstrated and highlight the effectiveness of proposed work.

2. We have proposed the DMF cooperative scheme to fully utilize adaptive modulation to maximize the throughput of cooperative systems. A closed-form approximation of BER for the DMF cooperative system has been derived. We also have proposed a solution for maximizing the throughput of user cooperative system by solving the optimization problem that jointly considers the modula-

tion schemes at the source and the relay nodes. Additionally, WLF matching algorithm has been employed to maximize the network throughput.

3. We have proposed the soft value combining scheme to utilize the spatial diversity gain and improve the spectrum efficiency. By defining the soft value from demodulation process, we also have conducted the analytical framework of SVC for wireless cooperative system with AF and DMF scheme and optimize the spectrum efficiency. We have designed the GNU radio/USRP2 platform based on OFDM transceiver system with soft values from demodulation process. Also the experiment results have verified the effectiveness of SVC.

4. We have developed a soft value-assist channel estimation algorithm for DMF scheme over Rayleigh fading channels. Two channel refinement schemes have been proposed to iteratively improve the channel estimation quality with the soft value information.

6.2 Future Work

The packet-level channel modeling and spectrum efficiency techniques for wireless cooperative systems also opens several important future work, which are listed as follows.

1. In Chapter 2, we have presented the FSMC model for wireless cooperative system with diversity combining, which can be used to bridge the physical layer and upper layer applications. So cross-layer design based on proposed FSMC model will provide efficient tools for system throughput and performance improvement. How to utilize the statistical information FSMC provided in the upper layer, such as MAC scheduling, frame pattern design and rate adaptation, will be studied.

2. Reliable information indicator, soft value, has been investigated in Chapter 4 and 5, respectively, for spectrum efficiency and channel estimation. Several practical issues may be encountered when we jointly consider the above two important performance features based on SVC. First, spectrum efficiency can be further improved by jointly considering power allocation and modulation configuration with SVC at both the source and relay nodes. Second, since the current modulation schemes only have discrete number of bits per symbol, which

mitigate the potential performance gain when channel qualities are in between of the consequent modulation thresholds. Including other modulation schemes, such as scalable modulations and trellis modulations, can help to retrieve the performance gain. Third, error bits detection at the relay node can improve the SVC performance by only forwarding the bits which are likely to be correctly received. At the relay node, how to use soft value to make the decision of forwarding the bit or not needs further investigation. Furthermore, the optimal pilot pattern design for S-CE scheme by considering the soft values and DMF structure is an interesting research direction.

3. Small cell networks (SCN) have the potential to meet the increasing capacity demand of current cellular system and attract lots of attentions, by densely deploying self-organized, low cost and low-power base stations. Packet-level channel modeling can be extended to SCNs, where the statistic information for each small cell can be used to analyze and optimize the network system design with fast reactions and reduced cost. Also SVC can be employed in SCNs with Coordinated Multi-point (CoMP) technique for data combining, when users receive signals from multiple cells to reduce the inter-cell interference, especially for the users in the cell edge.

4. To demonstrate the effectiveness and practical of proposed algorithm, a flexible hardware testbed is important for research investigation and verification in the realistic setting. To extend the current GNU radio/USRP2 platform to multiple nodes with cooperative protocol, is imperative and valuable as future research work.

Bibliography

[1] 3GPP TS 36.213. E-UTRA Physical layer procedures.

[2] Ettus research llc. http://www.ettus.com/.

[3] Gnu radio - the gnu software radio. http://www.gnu.org/software/gnuradio/.

[4] USRP prices and Specifications Ordering. http://www.olifantasia.com/.

[5] G. Benelli. An ARQ scheme with memory and soft error detectors. *IEEE Trans. on Communications*, 33(3):285–288, 2002.

[6] A. Bin Sediq and H. Yanikomeroglu. Performance analysis of soft-bit maximal ratio combining in cooperative relay networks. *IEEE Trans. on Wireless Communications*, 8(10):4934–4939, 2009.

[7] R.W. Butler and A.T.A. Wood. Laplace approximations for hypergeometric functions with matrix argument. *The Annals of Statistics*, 30(4):1155–1177, 2002.

[8] H. Chung, Y. Tsai, and M. Lin. IDMA using non-Gray labelled modulation. *IEEE Trans. on Communications*, (99):1–10, 2011.

[9] Cisco. Cisco visual networking index: Forecast and methodology, 2009-2014.

[10] D.V. Djonin and V. Krishnamurthy. MIMO transmission control in fading channelsa constrained Markov decision process formulation with monotone randomized policies. *IEEE Trans. Signal Proces.*, 55(10):5069–5083, 2007.

[11] M. Drini and T. Saadawi. Modeling wireless channel for ad-hoc network routing protocol. In *IEEE Symp. on Computers and Commun.*, pages 549 –555, July 2008.

[12] R. Farrell, M. Sanchez, and G. Corley. Software-defined radio demonstrators: An example and future trends. *International Journal of Digital Multimedia Broadcasting*, 2009, 2009.

[13] F. Gao, T. Cui, and A. Nallanathan. On channel estimation and optimal training design for amplify and forward relay networks. *IEEE Trans. on Wireless Communications*, 7(5):1907–1916, 2008.

[14] F. Gao, T. Cui, and A. Nallanathan. Optimal training design for channel estimation in decode-and-forward relay networks with individual and total power constraints. *IEEE Trans. on Signal Processing*, 56(12):5937–5949, 2008.

[15] B. Gedik and M. Uysal. Impact of imperfect channel estimation on the performance of amplify-and-forward relaying. *IEEE Trans. on Wireless Communications*, 8(3):1468–1479, 2009.

[16] D. Gesbert, M. Shafi, D. Shiu, P.J. Smith, and A. Naguib. From theory to practice: an overview of MIMO space-time coded wireless systems. *IEEE Journal on selected areas in Communications*, 21(3):281–302, 2003.

[17] E.N. Gilbert et al. Capacity of a burst-noise channel. *Bell Syst. Tech. J*, 39(9):1253–1265, 1960.

[18] I.S. Gradshteyn and I.M. Ryzhik. Table of integrals, series and products. *4th Ed.*, New York: Academic, 2000.

[19] D. Gunduz and E. Erkip. Opportunistic cooperation by dynamic resource allocation. *IEEE Trans. on Wireless Communications*, 6(4):1446–1454, 2007.

[20] Z. Hadzi-Velkov, N. Zlatanov, and G.K. Karagiannidis. On the second order statistics of the multihop Rayleigh fading channel. *IEEE Trans. Commun.*, 57(6):1815–1823, 2009.

[21] J. Hagenauer and P. Hoeher. A viterbi algorithm with soft-decision outputs and its applications. In *IEEE Globecom'89*, 1989.

[22] S. Han, S. Ahn, E. Oh, and D. Hong. Effect of channel-estimation error on BER performance in cooperative transmission. *IEEE Trans. on Vehicular Technology*, 58(4):2083–2088, 2009.

[23] S. Hares, H. Yanikomeroglu, and B. Hashem. Diversity-and AMC-aware routing in TDMA multihop networks. In *IEEE Globecom'03*, volume 1, 2003.

[24] S. Hassan and M. Ingram. A quasi-stationary Markov chain model of a cooperative multi-hop linear network. *IEEE Trans. Wireless Commun.*, (99):1–10, 2011.

[25] H. Huang and V.K.N. Lau. Delay-sensitive distributed power and transmission threshold control for S-ALOHA network with finite state Markov fading channels. *IEEE Trans. Wireless Commun.*, 8(11):5632 –5638, Nov. 2009.

[26] K.S. Hwang, Y.C. Ko, and M.S. Alouini. Two-way amplify and forward relaying with adaptive modulation. In *IEEE IWCMC*, pages 1370–1374. ACM, 2009.

[27] S.S. Ikki and M.H. Ahmed. Performance analysis of adaptive decode-and-forward cooperative diversity networks with best-relay selection. *IEEE Trans. on Communications*, 58(1):68–72, 2010.

[28] C.D. Iskander and P.T. Mathiopoulos. Fast simulation of diversity Nakagami fading channels using finite-state Markov models. *IEEE Trans. Broad.*, 49(3):269–277, 2003.

[29] C.D. Iskander and P. Takis Mathiopoulos. Analytical level crossing rates and average fade durations for diversity techniques in Nakagami fading channels. *IEEE Trans. Commun.*, 50(8):1301 – 1309, Aug. 2002.

[30] W.C. Jakes. *Microwave mobile communications*. Wiley-IEEE Press, 1994.

[31] K. Jamieson and H. Balakrishnan. PPR: partial packet recovery for wireless networks. In *ACM SIGCOMM*, pages 409–420, 2007.

[32] G.K. Karagiannidis. Performance bounds of multihop wireless communications with blind relays over generalized fading channels. *IEEE Trans. Wireless Commun.*, 5(3):498–503, 2006.

[33] K. Kim, H. Kim, and H. Park. OFDM channel estimation for the amply-and-forward cooperative channel. In *IEEE VTC2007-Spring*, pages 1642–1646. IEEE, 2007.

[34] N. Kong and L.B. Milstein. Average SNR of a generalized diversity selection combining scheme. *IEEE Commun. Letters*, 3(3):57–59, 1999.

[35] T. Kumagai and K. Kobayashi. Postdetection maximal ratio combining diversity receiver with scalar phase signals. In *IEEE ICUPC*, volume 2, pages 391–395, 2002.

[36] J.W. Kwon, Y.C. Ko, and H.C. Yang. Maximum spectral efficiency of amplify-and-forward cooperative transmission with multiple relays. *IEEE Trans. on Wireless Communications*, 10(1):49–54, Jan. 2011.

[37] T. Kwon, S. Lim, W. Seo, and D. Hong. Llr-based symbol selective transmission with a near-optimal threshold to minimize bep for demodulation-forward relay systems. *IEEE Trans. on Wireless Communications*, 9(2):540–545, 2010.

[38] J.N. Laneman, D.N.C. Tse, and G.W. Wornell. Cooperative diversity in wireless networks: Efficient protocols and outage behavior. *IEEE Trans. Inform. Theory*, 50(12):3062–3080, 2004.

[39] E.G. Larsson and B.R. Vojcic. "Cooperative transmit diversity based on superposition modulation". *IEEE Communications Letters*, 9(9):778–780, 2005.

[40] Y.N. Lee, A. Ashikhmin, and J.T. Chen. Impact of soft channel construction on iterative channel estimation and data decoding for multicarrier systems. *IEEE Trans. on Wireless Communications*, 7(7):2762–2770, 2008.

[41] Z. Lin, E. Erkip, and M. Ghosh. Adaptive modulation for coded cooperative systems. In *IEEE SPAWC2005*, pages 615–619. IEEE, 2005.

[42] Q. Liu, S. Zhou, and G.B. Giannakis. Cross-layer combining of adaptive modulation and coding with truncated arq over wireless links. *IEEE Trans. on Wireless Communications,*, 3(5):1746–1755, Sep. 2004.

[43] R. Liu, P. Spasojevic, and E. Soljanin. Incremental redundancy cooperative coding for wireless networks: Cooperative diversity, coding, and transmission energy gains. *IEEE Trans. on Information Theory*, 54(3):1207–1224, 2008.

[44] Y. Luo and L. Cai. Second order properties for wireless cooperative systems with Rayleigh fading. In *IEEE GLOBECOM*, 2010.

[45] Y. Luo and L. Cai. Throughput Maximization for User Cooperative Wireless Systems with Adaptive Modulation. In *IEEE ICC*, 2010.

[46] Y. Luo and L. Cai. Error recovery with soft value combining for wireless cooperative systems. In *IEEE WCNC'11*, 2011.

[47] Y. Luo and Cai L. Soft value-assisted channel estimation for demodulation and forward cooperative systems. *Plan to submit to IEEE Trans. on Communication*, 2013.

[48] Y. Luo and Cai L. Soft value combining for user cooperative systems with adaptive modulation. *Plan to submit to IEEE on Vehicular Technology*, 2013.

[49] Y. Luo, R. Zhang, Cai L., and S. Xiang. Finite-state markov modeling for wireless cooperative diversity system. *Submitted to IET Networks*.

[50] X. Ma, H. Kobayashi, and S.C. Schwartz. EM-based channel estimation algorithms for OFDM. *EURASIP Journal on Applied Signal Processing*, 2004:1460–1477, 2004.

[51] V. Mahinthan, L. Cai, J. W. Mark, and X. Shen. Maximizing cooperative diversity energy gain for wireless networks. *IEEE Trans. on Wireless Communications*, 6(6):2530–9, June 2007.

[52] V. Mahinthan, L. Cai, J. W. Mark, and X. Shen. Partner selection based on optimal power allocation in cooperative-diversity systems. *IEEE Trans. on Veh. Tech.*, 57(1):511–520, Jan. 2008.

[53] V. Mahinthan, C. Lin, J.W. Mark, and X. Shen. Maximizing cooperative diversity energy gain for wireless networks. *IEEE Trans. on Wireless Communication*, 6(7):2530–2539, 2007.

[54] M. Mardani, J.S. Harsini, F. Lahouti, and B. Eliasi. Joint Adaptive Modulation-Coding and Cooperative ARQ for Wireless Relay Networks. In *IEEE ISWCS'08*, pages 319–323, 2008.

[55] KO Mehmet and A. Huseyin. Channel estimation for wireless OFDM systems. *IEEE Communications Surveys & Tutorials 2nd Quarter. J*, pages 18–48, 2007.

[56] A.K. Miu, H. Balakrishnan, and C.E. Koksal. Improving loss resilience with multi-radio diversity in wireless networks. In *ACM MobiCom*, pages 16–30, 2005.

[57] T.K. Moon. The expectation-maximization algorithm. *IEEE Signal Processing Magazine*, 13(6):47–60, 1996.

[58] R.H. Morelos-Zaragoza, M.P.C. Fossorier, S. Lin, and H. Imai. Multilevel coded modulation for unequal error protection and multistage decoding. I. symmetric constellations. *IEEE Trans. on Communications*, 48(2):204–213, 2000.

[59] R.U. Nabar, H. Bolcskei, and F.W. Kneubuhler. Fading relay channels: Performance limits and space-time signal design. *IEEE JSAC*, 22(6):1099–1109, 2004.

[60] T. Nechiporenko, K.T. Phan, C. Tellambura, and H.H. Nguyen. Performance analysis of adaptive M-QAM for Rayleigh fading cooperative systems. In *ICC'08*, 2008.

[61] R. Nee and R. Prasad. *OFDM for wireless multimedia communications*. Artech House, Inc., 2000.

[62] M. Nicoli, S. Ferrara, and U. Spagnolini. Soft-iterative channel estimation: Methods and performance analysis. *Signal Processing, IEEE Transactions on*, 55(6):2993–3006, 2007.

[63] A. Nosratinia, T.E. Hunter, and A. Hedayat. Cooperative communication in wireless networks. *IEEE Communications Magazine*, 42(10):74–80, 2004.

[64] C.S. Patel and G.L. Stuber. Channel estimation for amplify and forward relay based cooperation diversity systems. *IEEE Trans. on Wireless Communications*, 6(6):2348–2356, 2007.

[65] C.S Patel, G.L Stuber, and T.G Pratt. Simulation of Rayleigh-faded mobile-to-mobile communication channels. *IEEE Trans. Commun.*, 53(11):1876–1884, 2005.

[66] C.S Patel, G.L Stuber, and T.G Pratt. Statistical properties of amplify and forward relay fading channels. *IEEE Trans. Veh. Technol.*, 55(1):1–9, 2006.

[67] G. Piro, N. Baldo, and M. Miozzo. An LTE module for the NS-3 network simulator. In *workshop on NS-3, SIMUTools*, 2011.

[68] R. Pyndiah, A. Picart, and A. Glavieux. Performance of block turbo coded 16-QAM and 64-QAM modulations. In *IEEE Globecom'95*, 1995.

[69] A. Ribeiro, X. Cai, and G.B Giannakis. Symbol error probabilities for general cooperative links. *IEEE Trans. on Wireless Communications*, 4(3):1264–1273, 2005.

[70] H. Rutagemwa, V. Mahinthan, J.W. Mark, and Xuemin Shen. Second order statistics of non-identical Nakagami fading channels with maximal-ratio combining. In *IEEE GLOBECOM*, pages 1 –5, Dec. 2006.

[71] P. Sadeghi, R. Kennedy, P. Rapajic, and R. Shams. Finite-state Markov modeling of fading channels - a survey of principles and applications. *IEEE Signal Proces. Magazine*, 25(5):57 –80, Sep. 2008.

[72] F. Sanzi, S. Jelting, and J. Speidel. A comparative study of iterative channel estimators for mobile OFDM systems. *IEEE Trans. on Wireless Communications*, 2(5):849–859, 2003.

[73] M. Schwartz, W.R. Bennett, and S. Stein. *Communication systems and techniques*. Wiley-IEEE Press, 1995.

[74] T.C. Seong and A.J. Goldsmith. Degrees of freedom in adaptive modulation: a unified view. *IEEE Trans. on Communications*, 49(9):1561–1571, Sep. 2001.

[75] H. Shin and J.B. Song. MRC analysis of cooperative diversity with fixed-gain relays in Nakagami-m fading channels. *IEEE Trans. Wireless Commun.*, 7(6):2069–2074, 2008.

[76] S. Song, A.C. Singer, and K.M. Sung. Soft input channel estimation for Turbo equalization. *IEEE Trans. on Signal Processing*, 52(10):2885–2894, 2004.

[77] E.C. Strinati, S. Yang, and J.C. Belfiore. Adaptive modulation and coding for hybrid cooperative networks. In *IEEE ICC'07*, pages 4191–4195, 2007.

[78] C.C. Tan and N.C. Beaulieu. On first-order Markov modeling for the Rayleigh fading channel. *IEEE Trans. Commun.*, 48(12):2032–2040, 2000.

[79] S. Ten Brink, J. Speidel, and R.H. Yan. Iterative demapping and decoding for multilevel modulation. In *IEEE Globecom'98*, volume 1, 1998.

[80] H.S. Wang and N. Moayeri. Finite-state Markov channel–a useful model for radio communication channels. *IEEE Trans. Veh. Technol.*, 44(1):163–171, 1995.

[81] T. Wang, A. Cano, G.B. Giannakis, and J.N. Laneman. High-performance cooperative demodulation with decode-and-forward relays. *IEEE Trans. on Communications*, 55(7):1427–1438, 2007.

[82] Z. Wang and G.B. Giannakis. A simple and general parameterization quantifying performance in fading channels. *IEEE Trans. on Communications*, 51(8):1389–1398, 2003.

[83] R. Wong. *Asymptotic approximations of integrals*, volume 34. Society for Industrial Mathematics, 2001.

[84] G.R. Woo, P. Kheradpour, D. Shen, and D. Katabi. Beyond the bits: cooperative packet recovery using physical layer information. In *ACM MobiCom*, pages 147–158, 2007.

[85] S. Xiang. Scalable streaming. https://sites.google.com/site/svchttpstreaming/.

[86] S. Xiang, L. Cai, and J. Pan. Adaptive scalable video streaming in wireless networks. In *ACM MMsys Accepted*, 2012.

[87] L. Xiao, T. Fuja, J. Kliewer, and D. Costello. A network coding approach to cooperative diversity. *IEEE Trans. on Information Theory*, 53(10):3714–3722, 2007.

[88] J. Xu, X. Shen, J.W. Mark, and J. Cai. Adaptive transmission of multi-layered video over wireless fading channels. *IEEE Trans. Wireless Commun.*, 6(6):2305–2314, June 2007.

[89] J. Yang, M. Ghosh, P.R.N. America, and B. Manor. A cooperative modulation scheme for wireless relay networks. In *IEEE VTC2007, Spring*, pages 1628–1632, 2007.

[90] Y. Yang, H. Hu, J. Xu, and G. Mao. Relay technologies for WiMAX and LTE-advanced mobile systems. *IEEE Communications Magazine*, 47(10):100–105, 2009.

[91] Q. Zhang and S.A Kassam. Finite-state markov model for rayleigh fading channels. *IEEE Trans. Commun.*, 47(11):1688–1692, 1999.

Appendix A

Appendix

APPENDIX I

FSMC for N multi-path cooperative systems

We briefly outline the general expression of LCR for N multi-path cooperative diversity system. Assuming received signals from N independent paths with SNR notated as $\Gamma_i, i = 1, 2, ..., N$. Each path, either performs as AF relay or direct channel, has the LCR, CDF and PDF as $N_{\Gamma_i}(\gamma)$, $F_{\Gamma_i}(\gamma)$ and $f_{\Gamma_i}(\gamma)$, respectively.

As for SC scheme, overall received SNR can be expressed as $\Gamma = \max\{\Gamma_i\}, i = 1, 2, ..., N$. Taking the above expression into (2.17), the general expression for N multi-path cooperative diversity system with SC, can be obtained as

$$N_{\Gamma}(\gamma) = \sum_{i}^{N} N_{\Gamma_i} \prod_{j,j\neq i}^{N} F_{\Gamma_j}(\gamma). \tag{A.1}$$

For MRC scheme with received SNR $\Gamma = \sum_{i=1}^{N} \Gamma_i$, the joint probability $f_{\Gamma\dot{\Gamma}}(\gamma, \dot{\gamma})$ can be expressed as

$$f_{\Gamma\dot{\Gamma}}(\gamma, \dot{\gamma}) = \int_{\Gamma_1=0}^{\infty} ... \int_{\Gamma_{N-1}=0}^{\infty} f_{\Gamma\dot{\Gamma}|\Gamma_1...\Gamma_{N-1}}(\gamma, \dot{\gamma}|\gamma_1, ..., \gamma_{N-1}) f_{\Gamma_1}(\gamma)...f_{\Gamma_{N-1}}(\gamma) d\gamma_1...d\gamma_{N-1} \tag{A.2}$$

and the conditional probability $f_{\Gamma\dot{\Gamma}|\Gamma_1...\Gamma_{N-1}}(\gamma, \dot{\gamma}|\gamma_1, ..., \gamma_{N-1})$ can be further simplified as

$$f_{\Gamma\dot{\Gamma}|\Gamma_1...\Gamma_{N-1}}(\gamma, \dot{\gamma}|\gamma_1, ..., \gamma_{N-1}) = f_{\dot{\Gamma}|\Gamma,\Gamma_1...\Gamma_{N-1}}(\dot{\gamma}|\gamma\gamma_1, ..., \gamma_{N-1}) f_{\Gamma|\Gamma 1,...\Gamma_{N-1}}(\gamma|\gamma_1, ..., \gamma_{N-1}) \tag{A.3}$$

By taking (A.2) and (A.3) into (2.23) and following the same procedure in Section 2.5, we can obtain the general expression for N multi-path cooperative diversity system with MRC.

APPENDIX II

Proof of Eq.(2.27)

Given that the derivative of direct channel, $\dot{\alpha}_D$ is zero-mean Gaussian distributed, where $\sigma^2_{\dot{\alpha}_D} = \pi^2 \bar{\gamma}_D f_3^2$ [30], the expectation of Γ_D under the condition of Γ and Γ_D, can be obtained as

$$E[\dot{\Gamma}_D] = E[2\Gamma_d \dot{\alpha}_D] = 0. \tag{A.4}$$

As for $\Gamma_R = \gamma_1\gamma_2/(C+\gamma_2)$, it can be rewritten as $\Gamma_R = (1/(\gamma_1\gamma_2 C^{-1}) + 1/\gamma_1)^{-1}$. To achieve more mathematically tractable form of the expression, we adopt the well-known inequality between harmonic and geometric means to derive an upper bound for Γ_R,

$$N(\sum_{i=1}^{N} \frac{1}{x_i})^{-1} \leq \prod_{i=1}^{N} x_i^{1/N}, \tag{A.5}$$

where the equality holds only when $x_1 = x_2 = ... = x_N$. Using (A.5), an upperbound for fixed-gain AF relay channel SNR, Γ_b, can be obtained as

$$\Gamma_R \leq \Gamma_b = \frac{1}{2}\gamma_1 \sqrt{\frac{\gamma_2}{C}}. \tag{A.6}$$

Normally each hop of the relay link will share the similar channel quality, and the constant amplify gain $C = \bar{\gamma_1} + 1$, thus Γ_b is a reasonable approximation of Γ_R.

Since the envelope of each hop from relay link $\alpha_i, i = 1, 2$ follows Rayleigh distribution, as discussed above, the derivative of α_i is also zero-mean Gaussian distributed. By using (A.6), the expectation of the derivative of AF relay link can be obtained as

$$E[\dot{\Gamma}_R] \approx \frac{1}{\sqrt{C}}\alpha_1\alpha_2 E[\dot{\alpha}_1] + \frac{1}{2\sqrt{C}}\alpha_1^2 E[\dot{\alpha}_2] = 0. \tag{A.7}$$

From (A.4), (A.7) and independence of each path, we can reach the conclusion

that the expectation of $\dot{\Gamma}$, $E[\dot{\Gamma}] = 0$. So the variance of $\dot{\Gamma}$ can be expressed as

$$Var[\dot{\Gamma}] \;=\; Var[\dot{\Gamma}_R] + Var[\dot{\Gamma}_D]. \tag{A.8}$$

which leads to the form of (2.27).

APPENDIX III

Derivation of Eq.(2.11)

Here we provide a brief outline for the close-form approximation of (2.11). Multivariate Laplace approximation theorem [20] can be applied for Laplace-type integral

$$J(\lambda) = \int_{\mathbf{x}\in R} u(\mathbf{x}) \exp(-\lambda w(\mathbf{x}))d\mathbf{x} \tag{A.9}$$

where u and w are real-valued multivariate functions. λ is a real parameter, and R is the unbounded domain of $\mathbf{x} = [x_1, ..., x_K]$.

When the above integral $J(\lambda)$ converges, while function $w(\mathbf{x})$ satisfies the following conditions: 1)$w(\mathbf{x})$ has an absolute minimum $\tilde{\mathbf{x}}$, i.e., $\nabla w(\tilde{\mathbf{x}}) = 0$; 2) The Hessian matrix $A = [(\frac{\partial^2 w}{\partial x_i \partial x_j})|_{\mathbf{x}=\tilde{\mathbf{x}}}] > 0$, then for larger λ, (A.9) can be approximated as

$$J(\lambda) \approx (\frac{2\pi}{\lambda})^{(K/2)} \frac{u(\tilde{\mathbf{x}})}{\sqrt{\det(\mathbf{A})}} \exp(-\lambda w(\tilde{\mathbf{x}})), \tag{A.10}$$

where det(.) denotes the matrix determinant.

Compare (A.9) and (2.11), we get

$$u(x) \;=\; \frac{\sqrt{f_1^2 \bar{\gamma}_1 x^4 (x^2 + C) + C^2 f_2^2 \bar{\gamma}_2 \gamma}}{x^2}, \tag{A.11}$$

$$w(x) \;=\; \frac{\bar{\gamma}_1 x^4 + C\bar{\gamma}_2 \gamma}{x^2 \bar{\gamma}_1 \bar{\gamma}_2}, \tag{A.12}$$

$$A \;=\; [\frac{d^2 w}{dxdx}] = \frac{2}{\bar{\gamma}_2} + \frac{6C\gamma}{\bar{\gamma}_1} x^{-4}, \tag{A.13}$$

$$\lambda \;=\; 1. \tag{A.14}$$

By definition, it is easy to obtain the interior critical point $\tilde{x} = (C\gamma\bar{\gamma}_2/\bar{\gamma}_1)^{\frac{1}{4}}$ by solving $dw(x)/dx = 0$. Although the approximation (A.10) is proven for large λ [83],

it also holds and performs very well when λ is small [7]. Therefore, by substituting (A.14) into (A.10) with the value of $\tilde{x}$, and after some simplification, we obtain the approximation expression given in (2.33).